JAEA-Review
2009-042

JAEA-Review

Annual Report of R&D Activities in Center for Computational Science & e-Systems from April 1, 2007 to March 31, 2009

Center for Computational Science & e-Systems

January 2010

Japan Atomic Energy Agency

日本原子力研究開発機構

本レポートは独立行政法人日本原子力研究開発機構が不定期に発行する成果報告書です。
本レポートの入手並びに著作権利用に関するお問い合わせは、下記あてにお問い合わせ下さい。
なお、本レポートの全文は日本原子力研究開発機構ホームページ（http://www.jaea.go.jp）
より発信されています。

独立行政法人日本原子力研究開発機構　研究技術情報部　研究技術情報課
〒319-1195　茨城県那珂郡東海村白方白根 2 番地 4
電話 029-282-6387, Fax 029-282-5920, E-mail:ird-support@jaea.go.jp

This report is issued irregularly by Japan Atomic Energy Agency
Inquiries about availability and/or copyright of this report should be addressed to
Intellectual Resources Section, Intellectual Resources Department,
Japan Atomic Energy Agency
2-4 Shirakata Shirane, Tokai-mura, Naka-gun, Ibaraki-ken 319-1195 Japan
Tel +81-29-282-6387, Fax +81-29-282-5920, E-mail:ird-support@jaea.go.jp

JAEA-Review 2009-042

Annual Report of R&D Activities in Center for Computational Science & e-Systems from April 1, 2007 to March 31, 2009

Center for Computational Science & e-Systems

Japan Atomic Energy Agency
Tokai-mura, Naka-gun, Ibaraki-ken

(Received November 6, 2009)

This report provides an overview of research and development activities in Center for Computational Science & e-Systems (CCSE), JAEA, during the fiscal years 2007 and 2008 (Apr 1, 2007 – March 31, 2009). These research and development activities have been performed by the Simulation Technology R&D Office and Computer Science R&D Office. These activities include development of secure computational infrastructure for atomic energy research based on the grid technology, large scale seismic analysis of an entire nuclear reactor structure, large scale fluid dynamics simulation of J-PARC mercury target, large scale plasma simulation for nuclear fusion reactor, large scale atomic and subatomic simulations of nuclear fuels and materials for safety assessment, large scale quantum simulations of superconductor for the design of new devices and fundamental understanding of superconductivity, development of protein database for the identification of radiation-resistance gene, and large scale atomic simulation of proteins.

Keywords: R&D Activities, CCSE, Computer Technology for Atomic Energy Research, Vibration Analysis, Grid, Superconductivity, Computational Fluid Dynamics, J-PARC, Plasma Simulation, Computational Materials Science, Computational Quantum Bioinformatics

JAEA-Review 2009-042

平成 19-20 年度　システム計算科学センター　研究開発年報

日本原子力研究開発機構

システム計算科学センター

（2009 年 11 月 6 日受理）

本報告書では、平成 19 年度および 20 年度(2007 年 4 月 1 日～2009 年 3 月 31 日)の日本原子力研究開発機構・システム計算科学センターにおける研究開発活動について報告する。これらの研究開発は、高度計算科学技術開発室とシミュレーション技術開発室により執り行われた。主な研究内容は、グリッド技術に基づく安全な計算環境の開発、 原子炉施設全体の大規模耐震計算、J-PARC 水銀ターゲットの大規模流体計算、核融合炉の大規模プラズマシミュレーション、原子炉材料および核燃料の安全評価のための大規模物性計算、新奇デバイス開発および超伝導現象解明のための大規模量子シミュレーション、照射耐性遺伝子特定のためのデータベース構築、およびたんぱく質の大規模分子シミュレーション等である。

原子力科学研究所(駐在)：〒319-1195 茨城県那珂郡東海村白方白根 2-4

Contents

目　次

Foreword

Computational science and technology has become a vital part of nuclear energy research, owing to the rapid expansion of computational capabilities which enabled many breakthroughs for the most demanding problems. The mission of the Center for Computational Science and e-Systems (CCSE) is to develop state-of-the-art computational techniques and infrastructure for nuclear energy research, and to promote cross-cutting computational research activities in Japan Atomic Energy Agency (JAEA). To achieve this mission, CCSE is carrying out vigorous research and development in the field of computational science for nuclear energy.

The R&D activities of CCSE during the fiscal year 2007 and 2008 are presented in the subsequent sections, and they can be summarized as follows:
1 Atomic Energy Grid Infrastructure: Development of secure computational infrastructure for nuclear energy research based on the grid technology
2 Computational Vibration Science and Fluid Dynamics: Large scale seismic analysis of an entire nuclear reactor structure, multiple bubble dynamics simulation for the J-PARC pulsed neutron source, large scale plasma simulation for nuclear fusion reactor, and two-phase flow simulation for nuclear engineering applications
3 Computational Materials Science: Large scale atomic and subatomic simulations of nuclear fuels and materials for safety assessment, and large scale quantum simulations of superconductor for the design of new devices and fundamental understanding of superconductivity
4 Computational Quantum Bioinformatics: Development of protein database for the identification of radiation-resistance gene, and large scale nuclear simulation of proteins

The CCSE will keep accelerating computational science R&D in the field of nuclear energy.

Toshio Hirayama
Director
Center for Computational Science and e-Systems,
JAEA

This is a blank page.

1. CCSE Research and Development Activities

1.1 Computer Science / Grid Computing

This is a blank page.

1.1.1 Application Program Interface for Grid-enabled Applications

Gridization of IMAGINE for the remote assistance of radiation therapy

Kimiaki Saito1), Naoya Teshima, Yoshio Suzuki, Norihiro Nakajima, Hidetoshi Saito2), Etsuo Kunieda3), Tatsuya Fujisaki4)

1) Quantum Beam Science Directorate, JAEA
2) Tokyo Metropolitan University
3) Keio University
4) Ibaraki Prefectural University of Health Science

We have been researching and developing IMAGINE (IT-based Medical Aiding Gear for Instantaneous Numeration of Energy Deposition Distribution) which is a dose calculation system to support the radiation therapy remotely[1]. At the radiation therapy, a doctor need decide a radiation condition, which includes the number of radioactive source, radiant intensity, radiation angle and so on. The Monte Carlo method is used for the dose calculation to estimate the radiation condition very precisely.

However, the method needs overnight calculation time by PC or workstation which is used in the general radiation therapy. Therefore, it is required to improve IMAGINE to execute the dose calculation by high performance computers (HPCs) and quickly response results to a medical facility.

When IMAGINE will be actually operated, IMAGINE is required to accept large amount of dose calculation jobs from many medical facilities at a same time. So far, IMAGINE could not use several HPCs at the samet time. Thus, it was difficult to quickly response results of dose calculations because of waiting time for job queuing.

To overcome this problem, we have carried out the gridization of IMAGINE, which enables to distribute jobs to job classes of HPCs and thus reduce the waiting time. We evaluated several methods to gridize IMAGINE by focusing on which is better to construct it in a shorter period and adopted the method to use grid commands. Thus, we designed the grid commands which can be replaced by present local execution modules. This method hardly changes the original configuration of IMAGINE at all.

We developed the grid commands on our grid infrastructure AEGIS (Atomic Energy Grid InfraStructure) [2] with the policy to implement the unix-like command functions and command interfaces. The list of grid commands (the command names and their descriptions) is shown in Tab.1.

We gridized IMAGINE by using the grid commands. The system configuration of gridized IMAGINE is shown in Fig.1. The period from the design phase to the test phase took about only a week.

We could successfully execute dose calculation jobs by using both SGI Altix3700Bx2 in Japan Atomic Energy Agency and Fujitsu HPC2500 in National Institute of Informatics at the same time [3].

Tab. 1: grid command list

command name	description
jstart	initialize grid environment
jend	finalize grid environment
jcp	copy file or directory
jmv	move file or directory
jmkdir	make directory
jrm	remove file or directory
jexec-command	execute command

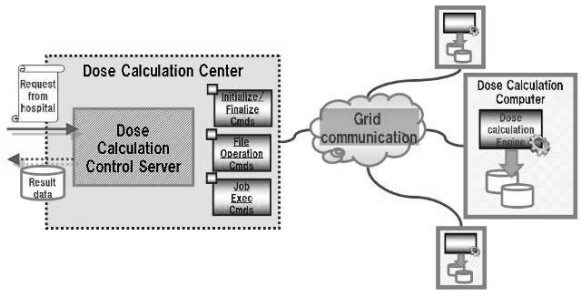

Fig. 1: System configuration of gridized IMAGINE.

References

[1] K. Saito, et al., Radiation Protection Dosimetry, 116, pp191-195 (2006).

[2] Y. Suzuki, A. Nishida, F. Araya, N. Kushida, T. Akutsu, N. Teshima, K. Nakajima, M. Kondo, S. Hayashi, T. Aoyagi and N. Nakajima, Journal of Power and Energy Systems, Vol.3, No.1, Special Issue on 16th International Conference on Nuclear Engineering pp.60-71 (2009).

[3] K. Saito, N. Teshima, Y. Suzuki, N. Nakajima, H. Saito, E. Kunieda, T. Fujisaki, Fujitsu Family Family Association FY2008 (2009) (Japanese).

1.1.1 Application Program Interface for Grid-enabled Applications

Development of Three-dimensional Virtual Plant Vibration Simulator on Grid Computing Environment ITBL-IS/AEGIS

Yoshio Suzuki, Akemi Nishida, Fumimasa Araya, Noriyuki Kushida, Taku Akutsu, Naoya Teshima, Kohei Nakajima, Makoto Kondo[1)], Sachiko Hayashi, Tetsuo Aoyagi and Norihiro Nakajima

1) O-arai Research and Development Center, JAEA

CCSE/JAEA, Center for computational science and e-systems of Japan Atomic Energy Agency is conducting R&Ds for extra large-scale simulation technologies of whole nuclear plants using state-of-the-art computational and IT technologies. Specifically we focus on establishing a virtual plant vibration simulator on inter-connected supercomputers, for seismic response analysis of a whole nuclear plant. In order to achieve a highly accurate simulation, we need to consider how connecting conditions among parts composing a plant affect integrated behaviors (stresses and deformations etc.) of a whole plant. A nuclear plant is generally composed of a gigantic number of parts. A simulation of a whole plant becomes a very difficult task because an extremely large dataset must be processed. To overcome this difficulty, we have established:

1. a simulation framework which allows model data preparation to be carried out in a part-wise manner, and allows the connecting condition of parts to be taken into consideration in an integrated simulation of a whole plant.
2. a computing platform which enables an extra large-scale simulation to be carried out on a grid computing platform called ITBL-IS, Information Technology Based Laboratory Infrastructure and AEGIS, Atomic Energy Grid Infrastructure (see Fig. 1).

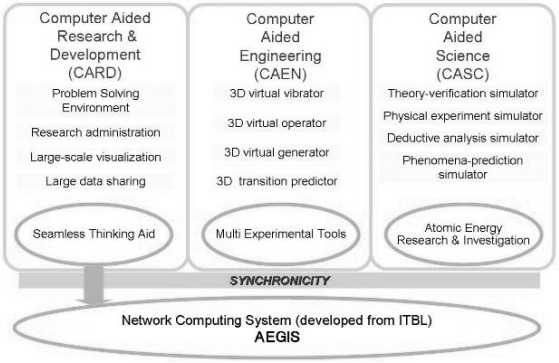

Fig. 1: Overview of AEGIS.

We have proposed a methodology of structural analysis for assembled structures ranging up to the size of a nuclear plant to estimate (1) the behavior by taking into account the heterogeneity conditions in assembly structures, (2) interactions and relative mechanical responses among the connected parts, and (3) the multi-dynamic behaviors in an assembly.

Also, we have launched R&D of grid middleware AEGIS for establishing computational infrastructure for nuclear field with the knowledge and skills in ITBL Infrastructure. The R&D aims at establishing predictable science and engineering to guarantee security and safety of atomic energy and preserve environment by constructing an environment of real-scale nuclear facility with computer aided research and development, computer aided engineering, computer aided science, and network computing system which enables those synchronicity.

The simulation framework using the computing framework has been applied to an elastic analysis of the reactor pressure vessel and cooling systems of the nuclear research facility, “HTTR: High Temperature engineering Test Reactor” at the O-arai Research and Development Center of Japan Atomic Energy Agency. The simulation framework taking advantage of grid distributed computing techniques showed early success in an extra large-scale simulation of major parts of the nuclear plant.

The simulation framework taking advantage of grid distributed computing techniques showed early success in the extra large-scale simulation of the major parts of the nuclear plant, and opens a possibility of new simulation technologies for building a whole virtual nuclear plant in computers for virtual experiments [1-2].

References

[1] Y. Suzuki, A. Nishida, F. Araya, N. Kushida, T. Akutsu, N. Teshima, K. Nakajima, M. Kondo, S. Hayashi, T. Aoyagi and N. Nakajima, Journal of Power and Energy Systems, Vol.3, No.1, Special Issue on 16th International Conference on Nuclear Engineering pp.60-71 (2009).

[2] Y. Suzuki, N. Nakajima, F. Araya, O. Hazama, A. Nishida, N. Kushida, T. Akutsu, N. Teshima, K. Nakajima, M. Kondo, S. Hayashi and T. Aoyagi, Proceedings of 16th International Conference on Nuclear Engineering (11-15 May 2008, Orlando, Florida, U.S.A.) CD-ROM (2008).

1.1.1 Application Program Interface for Grid-enabled Applications

Building an Application-specific Grid Computing Environment Using ITBL for Nuclear Material Engineering

Yuichi Tsujita[1)], Tatsumi Arima[2)], Kazuya Idemitsu[2)], Yoshio Suzuki, Hideo Kimura

1) School of Engineering, Kinki University
2) Faculty of Engineering, Kyushu University

Effective use of nuclear fuel is an important issue in nuclear material engineering. Pu recycle is refocused for effective use of nuclear fuel. MOX and inert matrix fuels (e.g., ZrO2-PuO2) are expected for effective burning Pu, however, Pu material is difficult to manage due to its radiotoxicity. As a result, cost of experimental facilities is very expensive. As computer simulation not only cuts cost for experimental researches but also provides deep understandings in atomic behavior, we have performed molecular dynamics (MD) simulations to research its material characteristics. In order to obtain realistic results, many atoms and many time steps are essential, however, such computation takes too much long time. So a parallelized program code is executed on a grid computing environment provided by an Information Technology Based Laboratory (ITBL) project. Its grid computing infrastructure (hereafter an ITBL system) provides users a seamless computing environment and many kinds of software tools such as a file manager, a program execution manager, and a cooperative tool for AVS/Express on a grid computing environment. Furthermore, a client application program interface (API) is provided to build a variety of grid applications on a client terminal PC for accessing the ITBL's functionalities. As there is a strong request from users in our material simulation research to utilize their native visualization software, we have selected the client API to build an application-specific grid computing environment which cooperates with the visualization software. We have built a customized graphical user interface (GUI) computing environment on a client terminal PC by using the Java client API. It provides a seamless access to ITBL's computational resources from a user's terminal PC. It also assists choosing parameters for the computation in parameter survey runs. Moreover, it enables successive processing of computation on remote parallel computers and visualization on a user's terminal PC in a single operation. The environment also provides a user friendly GUI interface for parameter controls and monitoring of submitted jobs. As a result, this computing environment removes difficulties in manual operations for parallel computations and visualizations in parameter survey runs. So, it prevents users from mistakes in the operations. This environment is expected to accelerate finding procedure for good nuclear fuel.

We have executed an MD program code, MXDORTOP. However, we have faced a usability problem in parallel computations because scientists are non-expert in a grid computing. Moreover, we have a difficulty in setting many parameters for MXDORTOP because MXDORTOP requests users to choose from among several such ensembles, e.g., a Busing-Ida-Gilbert type partially ionic pair potential, scaling in temperature, scaling in pressure, and constant volume.

We have presented a client GUI application for a grid computing by using the ITBL system [1]. The application is built by using a Java client API of the ITBL system. As the Java interface provides flexibility and portability in developing the GUI application, it is available on both the Linux and Windows without any modification in its code. With the help of the API library, we were able to realize single sign-on in user's authentication and authorization by using an X.509 certificate. Furthermore, the application provides control options for computations, file transfer, and visualization of simulated results on a client terminal by using computing resources of the ITBL system. Specifying parameters for a simulation program and job execution are available from the application by using a user-friendly GUI interface. We have succeeded in executing our simulation program by the client application without any attention to underlying communication software and location of each parallel computer. Moreover, seamless visualization of remote calculated results is supported by using native visualization software. The client application also prevents users from mistakes in parameter settings for many parameter survey runs. Furthermore, it provides seamless and successive operations of parallel computation and visualization.

References

[1] Y. Tsujita, T. Arima, K. Idemitsu, Y. Suzuki and H. Kimura, Proceedings of 16th International Conference on Nuclear Engineering (11-15 May 2008, Orlando, Florida, U.S.A.) CD-ROM (2008).

1.1.1 Application Program Interface for Grid-enabled Applications

Method to Unconsiously Use Grid middleware; Proposal of Seamless API and Its Application to Mechanics System

Kohei Nakajima, Yoshio Suzuki, Naoya Teshima, Shin-ichiro Sugimoto[1)], Shinobu Yoshimura[1)], Norihiro Nakajima

1) Institute of Environmental Studies, Graduate School of Frontier Sciences, The University of Tokyo

CCSE/JAEA, Center for computational science and e-systems of Japan Atomic Energy Agency is promoting R&D of grid computing middleware AEGIS (Atomic Energy Grid InfratStructure).

AEGIS equips several tools for job execution, file operation, and information management to execute scientific applications on supercomputers. These tools can be used from graphical user interface (GUI) and enables users to easily execute many applicationos.

However, users need to understand the structure of grid environment in order to make the fullset use of these tools. To overcome this, CCSE/JAEA has researched the method to unconsiously use grid middleware.

In general, in order to execute jobs by using a function of grid middleware, a user must describe a script file or acquire the usage of tool to generate the script file. We propose API (Application Program Interface) to automatically generate the script file to execute jobs (Script Generator API) and API to automatically execute a parameter survey (Parameter Survey API). Advantages of these APIs are as follows:

- Because job execution information can be specified using API, conditions of job execution can be dynamically decided in an application program including API.
- It is unnecessary for a user to generate the script file.
- It is unnecessary for a user to manage the script file.

A. Script Generator API

A user may not prepare the script file. Instead, the script file has to be generated automatically. We provide the function to automatically generate the script file as the Script Generator API.

The Script generator API demands job execution to grid middleware through the common API (Fig.1). The common API ,which has been developed on AEGIS by CCSE/JAEA, consists of authentication API, communication API, job execution API, file control API and information management API. The Script generator API has the job state monitoring function and the file staging function besides the script generation function.

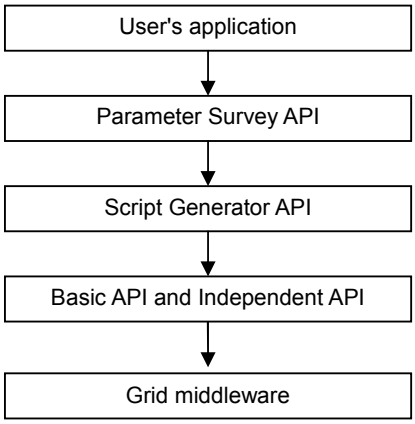

Fig. 1: Usage of API

B. Parameter Survey API

We provide the function to automatically execute parameter survey jobs as the Parameter Survey API. By using the Parameter Survey API, a user can execute jobs with different parameters to supercomputers at the same time.

We have applied these APIs to ADVENTURE (ADVanced ENgineering analysis Tool for Ultra large REal world). ADVENTURE has been researched and developed in the University of Tokyo. By using the Script Generator API and the Parameter Survey API, we have imploved "ADVENTURE Opt", which is the parameter survey module of ADVENTURE for structural optimization and can execute evaluation calculations based on the genetic algorithm.

We confirmed that many jobs with different parameters were executed on two or more computers and the structural optimization is completed without user's wathcing.

References

[1] K. Nakajima, Y. Suzuki, N. Teshima, S. Sugimoto, S. Yoshimura, N. Nakajima, FY2008 Collected Papers of NEC C&C Systems Users Association (2008) (Japanese).

1.1.1 Application Program Interface for Grid-enabled Applications

Research and Development of Fusion Grid Infrastructure Based on Atomic Energy Grid InfraStructure (AEGIS)

Yoshio Suzuki, Kohei Nakajima, Noriyuki Kushida, Chiaki Kino, Takahiro Minami, Nobuko Matsumoto, Tetsuo Aoyagi, Norihiro Nakajima, Katsuyuki Iba[1)], Nobuhiko Hayashi[2)], Takahisa Ozeki[2)], Toshiyuki Totsuka[2)], Hideya Nakanishi[3)] and Yoshio Nagayama[3)]

1) Research Organization for Information Science and Technology
2) Naka Fusion Institute, JAEA
3) National Institute for Fusion Science, NINS

In collaboration with the Naka Fusion Institute of Japan Atomic Energy Agency (NFI/JAEA) and the National Institute for Fusion Science of National Institute of Natural Science (NIFS/NINS), Center for Computational Science and E-systems of Japan Atomic Energy Agency (CCSE/JAEA) aims at establishing an integrated framework for experiments and analyses in nuclear fusion research based on the Atomic Energy Grid InfraStructure (AEGIS) [1]. AEGIS has been being developed by CCSE/JAEA aiming at providing the infrastructure that enables atomic energy researchers in remote locations to carry out R&D efficiently and collaboratively through the Internet.

Toward establishing the integrated framework, we have been applying AEGIS to pre-existing three systems: experiment system, remote data acquisition system, and integrated analysis system. For the experiment system, the secure remote experiment system with JT-60 has been successfully accomplished. For the remote data acquisition system, it will be possible to equivalently operate experimental data obtained from LHD data acquisition and management system (LABCOM system) and JT-60 Data System. The integrated analysis system has been extended to the system executable in heterogeneous computers among institutes.

CCSE/JAEA has been developing the integrated framework for experiments and analyses in nuclear fusion research in collaboration with NFI/JAEA and NIFS/NINS. We have been applying AEGIS to pre-existing three systems: 1) experiment system, 2) remote data acquisition system, 3) integrated analysis system.

The experiment system has been developed by NFI/JAEA to control JT-60 through the Intranet of JAEA. The extension of the system has been carried out aiming at securely controlling remote experimental devices through the Internet. By applying AEGIS network computing system to the original experiment system of JT-60, the secure remote experiment system with JT-60 has been successfully accomplished. We have confirmed that by demonstrating the remote experiment from Kyoto University.

For the remote data acquisition system, it will be possible to equivalently operate experimental data obtained from LHD data acquisition and management system (LABCOM system) and JT-60 Data System

The integrated analysis system has been extended to the system executable in heterogeneous computers among institutes. Since these three systems have been being constructed using a same network computing system, these three systems are easily integrated. We plan to accomplish these systems until FY2009 (Fig.1).

The integrated framework would become useful to use remotely ITER research center including a computational simulation centre for fusion science and a center for remote experimentation.

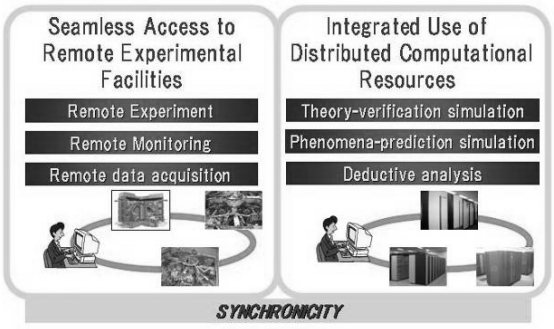

Fig. 1: Concept of framework for experiments and analyses in nuclear fusion research.

References

[1] Y. Suzuki, K. Nakajima, N. Kushida, C. Kino, T. Minami, N. Matsumoto, T. Aoyagi, N. Nakajima, K. Iba, N. Hayashi, T. Ozeki, T. Totsuka, H. Nakanishi and Y. Nagayama, Sixth IAEA Technical Meeting on Control, Data Acquisition, and Remote Participation for Fusion Research (4-8 June 2007, Inuyama, Japan), Fusion Engineering and Design Vol.83 pp.511-515 (2008).

1.1.1 Application Program Interface for Grid-enabled Applications

Development and verification of remote research environment based on “Fusion research grid”

Katsuyuki Iba[1)], Takahisa Ozeki[2)], Toshiyuki Totsuka[2)], Yoshio Suzuki, Takayuki Oshima[2)], Shinya Sakaba[2)], Minoru Sato[2)], Mitsuhiro Suzuki[2)], Kiyotaka Hamamatsu[2)] and Kimihiro Kiyono[2)]

1) Research Organization for Information Science and Technology
2) Naka Fusion Institute, JAEA

“Fusion research grid” is a concept that connects scientists far apart and let them collaborate effectively over the difference in time and distance in a nuclear fusion research. Fundamental technology of Fusion research grid has been developed at JAEA in the VizGrid project under the e-Japan project at Ministry of Education, Culture, Sports, Science and Technology (MEXT). We are conscious of needs to create new systems that assist researchers with their research activities. Remote research environments of experiments, diagnostics, analyses and communications were developed on “Fusion research grid”.

We have developed prototype systems that include a remote experiment system, a remote diagnostics system, and a remote analysis system. All users can access these systems from anywhere because “Fusion research grid” does not require a closed network like SuperSINet to maintain security. The prototype systems were verified in experiments at JT-60U and their availability was confirmed.

Complex and large experimental facilities are used at several research institutes in a nuclear fusion research field. International cooperative researches, such as International Thermonuclear Experiment Reactor (ITER) and JT-60U, are promoted. It is an important topic that excellent researchers from around the world and research resources of each laboratory are concentrated by Information Technology (IT). Especially, a system of remote experiment and analysis is demanded because movement of persons to an experimental facility causes a heavy loss of money and time. Because of these backgrounds, National Fusion Collaboratory project had started in America. In EU, Remote Participation project is progressing. In Japan, the VizGrid project under the e-Japan project at MEXT has started. With results of the IT Based Laboratory (ITBL) project, volume communication and Fusion research grid were developed in the VizGrid.

Our goal is to develop the remote research environment based on Fusion research grid and to confirm the efficiency of Fusion research grid [1].

Remote experiment system presents remote researchers with functions to give experimental information of JT-60U, and to submit experimental parameters. This system is divided into two parts. One is security part with ITBL grid infrastructure. The other is server computers to set experimental parameters, to monitor experimental status and to watch previous data.

Remote diagnostics system has a function to operate remotely via diagnostics CAMAC subsystem, and to acquire diagnostics data. Client computer of remote researchers is displayed GUI-based system control panel after this system based on X window function is logged into. Control panel has two functions. One is CAMAC control function which is allowed to reflect setting parameter of remote researcher in sync with JT-60 discharge sequence. The other is display control function which display diagnostics parameter and acquired data easily.

Remote cooperative analysis system assists that researchers analyze experimental data between widely separated places. Client computers access servers which analysis code and visualization tools are running through cashing server with shared page function.

We suggest “Fusion research grid”, which has advanced technology of security and a network, to solve many problems of the remote research. Prototype systems based on “Fusion research grid” was developed and verified under the VizGrid project. We confirmed that this system presented researchers with services of experiment, diagnostics and analysis. In addition, Fusion research grid was efficient for the remote research.

References

[1] K. Iba, T. Ozeki, T. Totsuka, Y. Suzuki, T. Oshima, S. Sakaba, M. Sato, M. Suzuki, K. Hamamatsu and K. Kiyono, Sixth IAEA Technical Meeting on Control, Data Acquisition, and Remote Participation for Fusion Research (4-8 June 2007, Inuyama, Japan), Fusion Engineering and Design Vol.83 pp.511-515 (2008).

1.1.1 Application Program Interface for Grid-enabled Applications

Web-based Java application to advanced JT-60 Man–Machine Interfacing System for remote experiments

Toshiyuki Totsuka[1)], Yoshio Suzuki, Shinya Sakata, Takayuki Oshima, Katsuyuki Iba[2)]

1) Naka Fusion Institute, JAEA

2) Research Organization for Information Science and Technology

It is expected that the JT-60SA experiment is conducted from a remote experiment center located in Rokkasho-mura, Aomori-ken, Japan as a part of the BA (Broad Approach) project. Functions required for this remote experiment are monitoring of the discharge sequence status, handling of the discharge parameter, checking of experiment data, and monitoring of plant data. All of them are included in the existing JT-60 Man–Machine Interfacing System (MMIF). The MMIF is now available to only on-site users at the Naka site due to network safety. The motivation for remote MMIF is prompted by the issue of developing and achieving compatibility with network safety.

The Java language has been chosen to implement this task. The paper [1] deals with details of the JT-60 MMIF for the remote experiment that has evolved using the Java language.

UNIX workstations have been employed for the JT-60 Man–Machine Interfacing System (MMIF). Each was interfaced to the JT-60 control system by a dedicated Ethernet cable. C language and X-window libraries have been used for the MMIF application software. Major application functions for MMIF are setting of discharge parameters, execution of the plasma discharge sequence, display of discharge result data, and monitoring of plant data. An event or an operator's action through the X-window interface initiates these functions. The MMIF workstations are also connected to JT-60 supervisory control system computers that supervise JT-60 plant subsystems via a local network. TCP/IP protocol is used as the standard for both the MMIF system and the control system network.

To perform the JT-60SA remote experiment, many functions must be executed distantly from the JT-60SA site via the Internet. However, the existing JT-60 MMIF functions have been designed only for on-site use due to network security concerns. New MMIF application software was developed in 2003 by modifying the existing X-window-based MMIF to support a remotely-executed JT-60 experiment distant from the JT-60 site.

The new X-window-based MMIF is capable of monitoring the discharge sequence, setting of discharge parameters, and displaying discharge result data at the remote location via an ITBL (Internet Technology Based Laboratory) server. The ITBL server is a gateway that enables advanced and secure network communication and was developed for this specific purpose.

Major functions of MMIF for remote experiments are as follows:

(1) Set discharge parameter,

(2) Monitor discharge sequence,

(3) Display discharge result data, and

(4) Monitor plant data.

The "Set discharge parameter" function is important for acquisition of the experimental requirements from the remote site. This function should be the same function used by on-site JT-60SA site users. The Java applet on the user's PC manages the parameter setting manipulation interface and the discharge parameter display function. Each parameter setting manipulation performed on the user's PC transfers the discharge parameters and action request number to the server process in the RES.

New Java-based MMIF software has resolved the problems caused by X-window-based software. The combination of the use of Java-based software and the ITBL server has brought the remote site experimental environment to the same level as the JT-60 on-site environment.

Java-based MMIF was successfully demonstrated in JT-60 remote experiments conducted from Kyoto University in 2006.

References

[1] T. Totsuka, Y. Suzuki, S. Sakata, T. Oshima and K. Iba, Sixth IAEA Technical Meeting on Control, Data Acquisition, and Remote Participation for Fusion Research (4-8 June 2007, Inuyama, Japan), Fusion Engineering and Design Vol.83 pp.511-515 (2008).

1.1.1 Application Program Interface for Grid-enabled Applications

Research and Development of Application Programming Interaface for Grid Environment

Yoshio Suzuki

At the Japanese national project “Development and Applications of Advanced High-Performance Supercomputer”, we have developed an application programming interface (API) for using grid computing environment. Here, we have developed the prototype of API by analyzing how grid-enabled applications in ITBL project use the grid computing environment. Using this prototype enables to develop grid-enabled applications easily, to use different grid environments without changing applications and to interoperate different grid environments without changing grid middleware.

We have researched and developed utilization technology of grid middleware toward the next generation national grid infrastructure which enables us to use integratedly computers in Japanese Universities and Institutions at the Japanese national project “Development and Applications of Advanced High-Performance Supercomputer”. In this project, we have researched and developed API for users to use user-friendly grid environment without caring kinds of grid middleware in order to shift the grid-enabled application developed in ITBL project to the next generation national grid infrastructure and cause the revitalization of grid-enabled applications. To realize this, we have developed the prototype of API by systematizing functions of API which enables uses to use user-friendly a grid environment from a user client and to use commonly various kinds of grid environment (Fig.1). Here, we analyzed how all grid-enabled applications developed in ITBL project utilize the ITBL grid environment.

Three concepts to improve the usability of various grid environments have been proposed. The first one is a common client API (Application Programming Interface). The client API makes it easy for users to develop grid-enabled application programs. The ITBL client API we have developed enables users to develop such programs on their client terminals without installing grid middleware into their terminals, and thus users to develop their programs independent of the modification of grid middleware. The concept of the common client API is the commonization of such a client API to various grid environments. The common client API has an advantage that users can use various grid environments without being conscious of the difference among various grid middleware. The second one is a common interoperable API. The interoperability among various grid environments enables users to access other grids from their own grid. The concept of the common interoperable API is the commonization of the interface to connect different grid middleware. The common interoperable API has an advantage that the particular development is not required to establish the interoperable environment. The third one is an unified API. The unified API is what unifies the common client API and the common interoperable API, and thus unifies the interface for access grid environments from the outside.

We have applied the API to the grid-enabled application which was developed in ITBL project to execute assembly structure analysis. We enabled a user to control many jobs from a client PC. In addition, we have developed the tool to display thumbnails of visualized images located on supercomputers at a client PC. This enabled users to view visualized images on a grid environment.

Users can use those system and tool in some grid environments (ITBL environment, NAREGI environment and so on) without changing them.

Furthermore, we can easily connect different grid environments by using API. We have confirmed that we can interoperate ITBL environment and NAREGI environment without changing those middleware then demonstrated API is effective to connect different grid environments.

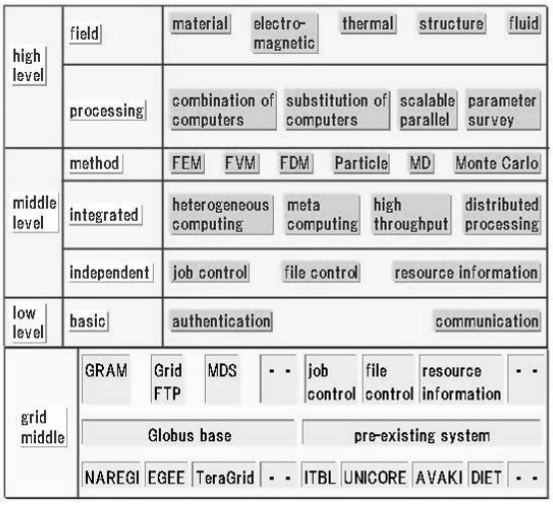

Fig.1: Definition of API.

References

[1] Y. Suzuki, FUJITSU Family Association FY2007 (2008) (Japanese).

1.1.2 Interoperability with Other Grids toward International Grid Environment

Atomic Energy Grid Infrastructure (AEGIS) and Interoperation with Other Grids

Yoshio Suzuki, Noriyuki Kushida, Naoya Teshima, Kohei Nakajima, Akemi Nishida and Norihiro Nakajima

Coordination of global knowledge is needed to advance the computational and computer science needed for nuclear research. The construction of a worldwide computing infrastructure network that would share and integrate worldwide computer resources, tools, and data with high security is an important step toward realizing this goal. For example, resources must be shared and integrated effectively to enable the execution of large-scale simulations, coupling simulations or parametric simulations, which are impossible or difficult to perform using only one computer in each institute or university. Such simulations are indispensable to the nuclear research field. Promising technology is being developed that would allow interoperability using different grid middleware to achieve a worldwide network computing infrastructure.

Research on the grid computing technology began approximately ten years ago and has resulted in the development of various grid middleware throughout the world. To date, research concerning the interoperability between different grid middleware has been promoted under the international programs of grid middle-ware standardization. One example is the UniGrids, which was funded under the 6th framework Specific Targeted Research Project (STREP) and was carried out for 2 years beginning in July 2004. The goal of the project was to attain the interoperability of the Uniform Interface to Computing Resources (UNICORE) system and Globus. The project enabled UNICORE users to utilize computers managed by Globus.

In the paper [1], we describe our research and development (R&D) of the interoperation technology using the Atomic Energy Grid Infrastructure (AEGIS), among other grids, and three actual experiments executed under three international collaborations (Fig.1).

R&D under AEGIS was conducted to provide a computational infrastructure for atomic energy research. International cooperation research in various fields has also been completed to advance computer science and to expand AEGIS.

In cooperation with the High Performance Computing Center Stuttgart (HLRS), we successfully executed a three-dimensional virtual plant vibration simulation using the interoperable environment between AEGIS and UNICORE. The simulation confirms that job controls, file controls, and acquisition of resource information are possible between computer resources in JAEA and HLRS using our interoperable system. As part of the cooperation with Grid-TLSE project partners, we established a prototype system for the inter-operable environment between AEGIS and DIET to execute the sparse solver prediction system, confirming that job execution from AEGIS to DIET is possible using the prototype system.

Under GNEP, we collaborated with DOE to implement a prototype system for network computing infrastructure. The prototype maintains high security between computer resources and data files in AEGIS and Globus.

Based on these results, we confirmed that our concept of the interoperable system can be applied to construct an interoperable environment between AEGIS and other grids without modifying each grid middleware. Improvements to each proto-type system will be needed to achieve research objectives as well as to advance the computational and computer science needed for nuclear research.

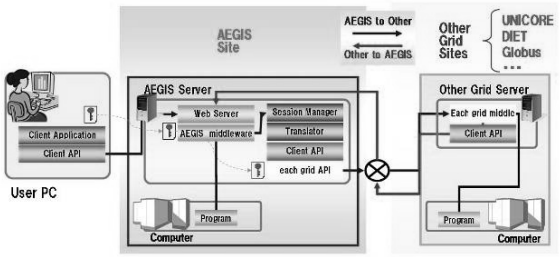

Fig. 1: Simplified configuration of an interoperable system between AEGIS and other grid middleware.

References

[1] Y. Suzuki, N. Kushida, N. Teshima, K. Nakajima, A. Nishida and N. Nakajima, High Performance Computing on Vector Systems 2008 M. Resch, S. Roller, K. Benkert, M. Gelle, W. Bez, H. Kobayashi, T. Hirayama (Eds.) Springer-Verlag Berlin Heidelberg, pp 65-77 (2008).

1.1.2 Interoperability with Other Grids toward International Grid Environment

Toward an International Sparse Linear Algebra Expert System by Interconnecting the ITBL Computational Grid with the Grid-TLSE Platform

Noriyuki Kushida, Yoshio Suzuki, Naoya Teshima, Norihiro Nakajima, Yves Caniou[1)], Michel Dayde[2)], and Pierre Ramet[3)]

1) Lip-ENS Lyon
2) Irit / INPT-Enseeiht
3) Inria Futur / LaBRI, Universit´e Bordeaux

The Japan Atomic Energy Agency (JAEA) Center for Computation Science and e-Systems (CCSE) and the Test for Large Systems of Equations (TLSE) partners (Cerfacs, Irit, LaBRI, and Lip-´ENS) have launched an international collaboration, within the framework of the Redimps Project (Research and Development of International Matrix Prediction System Project) [1]. In this collaboration, an international expert system for sparse linear algebra will be constructed using an international Grid computing environment. The TLSE Project [2] is an expert web site that aims at providing tools and software for sparse matrices. It allows the comparative analysis of a number of direct solvers (free or commercially distributed) on user-submitted problems, as well as on matrices from collections available on the site. The site provides user assistance in choosing the right solver for its problems and appropriate values for the control parameters of the selected solver. It also includes a bibliography on sparse matrices and access to collections of sparse matrices. The computations are carried over a computational Grid managed by the Distributed Interactive Engineering Toolbox (Diet) Grid middleware [3]. Diet is developed by the Graal Inria Project at Lip-´ENS Lyon. Implementing the GridRPC paradigm, it is designed to make the access to computers transparent from the users. On the other hand, JAEA has developed the middleware of “IT based laboratory” (ITBL). The ITBL middleware is deployed on the foundation of the Ministry of Education, Culture, Sports, Science and Technology of Japan from FY 2001 to 2005. ITBL was designed to have security network and a great variety of computers available in the ITBL Grid. The time to solution of linear equation solver strongly depends on the type of problem, the selected algorithm, its implementation and the target computer architecture. Thus we believe that extending the variety of computer architectures by Grid middleware interoperability between Diet and ITBL has a beneficial impact to the expert system.

In figure 1, illustration of interoperable system was shown. In the figure, SeD, MA and LA are Sever Daemon, master agent and local agent respectively. All of them are part of DIET program. MA and LA are the program which are employed to determine the computer which provides the best throughput in the DIET system and SeD is the program, which is usually numerical simulation code, made with DIET library. In the current interoperable system, we developed special SeD which can invoke the program installed in the ITBL system and get the result.

In the current literature, we introduced the prototype of interoperable system between ITBL and DIET, which enables international sparse linear algebra expert system. Thanks to the system, we could launch the sparse linear solver installed on the ITBL system from TLSE and then we could enlarge the number of solvers of TLSE [3].

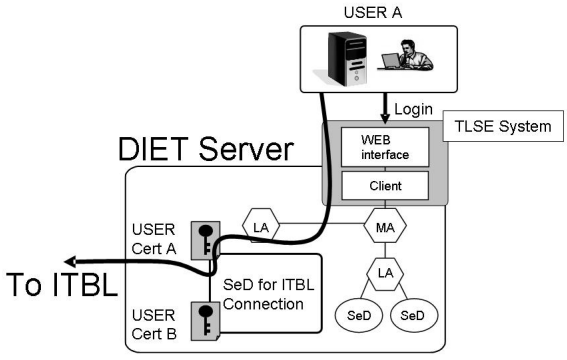

Fig 1: Illustration of interoperable system

References

[1] PREDIMPS web site. URL: http://www.redimps.org

[2] P. Amestoy, M. Dayd´e, C. Hamerling, M. Pantel, C. Puglisi, VECPAR’06 - Workshop on Computational Grids and Clusters (WCGC 2006), Rio de Janeiro, Br´esil, Springer-Verlag, LNCS 4395,(2006), 634–643.

[3] N. Kushida, Y. Suzuki, N. Teshima, N. Nakajima, Y. Caniou and M. Dayde, the Proceedings of 8th International Meeting High Performance Computing for Computational Science (24-27 June 2008, Toulouse, France) CD-ROM (2008).

1.1.2 Interoperability with Other Grids toward International Grid Environment

Developemnt of ITBL-UNICORE Grid interoperable system

Noriyuki Kushida, Yoshio Suzuki, Naoya Teshima, and Norihiro Nakajima

The Grid environment is the infrastructure in order to integrate computational resources, human resources or the other informational resources, which are distributed on the geographically distributed area. The ultimate goal of researchers of the Grid is achieving seamless sharing of the resources which are on the global. In order to achieve the global sharing of resources, several Grid project have been launched and several Grid middle-ware have been developed. Although every Grid project has been aiming to achieve the cooperation of computers on the global, each Grid middle-ware has lost the compatibility with each other, since each Grid middle-ware has been developed by each research group with their own policy. In order to resolve such problem, standardization is rapidly promoted[1], however, modification is required to the Grid-middleware in order to follow the standard, and it should be the overload to the administrator of Grids. Therefore, in this study, we develop the Grid interoperable system which realizes the cooperation of Grids without the halt of currently-operating Grid system and we apply interoperable system between ITBL and UNICORE.

In our interoperable system, following two aspects were additionally focused on other than achieving the interoperability:

- Primitive computational resource handling commands, e.g. file management, information collection of computer resources, or computational job management, should be performed without knowledge of each computer for the easy use.
- User certificate file should not be set any computers except user's computer.

Elaborate descriptions were introduced in the following. For the former aspect: In the present study, we formed the intent to implement the most primitive resource handling commands as the first step, since the others could make up with these primitive ones. For the latter aspect: In order to make the access to a Grid, we must identify the user using user certificate. One resolution to achieve identification is that one set the user certificate on the server and exhibits it when it is required. However, setting the certificate on the interoperable server is not acceptable because of the security reason: When the interoperable server is cracked, the entire system of Grid can be at the risk of cracking. Therefore, we employ the proxy certificate whose period of validity is enough shorter than the original, but the other functional is equivalent to the original one.

By considering all features described here, we designed the interoperable system. Our interoperable system consists with interoperable server which receives and passes the request of commands from one to another with translation. In figure 1, the behavior of the interoperable system in the case of the request of ITBL user to UNICORE is shown. Yellow boxes which include Arabic number with brackets mean the procedure of interoperable system. Thanks to the interoperable system, the user who tries to use UNICORE only need to login and issue commands to ITBL as shown in the figure.

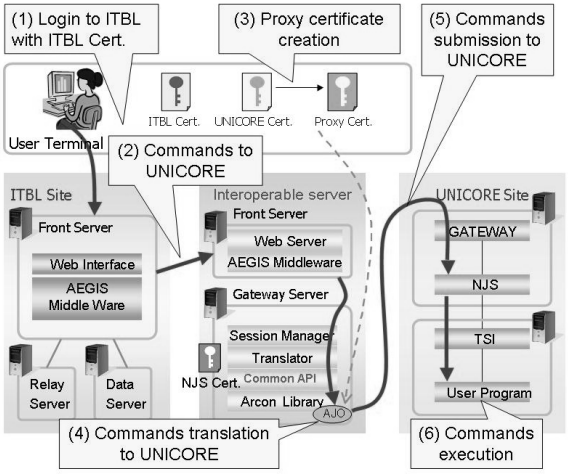

Fig. 1: Illustration of interoperable system

In this study, we developed the interoperable system which provides the cooperation of Grids. Thanks to the interoperable system, interoperation of ITBL and UNICORE was realized without any modification to both Grid middle-wares. This system can easily extend to the other Grid middle-wares and therefore enable global Grid system.

References

[1] B. Raluca et. al., http://www.abdn.ac.uk/~cms152/

[2] N. Kushida, Y. Suzuki, T. Aoyagi and N. Nakajima, FUJITSU Family Association FY2007 (2008) in Japanese.

[3] N. Kushida, Y. Suzuki, T. Minami, T. Aoyagi, N. Nakajima, NEC C&C Systems Users Association (2007) in Japanese.

1.1.3 Data Processing System for Validation & Verification of Simulation Results

Development of Cognitive methodology based Data Analysis System for Large Scale Data

Chikai Kino, Noriyuki Kushida, Yoshio Suzuki and Norihiro Nakajima

We have been developing Cognitive methodology based Data Analysis System (CDAS) [1-2]. At present, researchers of nuclear engineering fields must analyze ever-larger amounts of data because measuring equipments have higher performance, and techniques of computer and network are significantly advanced. The objective of the present study is the development of Data Analysis System which supports researchers to evaluate and judge numerical simulation results in data analysis processes.

Figure 1 shows a system configuration of CDAS. CDAS consists of three functions, namely Synthesis function, Verification & Validation function, and Data Diagnosis function. Synthesis function is has following abilities; namely cognizance ability of necessary information for data analysis and interpretation of findings from VV&DD functions.

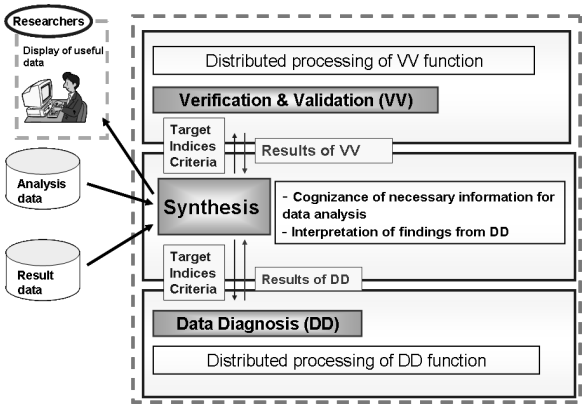

Fig. 1: System Configuration

To draw a conclusion, researchers must evaluate the reliability by validation and verification, because modeling or solutions always include some assumptions and approximations [3]. Additionally result data includes some scientific knowledge, so researchers must diagnosis the data and discover the scientific characteristic from reliable data. Finally, researchers try to draw a conclusion from reliable and meaningful information by consideration.

As an example of VV functions, estimation of mesh dependency by ZZ-method was implemented. This method uses error energy norm as index. In this study, CDAS verifies by combining Winslow method and SPR as evaluation of error energy norm.

Additionally, we adopted neural network using back propagation in order to evaluate and judge whether stress distributions are meaningful or not as DD functions. Stress concentration can be defined as stress distributions with a peak. That indicates a quadratic curve which is convex upward. So, the neural network is set to find such quadratic curve.

We have developed the function which makes computers process simple operations such as extraction of cross-section. It has been realized to process pattern recognition in a parallel and distributed manner and to reduce data transfer time in a few seconds, by using AEGIS.

We adopted the system to the seismic analysis [4]. The amount of data reaches to at least 1TB. Figure 2 shows that the system equipped with the functions enables to extract the reliable and meaningful stress concentration from large scale data reaching to 1TB. We have succeeded to reduce exertions and times to analyze data output from the seismic analysis and contributed to analyze data.

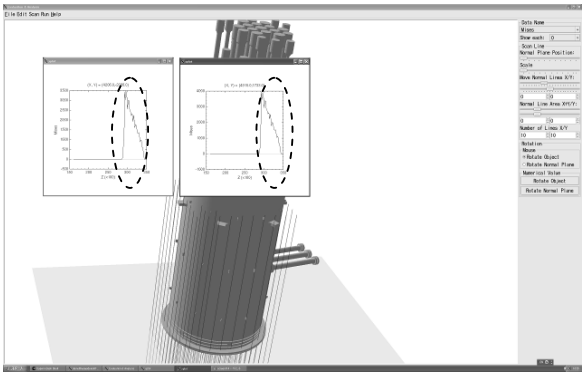

Fig. 2: Display of the results from CDAS

References

[1] C. Kino, N. Kushida, Y. Suzuki and N. Nakajima, International Conference for High Performance Computing, Networking, Storage and Analysis (SC07) Analytics Challenge Finalist (2007)

[2] C. Kino, Y. Suzuki, N. Kushida, A. Nishida, S. Hayashi and N. Nakajima, High Performance Computing on Vector Systems 2008, Springer-Verlag Berlin Heidelberg, pp.89-97 (2008)

[3] P. J., Roache, hermosa (1998)

[4] N. Nakajima, H. Matsubara, T. Minami, et al., SC05 HPC Analytic Challenge (2005).

1.1.3 Data Processing System for Validation & Verification of Simulation Results

Concept Design of Cognitive methodology based Data Analysis System

Chiaki Kino, Yoshio Suzuki, Akemi Nishida, Noriyuki Kushida, Sachiko Hayashi and Norihiro Nakajima

When the scale of data output from numerical simulation is extended larger and larger, a technical difficulty rises to analyze the calculated data due to limitation of human recognition ability. So, it is difficult for researchers to understand whether the data has enough accuracy, or whether the data includes a meaningful point like a stress concentration or a crack. Therefore, researchers need a system which enables efficient data analysis by informational technology to treat large and complex data without oversight or misunderstanding.

To meet these needs, various data analysis systems which equip informational technologies capable of human recognition ability have been developing in these days (for example). These almost systems are designed on the assumption that the systems target a specific problem. Generally, data analysis for numerical simulation need target various problems depending on researcher's aspect or objectives of the simulation and so on. It is difficult for the systems based on such an assumption to deal with data analysis of numerical simulation.

We have been developing Cognitive methodology based Data Analysis System (CDAS) [1]. The objective is the development of Data Analysis System with usable informational technologies capable of recognition abilities without targeting a specific problem. Using the information technologies, CDAS supports researchers to evaluate and judge numerical simulation results in data analysis processes. In the present study, the information model for recognition abilities of CDAS has been proposed.

To draw a conclusion from numerical simulation results, researchers must "evaluate" and "judge" the reliability by validation and verification (VV). Additionally the result data includes some scientific knowledge. So, researchers try to discover the scientific characteristic from the result data. In the process, researchers must "evaluate" and "judge" meaningfulness of the result data. We call this process Data Diagnosis (DD). Finally, researchers draw a conclusion from reliable and meaningful information by consideration.

For VV & DD functions, we need Evaluation & Judgment of reliability and meaningfulness by a system. To actualize Evaluation & Judgment by a system, we proposed the information model using Engineering Information and Aspect Information.

[Engineering Information]

Engineering Information is categorized into 3 groups, namely design data, analysis data and result data. Design data is information obtained by numerical conversion of modeling, such as kinds of components, shape of components or material information. Analysis data is information set to obtain numerical solution, such as mesh size, mesh shape or boundary conditions. Result data is information output data from numerical simulator.

[Aspect Information]

To actualize VV & DD functions, we need evaluate analysis targets by using the indices and criteria for judgment. As analysis targets, we can take various regions, components, parameter, time series data and so on. Additionally, we must use multiple evaluation indices and judgment criteria in order to analyze comprehensively without any bias. So, CDAS needs deal with the hierarchic structure of Analysis target, Evaluation index and Judgment criteria.

Analysis target, Evaluation index and Judgment criteria are arranged on Aspect information (See table1). From aspect of breaking, stress distribution of stand pipe as Analysis target, maximum value of stress and shape of stress distribution as Evaluation index and yield stress and convex upward as Judgment criteria are arranged. This information is input from an interface by user. CDAS can carry out VV and DD by using Aspect information.

Tab. 1: Examples of Aspect Information

Aspect	Analysis Target	Evaluation Index	Judgment Criteria
Breaking	Stress distribution of Stand pipe	Maximum Value of stress distribution	Yield stress
		Shape of stress distribution	Convex upward
Fatigue Crack	Strain distribution of Pressure vessel	Average value of stress distribution	Strain range
	Stress distribution of Pressure vessel	Maximum Value of stress distribution	Yield stress

References

[1] C. Kino, Y. Suzuki, A. Nishida, N. Kushida, S. Hayashi and N. Nakajima, Transactions of JSCES, Paper No.20080018 pp.1-8 (2008) (Japanese).

1.1.3 Data Processing System for Validation & Verification of Simulation Results

Cerebral Methodology Based Computing for Estimating Validity of Simulation Results

Yoshio Suzuki, Akemi Nishida, Tomonori Yamada, Fumimasa Araya, Sachiko Hayashi, Norihiro Nakajima, and Toshio Hirayama

Our challenge is to estimate the validity of simulation results by establishing “Cerebral Methodology Based Computing (CMC)”. The estimation of the validity is indispensable to accurately predict phenomena by using simulation. It is difficult to estimate the validity from a single simulation because the simulation contains uncertainties and ambiguities. We have proposed CMC as the computing methodology which enables us to estimate the validity of results with both deductive and inductive approaches, similar to the human thinking process. To realize CMC, we have constructed the system which enables us to execute both deductive simulations and inductive simulations, and then combine results of those simulations in an integration process. We have applied the system to a thermal displacement analysis of a nuclear power plant and confirmed the usefulness of the system.

The estimation of validity of simulation results is indispensable to accurately predict phenomena by using simulation. So far, the simulation has successfully contributed to reveal various mechanisms of phenomena in various fields of physics, chemistry, biology, and so on. The simulation has also successfully predicted phenomena in some of those fields. However, in some other fields such as the nuclear field, the simulation has only been used to complement results obtained from experiments and/or theories and has not had complete trust by itself. One of the most essential problems is how to estimate the validity of simulation results.

It is difficult to estimate the validity from a single simulation because the simulation includes uncertainties and ambiguities. Uncertainties arise from the calculation processing such as computational error. The computational error includes the rounding error, the truncation error, the loss of information, cancellation. Ambiguities arise from projection of the real space to the computational space. Ambiguities include variety of model constructions, condition selection, equation approximations, and the combination of these items. The extraction of simulation region, the mesh division, and the shape simplification are carried out to construct the simulation model. The boundary condition, the initial condition, and the convergence condition are defined to prepare the simulation condition. Ordering of equations and generation of differential equations are used to approximate equations.

We have proposed CMC as the computing methodology which enables us to estimate the validity of results with both deductive and inductive approaches, similar to the human thinking process. So far, it has been usual that only a few methods are used to confirm the validity of simulation results. For example, researchers execute sequentially a few simulation cases with different resolutions and/or different accuracies. Although such the execution is useful to confirm the validity of simulation results to some extent, it is not always enough to estimate the validity. The human being has thought out the deductive and inductive methods as a more correct thinking process to find a more correct answer. A more correct answer can be obtained by integratedly using those methods. Our idea is to project the human thinking process to grid computers in a parallel and distributed manner. To realize CMC, we have proposed the system which enables us to execute both deductive simulations with neural network, knowledge processing and so on and inductive simulations with scale-model calculations and to estimate a probability of validity by combining results of those simulations.

We have applied the system to a thermal displacement analysis of a nuclear power plant. It is indispensable to estimate the validity of simulation results in nuclear field to improve the safety and security of a nuclear power plant. As a result, the difference between results of deductive and inductive simulations is shown by graphs and the estimation of validity is shown by the natural language expression.

We have provided the CMC to estimate the validity of simulation results. We have constructed the system by implementing a deductive simulation function, an inductive simulation function, and a combination function to provide a probability of validity. We have applied the system to the thermal displacement analysis and confirmed the usefulness of the system.

References

[1] Y. Suzuki, A. Nishida, T. Yamada, F. Araya, S. Hayashi, N. Nakajima and T. Hirayama, SC08 Analytics Challenge Finalist (2008).

1.2 Computational Vibration Science

This is a blank page.

1.2.1 Grid-based Large-scale Assembled Structure Analysis of an Entire Nuclear Plant

A Methodology of Structural Analysis for Nuclear Power Plant Size of Assembly

Masayuki Tani, Norihiro Nakajima, Akemi Nishida, Yoshio Suzuki, Hitoshi Matsubara, Fumimasa Araya, Noriyuki Kushida, Osamu Hazama , Makoto Kondoh and Kozo Kawasaki[1)]

1) O-arai Research and Development Center, JAEA

It is proposed a methodology of structural analysis for nuclear plant size of assembled structures to estimate (1) the behavior by taking account of heterogeneity condition in assembly structures, (2) what could be happened among the connected parts, and (3) the multi dynamic behaviors in assembly. A part of the first approach is introduced in this paper so named FIESTA, Finite Element Structural Analysis for Assembly for structural analysis of nuclear power plant size of assembly. FIESTA is executed on the computers connected with networking in continuous processing space such as grid computing environment to distribute the computational load by giving each part data to distributed parallel computers. The verification was carried out for JAEA (Japan Atomic Energy Agency)'s High Temperature Engineering Test Reactor (HTTR) plant data, which consist of approximately 2000 functional parts. The objected finite element model is 250 million tetrahedrons in 20 GB memory space. The result data was successfully obtained with 2.3TB disk space. The chronicle data are visualized by developing a parallel support toolkit on the grid computing environment.

A methodology of structural analysis for assembly by taking account of heterogeneous condition is to treat the assembly by parts. To solve the complex structure, each part should be analyzed under heterogeneous condition, otherwise, part needs to be solved under each own necessary condition. For connected parts, parts may be connected by fasten bolts, means giving certain loads and constraints, to be solved in assembly. In order to manage heterogeneity condition in assembled structures, the method needs to treat the structure as part by part. The assembly is treated to provide boundary condition data for its parts. By preparing the input data one by one for analysis, and gathering ones, the complex object is easily generated and practically solved in distributed circumstance. FIESTA computes each part data in parallel computing, one by one, on the distributed computers to concerns functionality of part. Each part solved in distributed computers gathers to be assembling as a structure. It is introduced a mesh connection algorithm for different mesh density among parts, since part-wised mesh generation was carried out.

The grid computing environment used in FIESTA's verification is so-named AEGIS, Atomic Energy Grid Infrastructure, which was based on ITBL, Information Technology Based Laboratory conducted by MEXT, Ministry of Education, Cultures, Sports, Science and Technology of Japan as one of the national project, e-Japan. The reason why ITBL was ready to operated at the start of the project is that ITBL's grid computing functions were utilized the STA, Seamless Thinking Aid. AEGIS is a grid computing environment of JAEA, which connects super computers located in multiple sites, such as Altix3700 by SGI, PrimePower by Fujitsu, SX-6 by NEC, pS-690 by IBM, SR8000 by Hitachi, and so on.

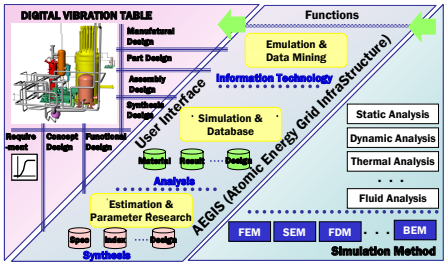

Fig. 1: Design by ASA (Assembled Structure Analysis System)

A concept of Assemble Structural Analysis (ASA) is introduced to the digital vibration table for nuclear power plant as a part of digital space science and engineering. As one of a methodology of ASA to analyze assembly structure, Finite Element Structural Analysis for Assembly (FIESTA) is proposed to analyze the structural behavior of nuclear power plant. The methodology of FIESTA has introduced the way it implements and it demonstrated with numerical experiments to function. FIESTA proved the part connection computing can be calculated with same accuracy as finite element analysis for uniform structure. FIESTA proceeds on grid computing environment, AEGIS, and gave a requirement to improve its efficiency.

References

[1] M. Tani, N. Nakajima, A. Nishida, Y. Suzuki, H. Matsubara, F. Araya, N. Kushida, O. Hazama , M. Kondoh, and K.Kawasaki, Joint International Topical Meeting on Mathematics & Computation and Supercomputing in Nuclear Applications (M&C + SNA 2007) (15-19 April 2007, Monterey, California, U.S.A.) CD-ROM (2007).

1.2.1 Grid-based Large-scale Assembled Structure Analysis of an Entire Nuclear Plant

Application and accuracy of basis functions implementated in a patch-by-patch approximation of mixed-type finite element

Hitoshi Matsubara and Genki Yagawa

With the finite element method, each process, such as defining geometrical shapes, physical fields, setting material properties and assigning boundary conditions, is done on an element-wise basis, in which the meshing is the most important and time consuming process among others. For example, it is well known that the aspect ratio of the element plays the especially important role with respect to approximation accuracy. Required is a robust mesh-generation technology that does not deteriorate this ratio.

On the other hand, the adaptive finite element method is developed to overcome the mesh dependencies problem in the finite element method by evaluating the error norms at the post-processing, which improves the geometrical state of elements with a large error norm. In order to calculate the error norms, Zienkiewicz and Zhu employed the localized least squares method on the stress or strain values of local patch, which is so called patch-by-patch approximation. By the smoothing effects based on the least squares method, this method has successfully achieved more accurate solutions than those of the original finite element method.

In this research, to acquire a highly accurate solution in main-processing, we have proposed the patch-by-patch approximation of mixed-type finite element. In this approximation, not only a displacement field for each element but also stress and strain fields for each patch are defined as shown in Fig. 1. In order to determine unknown parameters of stress and strain fields of a patch, the Hu-Washizu principle is employed.

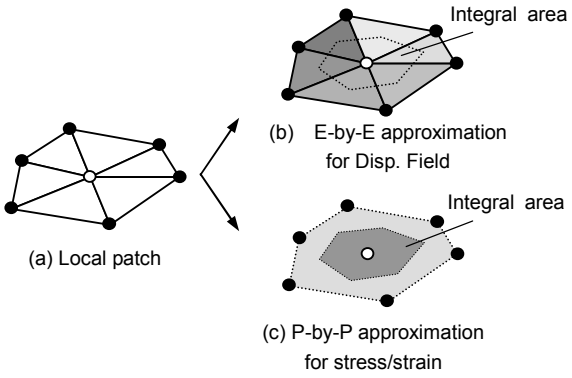

Fig. 1: Concept of patch-by-patch approximation

To show the effectiveness of this approximation in the singular field analyses, the singular stress field is implemented as a basis function. The numerical model is illustrated in Fig. 2 for the problem of a plate with a slanted center crack under uniform tension. The stress intensity factors, KI and KII are obtained for various crack angles. Fig. 3 shows the stress intensity factors KI and KII, respectively, versus the angle of the crack. For the sake of comparison, the extrapolated stress intensity factors by the least-squares method based on the linear finite element method are shown. It is seen from the figure that KI and KII values of the proposed method are much closer to the theoretical ones than those of the linear finite element method.

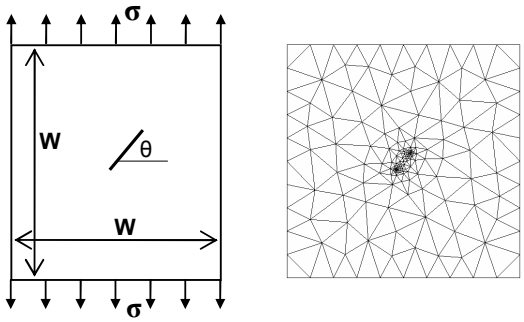

(a) Condition (b) Mesh

Fig. 2: Square plate with a slanted crack

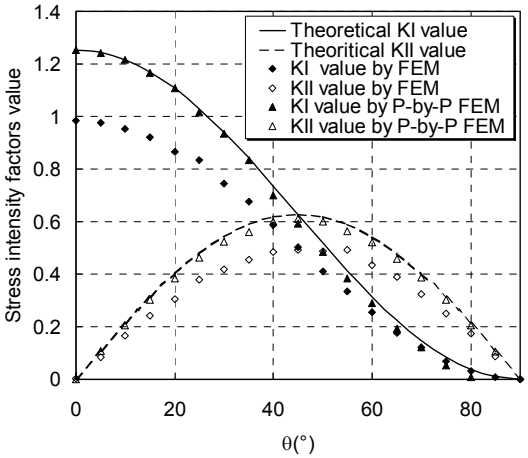

Fig. 3: Comparison of stress intensity factors

References

[1] H. Matsubara and G. Yagawa, Journal of Applied mechnics, JSCE, Vol.10 (2007).

1.2.1 Grid-based Large-scale Assembled Structure Analysis of an Entire Nuclear Plant

Development and Application Research of Vibration Simulator for Full-scale Nuclear Power Station

Akemi Nishida, Fumimasa Araya, Tomonori Yamada, Noriyuki Kushida, Hitoshi Matsubara, Osamu Hazama, Hiroshi Takemiya and Norihiro Nakajima

1. Overview of Research

We report a so-called three-dimensional nuclear power station simulator that can be used to study the structural behavior of a plant, evaluate its soundness, and perform structural and dynamic analyses under the influence of an earthquake. An actual nuclear power station can be simulated by using information about its structure and its components such as pipes, containers and so on. The investigation proceeds by applying it against the evaluation of the conservativeness of conventional response analyses based on spring-mass models and the probabilistic fragility evaluation in a seismic Probabilistic Safety Assessment (PSA), to determine if the suggested methodology can contribute toward an improvement in the operational safety of a nuclear power stations. In order to do so, we start to develop the simulator to be able to compare the results with the conventional response analysis results and the observed data. The suggested methodology may be utilized in Probabilistic Risk Assessment/ Quantitative Risk Assessment (PRA/QRA) in the future.

2. Research Details

2.1. Objective of Research

An amendment to the “Regulatory Guide for Reviewing Seismic Design of Nuclear Power Reactor Facilities” of the National Safety Commission (NSC) has led to great emphasis being placed on the verification of listed risks, that is, the risks introduced by seismic excitations exceeding the basic design earthquake ground motion. Although the acceleration values produced by the Niigata-ken Chuetsu-oki Earthquake of 2007 significantly exceeded the design basis levels for a very wide range of frequencies, the resulting damage was limited, and it was confirmed that the designed nuclear facilities according to the present regulatory guide had enough strength margin . The NSC has requested institutions to perform quantitative assessments of the seismic designs of nuclear power stations on an urgent basis. However, since there clearly are limitations to the actual scale on which such assessments can be made, JAEA began developing a vibration simulator for a full-scale nuclear power station, i.e., a three-dimensional nuclear power station simulator based on computational science technologies in order to study the structural behavior of a plant and to evaluate its soundness. The vibration simulator simulates an actual plant system in a computing environment by using three-dimensional data about the actual structure and components of the plant. It is expected that this technique can be used for both of the evaluation of the conservativeness of conventional response analyses and the probabilistic fragility evaluation in a seismic PSA.

2.3. Outcome of Research (Expected outcome)

The numerical capability of the simulator has already been confirmed; presently, the accuracy of the dynamic response results is being investigated by means of a comparison with the recorded data of an actual plant system. The simulator will be further developed so as to demonstrate the dynamic response calculation capability by continuing the investigation on the accuracy of the dynamic response results.

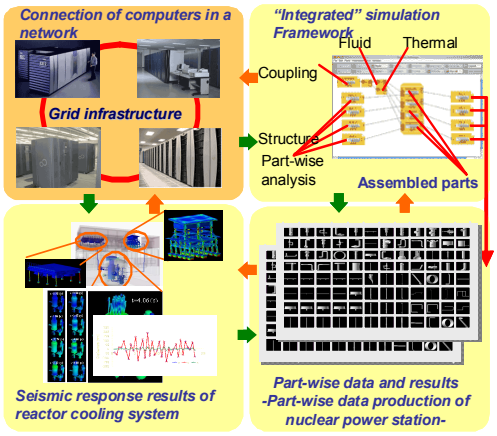

Fig. 1: Concept of vibration simulator for full-scale nuclear power station

References

[1] A. Nishida, F. Araya, T. Yamada, N. Kushida, H. Takemiya and N. Nakajima, Additional Materials of Nuclear Safety Research Forum 2009, pp.25-29 (2009).

[2] A. Nishida, F. Araya, H. Matsubara, O. Hazama and N. Nakajima, Additional Materials of Nuclear Safety Research Forum 2008, pp.93-97 (2008).

1.2.1 Grid-based Large-scale Assembled Structure Analysis of an Entire Nuclear Plant

Proposal of Vibration Table in an Extended World by Grid Computing Technology for Assembled Structures

Tomonori Yamada, Fumimasa Araya, Akemi Nishida, Noriyuki Kushida and Norihiro Nakajima

We realize a vibration table in an extended world for simulation, which is capable of emulating the real world's earthquake in digital space and brings concurrent experiments between real and digital one. There is currently a lack of methodologies and technologies for simulating huge and complex structures such as a nuclear facility. In this paper, the purposes for reproducing facilities in an extended world are clearly summarized through analysis of assembled structures, as well as introduction of the computing framework used. The first attempt at analyzing an assembly was accomplished by structural finite element analysis and by integrating the components of an actual facility. Since the assembly analysis necessitates a massive computational cost, a grid computing environment was applied to the computational resources.

The idea of virtual reality or virtual facilities has been proposed previously; however, its realization has been restricted because of the limited computer resources that are available. The proposal of using the 3D vibration table in an extended world has also been limited in terms of its analysis capability and the maximum number of degrees of freedom to analyze. JAEA overcame this limitation by using Atomic Energy Grid Infrastructure (AEGIS), which is a grid computing environment. AEGIS is an effective grid computing technology succeeding IT-Based Laboratory (ITBL), which was developed in a national project as part of the e-Japan Priority Policy Program, which aimed to establish a environment for conducting research in an extended world using computer resources connected by high-speed networks. ITBL integrated computer resources owned by various research institutions and universities in Japan having a combined computing power of approximately 73Tera FLOPS. These grid computing activities have been conducted by JAEA since 1995 in an effort to acquire the huge computer resources required for the field of nuclear engineering. The research and development conducted for AEGIS aims to establish predictable engineering and science to guarantee the safety of atomic energy and to foster synchronicity of computer-aided engineering and computer science. In addition, some international cooperative operations have been conducted between AEGIS and other grid middleware such as UNICORE (HLRS, Stuttgart University, Germany) and DIET (IRIT, France) to foster international cooperation in the development of atomic energy.

The purposes for developing the 3D vibration table in an extended world are summarized as follows:

1) Monitoring appropriate conditions (stress, displacement, acceleration and so on) for each component in an entire facility by a large scale structural analysis

2) Clarifying simulation conditions, such as the boundary conditions, to enable detailed component-wise analysis based on the results of assembly analysis

3) Evaluating the integrity of an assembly, including independent and/or locally connected components

In this study [1], in order to validate the computational framework and as a first step towards realizing the 3D vibration table in an extended world for an actual nuclear power plant, we focus on simulating the major components in the test reactor (see Fig.1). Our finite element analysis code can construct a finite element model for an entire nuclear power plant by meshing each component independently and bonding inconsistent meshes together. This strategy can drastically reduce the modeling cost compared to meshing the entire model at once, although an effective meshing procedure still needs to be investigated. Assembly analysis using the finite element method was confirmed to be capable of analyzing a huge and complex facility.

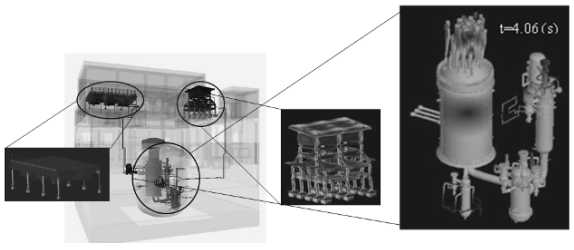

Fig. 1: An assembled simulation result of test reactor

References

[1] Tomonori Yamada, Fumimasa Araya, Akemi Nishida, Noriyuki Kushida, and Norihiro Nakajima, Theoretical and Applied Mechanics Japan, Vol.57, pp.81-87 (2009).

1.2.2 Vibration Analysis Technology to Handle a Different Wavelength

Effect of Timoshenko Coefficient in Wave Propagation Analysis of a Three-Dimensional Frame Structure

Akemi Nishida

It is necessary to perform maintenance management experiments and aging inspection experiments under real conditions for the highly reliable inspection of the safety and conservation of nuclear plants. However, it actually requires a long time with enormous costs. Therefore, at our center, a trial investigation was recently performed on the secure and effective integrity evaluation of nuclear plants using computer science technology. In the first step of this trial, a three-dimensional vibration simulation system of the entire scale of the nuclear plant, which cannot be vibrated on a real shaking table, is researched and developed. As one of the technology components, the physical modeling for the simulation of vibration energy that propagates between the enormous parts of nuclear plants is performed for frame structures such as piping system.

Recently, an analytical method that uses Fourier transformation and the finite element method have been used to estimate the natural frequencies and wave propagation properties of the beam structure. This method is called the spectral finite element method (SFEM) or spectral element method (SEM), etc.; this method has a great advantage that can compute wave propagation phenomenon of structures. Also it has an advantage of computational speed with regard to its ability to use the FFT algorithm. In this paper, we are planning to use SFEM for analysis of piping structures in a nuclear plant.

In order to treat a bending deformation in vibration analysis of a beam, the Bernoulli-Euler theory or the Timoshenko theory is generally used. The Bernoulli-Euler theory is frequently used for the vibration analysis of a beam in the low-frequency domain such as that in earthquakes. However, the Timoshenko theory is widely used for the mechanical vibration analysis or collision analysis of facilities and machinery for obtaining a comparatively good approximation in the high-frequency domain. Therefore we introduced the Timoshenko theory for SFEM. The Timoshenko coefficient is introduced by taking account of the interactions between the bending and the shear deformations in the Timoshenko theory. This coefficient is calculated by the shear deformation distribution in a section that is generated by the bending deformation of the beam. The shear deformation distribution in a section must be calculated on the basis of plausible assumption. Various assumptions or theories have been suggested to date. The theory by Cowper introduces the least assumptions in computing the Timoshenko coefficient and is widely used. It is said that the assumption is good for the problem of static loading. However, the references that discussed for the problem of dynamic loading, especially wave propagation problem, are very few as far as we examined. Therefore, the theory by Cowper is reexamined in this study to introduce in SFEM for analysis of three-dimensional piping structure in the view point of dynamic behavior. The examination of the influence of the dispersion characteristics of the phase velocity of the beam and the investigation of the sectional stress distribution by the Timoshenko coefficient are shown in this paper. Some numerical simulations by using the Timoshenko coefficient obtained by Cowper's theory are shown and the effects of the Timoshenko coefficient are considered.

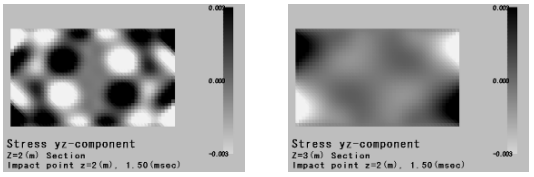

(a) Point A (b) Point B

Fig. 1: Shear stress distribution by the FDTD method (Point A is an impact point. Point B is one meter a part from the impact point.)

It was shown that the convergence value of the phase velocity at high frequency, i.e. short wave length limit, is influenced by Timoshenko coefficient. This effect could not be ignored in the accurate evaluation of wave propagation or vibration. In addition, it was shown that Cowper's formula was effective for the evaluation of the Timoshenko coefficient until reflection waves reached by showing the shear stress distribution in a cross section. As an example, the wave propagation phenomenon and shear stress distribution were analyzed by numerical simulations for an example of the piping system, and it was able to be a pre-examination for the analysis of the wave propagation phenomenon in a real complex piping system, which will be analyzed in the near future.

References

[1] A. Nishida, Theoretical and Applied Mechanics Japan, Vol,56, pp.57-65 (2007).

1.2.2 Vibration Analysis Technology to Handle a Different Wavelength

A Large Scale Simulation for Impact and Blast Loading Issues

Norihiro Nakajima, Fumimasa Araya, Akemi Nishida, Yoshio Suzuki, Masato Ida, Tomonori Yamada, Noriyuki Kushida, Guehee Kim, Chiaki Kino and Hiroshi Takemiya

Japan is so said an energy consumption country of the fourth place world, but the energy resources such as petroleum, the natural gas are poor and depend on import for the most, and stable supply becomes a big problem. For the greenhouse gas restraint, the promotion of the energy saving is featured. A nuclear power plant for commerce in Japan has been started in 1966. The supply occupies about 30% of the now Japanese electricity generating. Due to the nature of Japan, earthquake proof is an important subject for social infrastructure operation. To encourage its proofing, many approaches have been applied into many infrastructures, not only computational approach. A computational science approach for earthquake proof is suggested with FIESTA (Finite Element Structural analysis for Assembly), a large scale simulation. A methodology is discussed from the point of view of impact and blast loadings. Examples of loadings in the nuclear engineering are introduced.

For stable electricity supply, and for the saving of fossil fuel resources, such as petroleum and coal, the nuclear power generation is contributing and playing a big role in an anti-warming measure as the electricity generating system that does not drain CO2.

Japan Atomic Energy Agency, JAEA has mission to carry out long-term energy security countermeasures to environmental problems and to create advanced science and technology with competitive edges, emphasizing in the field of nuclear fuel cycles, nuclear fusion energy, hydrogen economy by nuclear process heat, and quantum beam technology. Computational science is a cross-cutting technology in JAEA, and playing very important role as the third generation research methodology besides experimental and theoretical.

To support nuclear power generation for stable electricity supply, one of big issues is the earthquake proofing technology in Japan. Center of Computational Science and E-systems, CCSE is carrying out research and development of a vibration table by the real space simulation with reality modeling for assembly structure.

FIESTA has been practiced in actual plant data and its verification is carrying out by comparing other numerical experiments and observed data. FIESTA is so far validated as a tool for structural analyses.

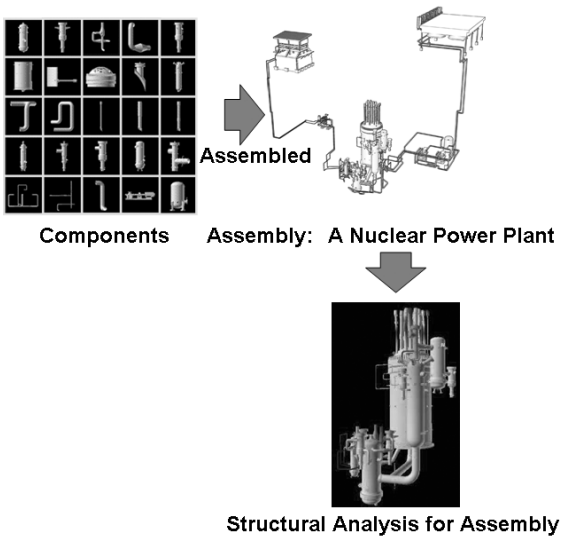

Fig. 1: Nuclei Breaking in Spallation reactions

Impact and blast loadings in nuclear engineering are introduced to treat the higher frequency problem in FIESTA. There is no consolidated solution to manage this issue in FIESTA, but coupling simulation technology was suggested to take into account effects of fluid dynamics.

To support nuclear power generation for stable electricity supply, a large scale simulation technology may help understanding of phenomenon to predict the life time.

References

[1] N. Nakajima, F. Araya, A. Nishida, Y. Suzuki, M. Ida, T. Yamada, N. Kushida, G. Kim, C. Kino and H. Takemiya, Proceedings of International Symposium on Structures under Earthquake, Impact, and Blast Loading 2008(IB08), pp.119-123 (2008).

1.2.2 Vibration Analysis Technology to Handle a Different Wavelength

Impact Analysis of Three-Dimensional Frame Structures -An Application for Piping Structures of a Nuclear Power Plant-

Akemi Nishida

Generally, it is difficult to predict the occurrence of natural disasters such as earthquakes. Therefore, a performance management system that constantly maintains the safety and functionality of structures is imperative, particularly for critical structures like nuclear power plants. In order to realize such a system, it is becoming important to carry out detailed modeling procedures and analyses to better understand the actual phenomena. Such details are important in understanding the phenomena occurring in frame structures such as piping systems, which are considered to be among the weakest and most vulnerable components of nuclear power plants. The aim of our research is to develop detailed analysis tools and to determine the dynamic behavior of piping systems in nuclear power plants, which are complicated assemblages of different parts.

The elastic wave theory has been primarily used to investigate the response of a structure subjected to an impact load in a structural field. The Laplace transformation is generally used to analyze the wave equation, which is expressed by a partial differential equation. However, it is difficult to analytically perform the inverse transformation for the solution in the frequency domain, except in some special cases. Due to this difficulty, many approximate methods have been proposed. On the other hand, Krings et al. modified the equation of the Laplace inverse transformation such that the fast Fourier transformation (FFT) algorithm could be used. Doyle proposed another method that uses Fourier transformation instead of Laplace transformation and showed that the method is applicable to the analysis of structures with multiple degrees of freedom. This analytical method is called the spectral element method or finite spectral element method and has an advantage with regard to its ability to use the FFT algorithm. Nishida et al. extended this method for three-dimensional frame structures including shear and torsional deformation effects. In this paper, a comparison of the Bernoulli–Euler beam theory and Timoshenko beam theory is shown. Next, it is shown that the proposed method is effective to resolve the eigenvalue problem. Finally, a multi-connected structure is analyzed by using this method and the obtained results are compared with the experimental results. Consequently, the applicability of the presented element is shown.

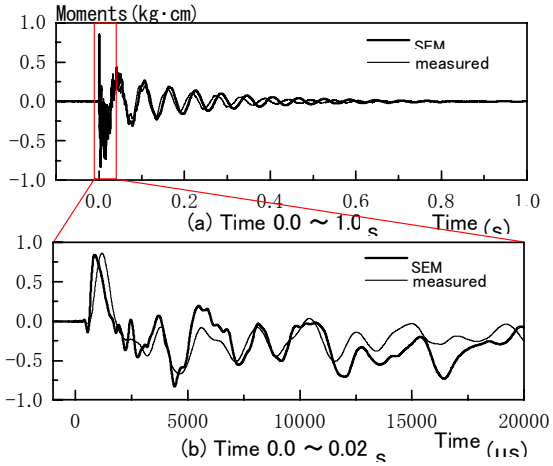

Fig. 1: Moment histories at point No.2

A comparison of the Bernoulli–Euler beam theory and Timoshenko beam theory shows the necessity of the latter in piping structure analyses of nuclear power plants. Further, it is shown that the SEM is effective for resolving the eigenvalue problem in high frequency domain. Finally, the application of the SEM for a multi-connected frame structure was shown and the results were compared with the experimental results. It was found that the spectral element could effectively represent the wave propagation phenomena and that the modeling of the boundary condition was crucial for estimating the phase properties of a multi-connected frame structure. As a topic for future study, we are preparing to conduct the numerical simulation of more complicated piping structures in a nuclear plant system.

References

[1] A. Nishida, Proceedings of International Symposium on Structures under Earthquake, Impact, and Blast Loading 2008(IB08), pp.129-134 (2008)

1.2.3 Thermal Stress Analysis of Double-Wall-Tube Steam Ganerator Tubesheet for FBRs

Transient Thermal Stress Analysis of a Spherically Curved Tubesheet

Osamu Hazama[1)]

1) Presently Itochu Techno-Solutions Corporation

A new concept of double-wall-tube steam generator (SG) is being introduced and investigated as an innovative technology to realize next-generation sodium-cooled Fast Breeder Reactors (FBRs). This new concept is posing great challenges in the engineering design of a tubesheet which must bundle over 7000 double-wall heat transfer tubes under several mechanical and thermal loads. R&D efforts concerning the development of a feasible design for the new concept tubesheet structure have been performed by a cooperation of CCSE with the design group in the O-arai Research and Development Center.

Since there are many cylinder-shaped stubs on the tubesheet, which hold double-wall-tubes, it has complex configuration which results in complex stress distributions in the tubesheet. Also, since an FBR design provides fast and large temperature transients, a large thermal stress in the tubesheet was predicted. Therefore, a rigorous estimation of the location and magnitude of highest stress becomes important in the structural design. In order to realize the estimation, two series of FEM calculations were performed in the transient thermal stress analysis[1][2].

1. Calculations to investigate effects of stub on stress distribution with simple FEM models

To investigate effects of the stub on stress distributions, simple FEM models were used in which one model has no stub on the tubesheet and the others have single stub with different filet radius, R=4 and 7.4 mm. The calculated results showed that the stub can reduce the stress generated on the tubesheet surface as shown in Fig. 1. However, as Fig. 2 shows, larger stresses are arisen on the hole surface inside the stub and the stub has no effect to reduce the surface stress inside the hole.

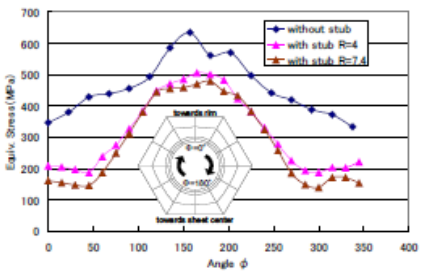

Fig. 1: Equivalent stress distribution in the circumferential distribution of a stub hole and fillet

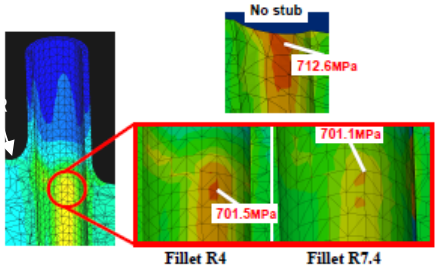

Fig. 2: Equivalent stress distribution on the inner surface of stub hole

2. Calculation to identify location and magnitude of highest stress

In order to identify location and magnitude of the highest stress, large scale FEM calculation was performed on a parallel .super computer. The FEM model presents real configuration with 10M DOF as shown in Fig. 3. The calculated results in Fig. 4 shows the highest stress is arisen on the hole surface of the outermost stub and the magnitude is about 1GPa.

The results shown here were used to optimize the tubesheet configuration so as to minimize the stress.

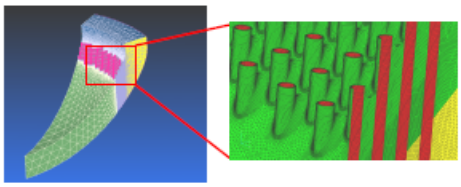

Fig. 3: FEM model for investigating highest stress

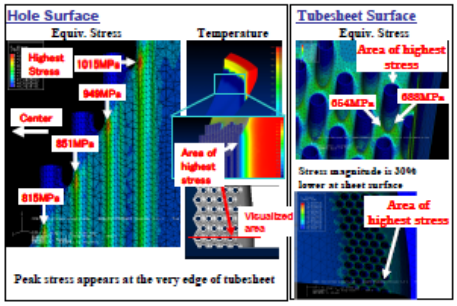

Fig. 4: Temperature and equivalent stress distributions in the vicinity of highest stress area

References

[1] O. Hazama and F. Araya, JSME Annual Conf. 2007, Osaka (2007).

[2] O. Hazama, REDIMPS, Tokyo (2007).

1.3 Computational Fluid Dynamics & Fusion Science

This is a blank page.

1.3.1 Numerical Study of Cavitation Bubbles in Liquid Mercury

Supression of Cavitation Inception by Microbubble Injection

Masato Ida, Takashi Naoe[1)], and Masatoshi Futakawa[1)]

1) J-PARC Center, JAEA

Cavitation in liquid mercury is now a significant issue in the development of pulsed high-power spallation neutron sources, in which liquid mercury is bombarded by a high-intensity proton beam to produce high neutron fluxes. Recent off-beam experiments [1-2] suggested that strong pressure waves originating from the energy release due to spallation reactions should cause cavitation in liquid mercury and the associated damage (i.e., cavitation erosion) will significantly reduce the lifetime of the metal vessel in which liquid mercury flows.

One of the potential approaches to suppress the cavitation is to inject gas microbubbles into liquid mercury [3-5]. From an experiment using an impact test machine, which induces a rapid pressure change in liquid mercury, we found that the injection of a small amount of microbubbles can significantly reduce cavitation erosion [2]. Toward clarifying the underlying mechanism of this observation, we have performed a numerical study [3, 5].

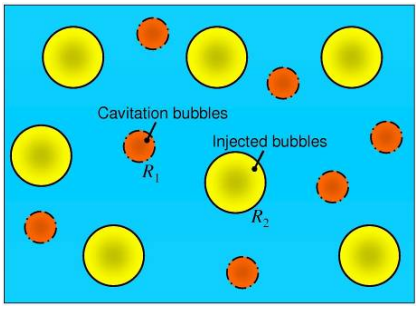

Fig. 1: Settings. A large 3D bubble cluster that consists of cavitation and injected bubbles is considered. Both kinds of bubbles are assumed to be spherical, and bubbles of the same kind are assumed to be identical.

The theoretical model used is based on the coupled Keller-Miksis equations, which govern the radial motion of acoustically coupled bubbles. We extended the model so that the coexistence of different kinds of bubbles (cavitation bubbles and injected gas microbubbles) is allowed and the interaction of a large number of bubbles is considered (Fig. 1). An experimentally observed pressure-time curve is used as the external pressure field which drives the radial motion of bubbles.

Computed expansion ratios (maximum radius / initial radius) of bubbles are shown in Fig. 2. From this it was found that for sufficiently large injected bubbles, cavitation bubbles have a very small expansion ratio, meaning that cavitation inception is suppressed. Also, it can be seen that large injected bubbles have a small expansion ratio, implying that the injected bubbles themselves will not cause remarkable damage.

Carefully examining the numerical results, we found that the suppression of cavitation inception is caused by the positive pressure waves radiated by the injected bubbles: The pressure waves reduce the magnitude of negative pressure in liquid mercury, the driving force of cavitation.

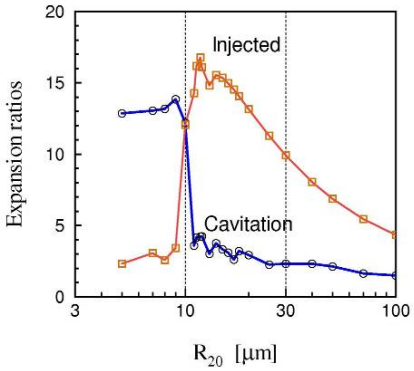

Fig. 2: Computed expansion ratios of bubbles as functions of the equilibrium radius of the injected bubbles (R_{20}). The equilibrium radius of the cavitation bubbles and the mean interbubble distance are assumed to be 10 μm and about 860 μm, respectively.

References

[1] M. Ida, T. Naoe, and M. Futakawa, Physical Review E 75(4), 046304 (2007).

[2] T. Naoe, M. Ida, and M. Futakawa, Nuclear Instruments and Methods in Physics Research Section A 586(3), pp.382-386 (2008).

[3] M. Ida, T. Naoe, and M. Futakawa, Physical Review E 76(4), 046309 (2007).

[4] M. Futakawa, H. Kogawa, S. Hasegawa, T. Naoe, M. Ida, K. Haga, T. Wakui, N. Tanaka, Y. Matsumoto, and Y. Ikeda, Journal of Nuclear Science and Technology 45(10), pp.1041-1048 (2008).

[5] M. Ida, T. Naoe, and M. Futakawa, Nuclear Instruments and Methods in Physics Research Section A 600(2), pp.367-375 (2009).

1.3.1 Numerical Study of Cavitation Bubbles in Liquid Mercury

New Mechanism of Cavitation Noise Generation

Masato Ida

Cavitation noise is a loud acoustic noise emitted by bubbles emerged in a liquid through cavitation phenomena. Cavitation bubbles emit strong pressure pulses when they collapse violently, and the pressure pulses form an acoustic signal, which is measured as a loud noise. Cavitation noise in general contains a broadband signal which seems to consist of positive and negative pressure pulses. However, theoretical models for single bubbles fail to describe negative pressure pulses [1, 2]. How the negative pressure pulses are created is thus still an open question.

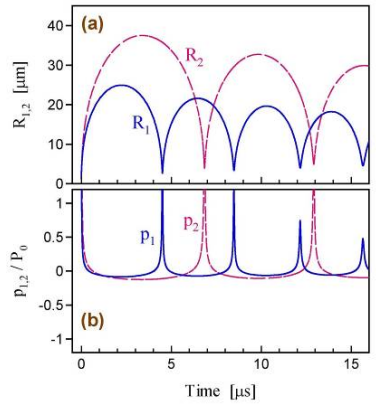

Fig. 1: Bubble radii (a) and bubble-emitted pressures (b) in a single bubble case as functions of time. P_0 is the atmospheric pressure. Only positive pulses are emitted.

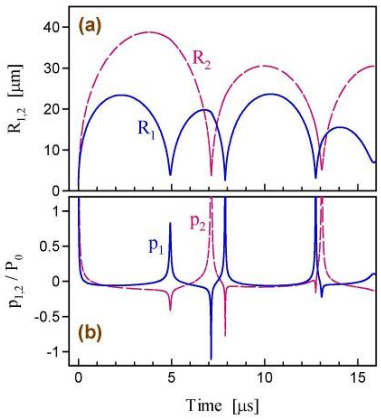

Fig. 2: Same as Fig. 1 but in a double bubble case. Both positive and negative pulses appear.

We hypothesized that the interaction between cavitation bubbles through pressure pulses is a source of the negative pulses [2]. When a number of bubbles exist and undergo volume change, they interact with each other through the pressure waves that they emit. This acoustic interaction of bubbles is known to lead to a variety of phenomena that single bubbles can never cause. We found numerically that the negative pulses are explained by considering the interaction between bubbles through the pressure pulses [2].

Figure 1 shows the radii of two bubbles and the pressures from the bubbles in a single-bubble case (i.e., with an infinite interbubble distance) as functions of time. The theoretical model used is the coupled Keller-Miksis equations [3]. Since the initial radii of the bubbles are set to be smaller than their equilibrium radii, the bubbles first expand and then collapse violently to emit positive pressure pulses. For a finite interbubble distance, the pressures have a clearly different profile. As shown in Fig. 2, not only positive pulses but also negative pulses are emitted when the bubbles interact.

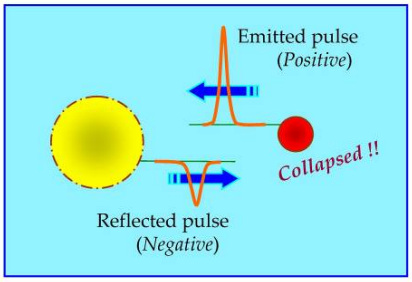

Fig. 3: Noise generation process. Positive pressure pulses emitted by a collapsed bubble (the right sphere) create negative reflected pulses when hitting neighboring bubbles (the left sphere).

The mechanism of negative pulse generation that we proposed is as follows (see also Fig. 3): A bubble emits a strong positive pulse while it collapses. When the positive pulse hit a neighboring bubble, the bubble is impulsively compressed and a strong tension is created in the surrounding liquid. This tension will propagate through the liquid as a reflected pulse whose amplitude is negative. If many bubbles exist, the positive and negative pulses will make up a broadband signal.

References

[1] M. Versluis *et al.*, Science 289(5487), 2114 (2000).
[2] M. Ida, Physical Review E 79(1), 016307 (2009).
[3] M. Ida, T. Naoe, and M. Futakawa, Physical Review E 76(4), 046309 (2007)

1.3.2 Development of Conservative Gyrokinetic Vlasov Simulation

New conservative gyrokinetic full-f Vlasov code and its comparison to gyrokinetic δf particle-in-cell code

Yasuhiro Idomura[1),2)], Masato Ida[2)], Shinji Tokuda[1),2)], Laurent Villard[3)]

1) Naka Fusion Institute, JAEA
2) Center for Computational Science and e-systems, JAEA
3) Ecole Polytechnique Federale de Lausanne, Switzerland

In this work [1-3], we have developed a new conservative gyrokinetic full-f Vlasov code, G5D, using the Morinishi scheme. In the scheme, the skew-symmetric finite difference operator conserves both the $L1$ and $L2$ norms. Numerical properties of the new Vlasov code have been discussed by comparing the results from Ion Temperature Gradient driven (ITG) turbulence simulations with the skew-symmetric operator and with the divergence operator. Here, the latter scheme is equivalent to a finite volume method or a centred finite difference method. The comparison has shown that the former scheme is numerically stable and robust in a long time simulation, while the latter scheme breaks down in the nonlinear phase. The ITG simulation with the skew-symmetric operator shows an exact conservation of the $L1$ norm and an approximate conservation of the $L2$ norm. Here, the small error of the $L2$ norm comes not from the nonlinear convection term but from the time integration scheme. From these results, it has been demonstrated that the conservation of the $L2$ norm is very helpful for avoiding the growth of numerical oscillations. In addition to the conservations of the $L1$ and $L2$ norms, the total energy conservation is confirmed. Although small spurious negative values of f, which violate the definition of the kinetic entropy, are observed, the simulation satisfies the entropy balance relation of the fluctuation entropy, which is much more relevant in dictating the turbulent heat flux.

The new Vlasov code has been successfully benchmarked against a conventional δf Particle-In-Cell (PIC) code, G3D. ITG turbulence simulations with the Vlasov and PIC codes show reasonably good agreement both in the linear and early nonlinear phases. In a long time simulation, the new Vlasov code shows the good total energy conservation as well as the exact particle number conservation, while in the PIC simulation, the particle number is not conserved and the total energy slowly increases due to the numerical heating (see Fig.1). Conservations of the total particle number and the total energy are essential properties for a long time full-f Vlasov simulation with evolving background profiles. The results show that the new conservative gyrokinetic full-f Vlasov code satisfies these requirements. In the present benchmark parameters, the computational cost of the Vlasov simulation is comparable to that of the PIC simulation, although the memory usage of the Vlasov simulation is larger by ~5 times.

The effect of the $v_{\parallel}$ nonlinearity has been clarified both in the Vlasov and PIC simulations. The entropy balance relation shows that the contribution from the $v_{\parallel}$ nonlinearity is physically unimportant. However, comparisons between the simulations with and without the $v_{\parallel}$ nonlinearity have shown that it affects conservation properties numerically. The simulation without the $v_{\parallel}$ nonlinearity produces the error of the particle number in the PIC simulation, while it leads to the error of the $L2$ norm in the Vlasov simulation.

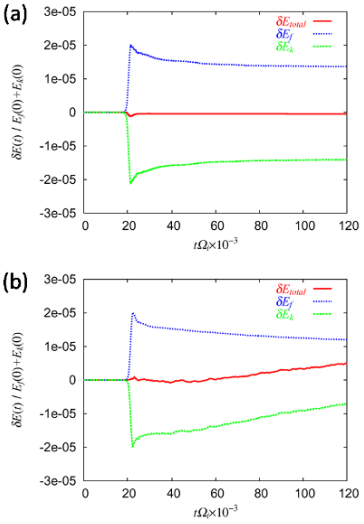

Fig.1 The time histories of the total energy, δE_{total}, the field energy, δE_f, and the kinetic energy, δE_k, observed in ITG turbulence simulations using (a) G5D and (b) G3D. The errors of δE_{total} at $t=120\times10^3\Omega^{-1}$ are ~3% and ~40% of δE_f in G5D and G3D, respectively.

References

[1] Y. Idomura, M. Ida, S. Tokuda, and L. Villard, J. Comput. Phys., 226, 244-262 (2007).

[2] Y. Idomura, M. Ida, and S. Tokuda, Commun. Nonlinear Sci. Numer. Simul. 13, 227-233 (2008).

1.3.2 Development of Conservative Gyrokinetic Vlasov Simulation

Conservative global gyrokinetic toroidal full-f five-dimensional Vlasov simulation

Yasuhiro Idomura[1),2)], Masato Ida[2)], Takuma Kano[2)], Nobuyuki Aiba[1)], Shinji Tokuda[1),2)]

1) Naka Fusion Institute, JAEA

2) Center for Computational Science and e-systems, JAEA

In this work [1], we have developed a new conservative global gyrokinetic toroidal full-f 5D Vlasov code, GT5D, using novel numerical techniques. By using new discrete forms of the Hamiltonian flows, the Non-Dissipative Conservative Finite Difference method is successfully extended for the toroidal gyrokinetic equation in general curvilinear coordinates. The scheme guarantees numerical stability by satisfying relevant first principles, the conservations of two invariants, f, f^2, and the phase space volume. In GT5D, the scheme is implemented in the cylindrical coordinates, and the gyrokinetic equation is solved including the magnetic axis, the separatorix, the X-point, and an open field region either in model circular tokamak configurations or in real MHD equilibrium configurations (see Fig.1). The quasi-neutrality equation with the integral flux-surface average operator is solved using a finite element approximation in the flux coordinates, and two coordinate systems are connected through a new full finite larmor radius operator, which is developed by applying a finite point sampling technique in Particle-In-Cell (PIC) simulations. The Additive Semi-Implicit Runge-Kutta method (ASIRK) is applied to overcome severe Courant-Friedrichs-Lewy conditions in GT5D. In the ASIRK, stiff linear and non-stiff nonlinear operators are decomposed using the Poisson bracket operator and the Hamiltonian, so that both operators keep the above first principles. All these techniques enable robust and accurate simulations of the Ion Temperature Gradient driven (ITG) turbulence with reasonable computational costs.

In order to demonstrate the validity of GT5D, linear and nonlinear benchmark tests have been performed against a global gyrokinetic toroidal δf PIC code, GT3D. Linear zonal flow damping tests and linear ITG benchmark calculations show quantitative agreements between GT3D and GT5D, and it is shown that in simulating the ITG turbulence, GT5D has enough resolutions both in a configuration space and in a velocity space. Nonlinear benchmark tests are performed for the ITG turbulence without sources and collisions, which are not implemented in GT3D. In the present benchmark parameters, the computational cost and memory usage of GT5D are respectively ~5 and ~3 times larger than those of GT3D. As for the numerical accuracy, it is found that GT5D shows exact and approximate conservation of the total particle number and the total energy, respectively, while these quantities monotonically increases in GT3D. The exact particle number conservation is important for long time simulations of the ITG turbulence, because an accumulation of the erroneous particle density produces spurious electric fields, leading to stronger geodesic acoustic mode activities. When particle and grid numbers are large enough, GT3D and GT5D show reasonably good quantitative agreements in the saturated turbulent levels, the radial and poloidal turbulent correlation lengths, the spatio-temporal evolutions of zonal flows, and the quasi-steady temperature gradients. From the benchmark results, a global solution of the ITG turbulence is identified for the first time by using two gyrokinetic codes based on completely different numerical approaches. This solution shows that without sources and collisions, the system is quickly relaxed to an effective marginal state in turbulent time scales. In this state, the system is dominated by steady meso-scale zonal flows, the temperature gradient is slightly below the effective critical gradient given by so-called Dimits shift, and the turbulent transport is almost quenched by residual zonal flows. This is consistent with a collisionless steady solution of the entropy balance relation.

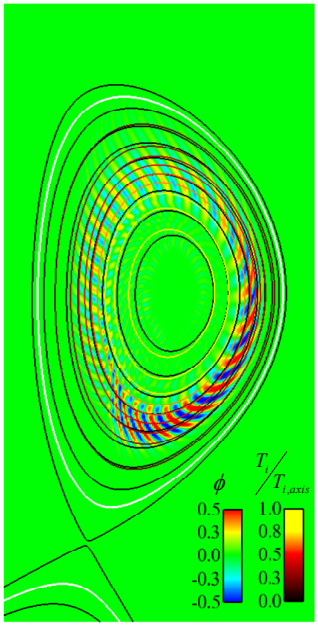

Fig. 1: An eigenfunction of the ITG mode in ITER like configuration of JT60-SA tokamak. The electrostatic potential ϕ is shown by color contour plot. Color solid lines show constant temperature T_i surfaces.

References

[1] Y. Idomura, M. Ida, T. Kano, N. Aiba, and S. Tokuda, Comput. Phys. Commun., 179, 391-403 (2008).

1.3.3 Development of Evaluation Method for Oscillating Interface in Two-phase Flows

Simulation of an oscillating liquid droplet : development of two-phase flow simulation code

Tadashi Watanabe

Simulation system of whole nuclear plant is being developed by CCSE for evaluation of seismic effects on plant components. Development of simulation method for oscillating fluid including two-phase interfaces is one of the important parts for the plant simulation system. Shape oscillation of a liquid droplet has been simulated in the developmental stage of the two-phase flow simulation code. In the nuclear engineering fields, droplets are not only seen in power plants but also used to measure material properties. For instance, properties of molten material are measured by using a levitated droplet, since the effect of container wall is eliminated. Viscosity and surface tension are, respectively, obtained from the damping and the frequency of shape oscillations. Large-amplitude oscillations are desirable from the viewpoint of measurement. However, the relation between material properties and oscillation parameters is based on the linear theory, and small-amplitude oscillations are necessary. Slight rotation is also needed to stabilize the levitated droplet. Numerical simulations of an oscillating liquid droplet were thus performed to study the effects of amplitude and rotation on the oscillation frequency.

Three-dimensional Navier-Stokes equations were solved using the level set method. The level set function, which is the distance function from the droplet surface, was calculated by solving the transport equation. The period and the damping of small-amplitude oscillations were in good agreement with the linear theory. For large amplitude, the oscillation frequency decreased as the amplitude increased as shown in Fig.1. The flow fields around the oscillating droplet were visualized as shown in Fig. 2, and the three-dimensional vortex structures were found to appear. It was also found that the number of vortices was the same as the order of oscillation. As the rotation rate increased, in contrast to the effect of amplitude, the oscillation frequency increased as shown in Fig. 3. Theoretical predictions taking into account small nonlinear effects are also indicated in Figs. 1 and 3. It was found that the frequency shift was overestimated by these theoretical predictions.

Through this study, the two-phase flow simulation code was developed and the level set method was found to simulate oscillating fluid interfaces with sufficient accuracy. This method would be applied for the plant simulation system in the near future.

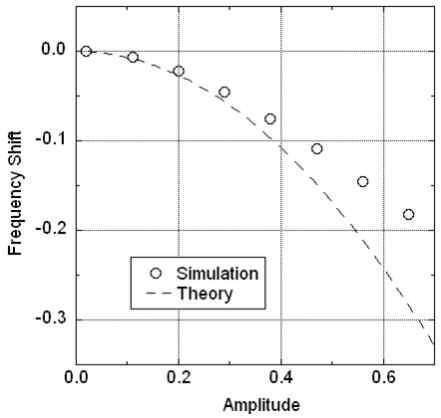

Fig. 1: Effect of amplitude on oscillation frequency.

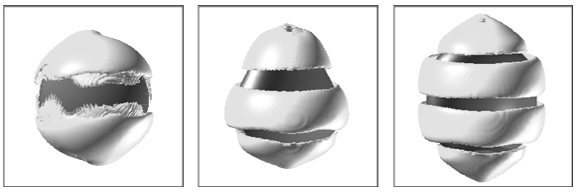

Fig. 2: Vortex structure around the droplet.

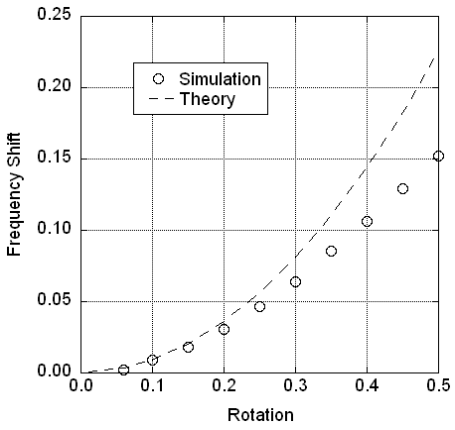

Fig. 3: Effect of rotation on oscillation frequency.

References

[1] T. Watanabe, Computers and Fluids, 37(2008)91-98.

[2] T. Watanabe, Proc. Int. Conf. Parallel CFD, Antalya, Turky, May 21-24 (2007).

1.3.3 Development of Evaluation Method for Oscillating Interface in Two-phase Flows

Efficiency of parallel computations of incompressible two-phase flows : code speed up

Tadashi Watanabe

As described in the previous chapter, the simulation system of whole nuclear plant is being developed by CCSE, and the simulation of two-phase flows is one of the important parts for the plant simulation system. The level set method has been shown to simulate oscillating fluid and interfaces with sufficient accuracy. The plant simulation system is a large-scale computational tool and needs huge amount of computational resources. Numerical efficiency of two-phase flow simulations is thus of importance for the plant simulation system, and the efficiency of the level set method has been studied.

The sample problem was the oscillating droplet shown in the previous chapter, where the three-dimensional incompressible Navier-Stokes equations were solved using the finite difference method. The most time consuming part was to solve the pressure Poisson equation using the Bi-CGSTAB method. The domain decomposition technique was applied and the message passing interface library was used for parallel computations. The schematic of matrix calculation is shown in Fig. 1. Three preconditioners were compared; the point Jacobi (PJ: diagonal part in Fig. 1), the block Jacobi (BJ: solid square), and the overlapping additive Schwarz (AS: dotted square) schemes. The problem size was 96x96x96, and parameters for each preconditioner were determined by sensitivity calculations. The average speed up of parallel calculation is shown in Fig. 2, where the total calculation time is indicated by Elapse, while the time for matrix calculation by Matrix. The speed up of the PJ scheme was larger than that of the BJ and AS schemes, and the BJ scheme was almost the same as the AS scheme as shown in Fig. 2. The data array in each processor became small as the number of processors increased, and the effect of cache became large. The diagonal elements are used as the preconditioner in the PJ scheme, while the block diagonal elements are used in the BJ and AS schemes as shown in Fig. 1. The size of the matrix was thus the smallest for the PJ scheme since the compressed row form was used, and the effect of cache was found to be notable. The relative calculation time using one processor was 1.0, 0.63 and 0.63, respectively, for the PJ, BJ and AS schemes. It was found that the BJ and AS schemes were better when the number of processors was small. It was also shown that the AS scheme was not effective in this problem, since the matrix was sufficiently large and the characteristics of the matrix were not much improved by the overlapping scheme.

The simulation code for incompressible two-phase flows has been developed and parallelized, and the effects of preconditioners were made clear. Sufficient speed up of flow calculations was achieved for the plant simulation system.

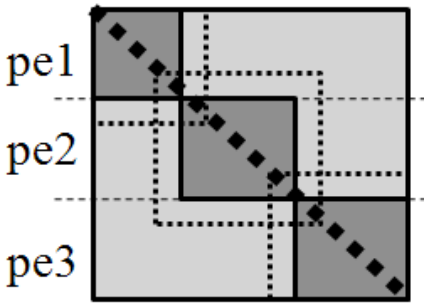

Fig. 1: Schematic of matrix calculation.

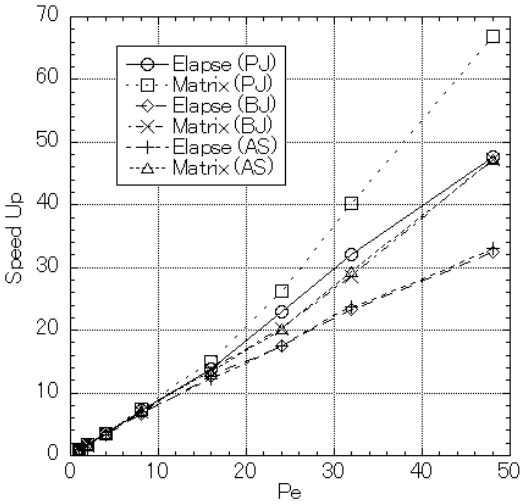

Fig. 2: Speed up with different preconditioners.

References

[1] T. Watanabe, Proc. IASME/WSEAS Int. Conf. Continuum Mech., Cambridge, UK, Feb. 23-25 (2008).

[2] T. Watanabe, Proc. Int. Conf. Parallel CFD, Antalya, Turky, May 21-24 (2007) .

[3] T. Watanabe, WSEAS Trans. Fluid Mech. 2(2008)164-174.

1.3.3 Development of Evaluation Method for Oscillating Interface in Two-phase Flows

Characteristics of a rotating-oscillating liquid droplet : code application 1

Tadashi Watanabe

An oscillating liquid droplet has been simulated, as shown in the previous chapter, as an example problem of two-phase flows for development of the simulation system of whole nuclear plant. The incompressible Navier-Stokes equations were solved together with the transport equations for interfaces, and the level set method was shown to predict droplet dynamics with sufficient accuracy and efficiency. The developed simulation code was applied to study characteristics of a rotating-oscillating liquid droplet, since a levitated droplet is used to measure material properties in the nuclear engineering fields. Measurement of properties of high-temperature and highly reactive molten core material is an important issue, since the material properties under accidental conditions are necessary for safety analyses. Surface tension is, for instance, obtained from the frequency of drop-shape oscillations based on the linear theory. The oscillation frequency is, however, affected much by the amplitude and rotation as shown in the previous chapter.

In order to study the combined effects of oscillation amplitude and rotation rate, axisymmetric oscillations of a rotating droplet were simulated. The variation of pressure difference in the droplet, which is defined as the pressure difference between the equator and the pole, is shown in Fig. 1. The pressure difference was found to decrease as the amplitude increased, while it increased as the rotation rate increased. The pressure difference was shown to have the same tendency as the frequency shift. It was also found that zero pressure difference was possible by an appropriate combination between the amplitude and the rotation rate. The condition for zero pressure difference is shown in Fig. 2, along with the condition for zero frequency shift. It was found that both the conditions were represented by the linear relation between the amplitude and the rotation rate. It indicated that the dependencies of the frequency shift and the pressure difference on the amplitude were the same as those on the rotation rate. It was confirmed that the frequency shift was corresponding to the unbalanced force field in the droplet, which was given as the combination of surface tension, centrifugal and Coriolis forces.

Through this study, the detailed flow fields in a rotating-oscillating droplet were shown, and the origin of the frequency shift was clearly shown. An application of the developed two-phase flow simulation code for the plant simulation system was demonstrated.

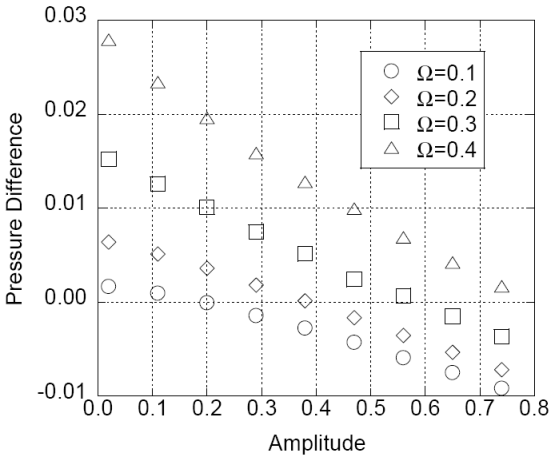

Fig. 1: Pressure difference due to amplitude and rotation.

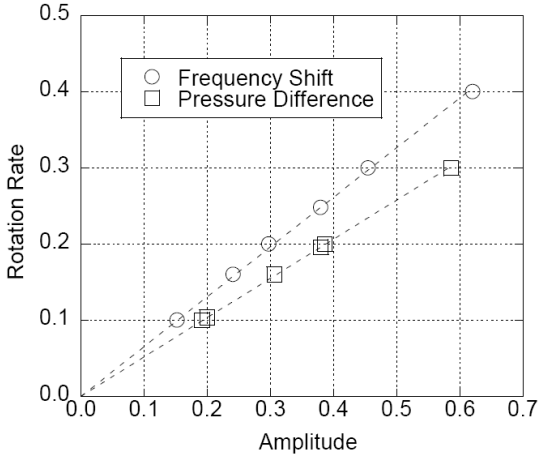

Fig. 2: Condition for zero frequency shift and zero pressure difference.

References

[1] T. Watanabe, Proc. IASME/WSEAS Int. Conf. Continuum Mech., Cambridge, UK, Feb. 23-25 (2008).

[2] T. Watanabe, Phys. Lett. A, 372(2008)482-485.

[3] T. Watanabe, Comp. Sim. Mod. Sci. 1(2008)81-85.

[4] T. Watanabe, WSEAS Trans. Fluid Mech. 2(2008)164-174

1.3.3 Development of Evaluation Method for Oscillating Interface in Two-phase Flows

Accurate measurement of surface tension : code application 2

Tadashi Watanabe

A two-phase flow simulation code has been developed for the simulation system of whole nuclear plant, as shown in the previous chapter. Oscillations of a rotating liquid droplet have been simulated as an application of the developed code, and it was shown that the detailed flow fields were simulated well together with the oscillatory interface. The relation between the force balance in the droplet and the frequency shift of the drop-shape oscillation was made clear. This result is of importance for the measurement of material properties in the nuclear engineering field, since the oscillation of a levitated droplet is used to measure properties of high temperature molten material. It is, however, not easy to observe and control the force balance in the droplet directly.

Measureable variables and controllable parameters for a rotating-oscillating droplet have been studied In order to utilize the characteristics found in the previous chapter. The effects of amplitude and rotation on the aspect ratio and the frequency shift are shown in Figs. 1 and 2, respectively. Large amplitude and small rotation were found to result in large aspect ratio and negative frequency shift. This relation is given through the force balance in the droplet as shown in the previous chapter. Figure 3 shows the frequency shift as a function of the aspect ratio. Effects of material properties such as viscosity and surface tension are also indicated in Fig. 3 in terms of the Reynolds and Weber numbers, respectively. From these figures, large-amplitude oscillations with no frequency shift were found to be possible when the aspect ratio was unity, regardless of the viscosity and surface tension. This finding is important for measurement, since the aspect ratio of the droplet shape can be observed and the oscillation amplitude and the rotation rate are controlled easily. This result indicates that the accurate measurement of oscillation frequencies, which are not suffered from frequency shift, could be conducted by controlling the rotation rate and the amplitude, and thus more reliable surface tension would be obtained.

Through this study, the accurate measurement method was proposed based on the simulation results obtained by the developed two-phase flow simulation code, and an application of the developed code for the plant simulation system was also demonstrated.

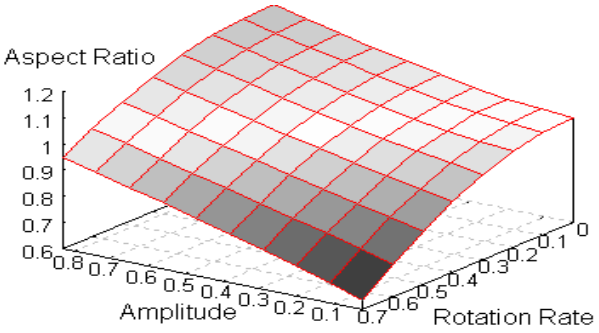

Fig. 1: Effects of amplitude and rotation on aspect ratio.

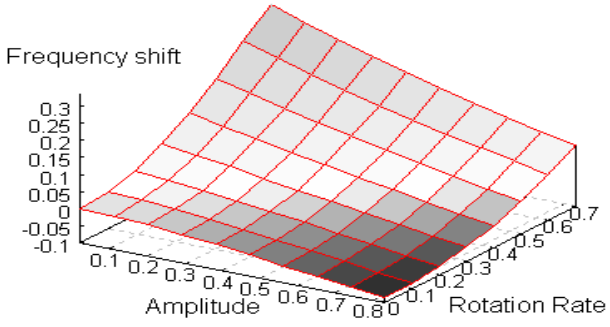

Fig. 2: Effects of amplitude and rotation on frequency shift.

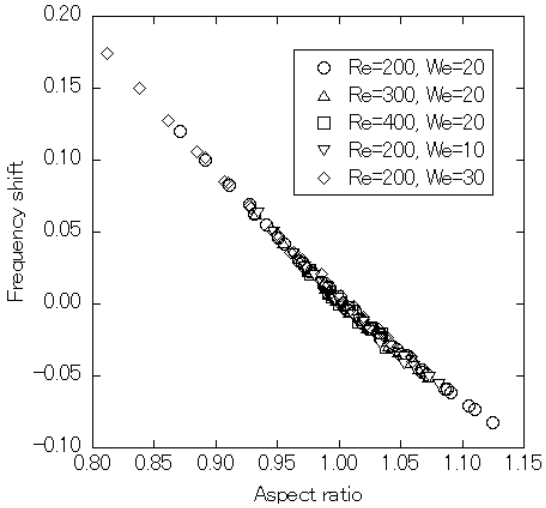

Fig. 3: Relation between frequency shift and aspect ratio.

References

[1] T. Watanabe, Proc. Int. Congress Theo. Appl. Mech., Adelaide, Austraria, Aug. 24-29 (2008).

[2] T. Watanabe, Phys. Lett. A, 373(2009)867-870.

1.4 Computational Materials Science

This is a blank page.

1.4.1 Cooperation with superconductor experiment

Superconducting Pb Island Nanostructures Studied by Scanning Tunneling Microscopy and Spectroscopy

T. Nishio[1)], T. An[1)], A. Nomura[1)], K. Miyachi[1)], T. Eguchi[1)], H. Sakata[2)], S. Lin[3)], N. Hayashi, N. Nakai, M. Machida and Y. Hasegawa[1)]

1) ISSP, University of Tokyo 2) Tokyo University of Science 3) NIMS

Mesoscopic superconductors, whose sizes are of the order of their coherence length, exhibit properties significantly different from those of their bulk counterparts. In bulk superconductors, the penetrating vortices form a triangular Abrikosov lattice. On the other hand, small superconductors exhibit various states of vortices, such as a giant vortex and an antivortex, depending on their size and shape. These unique features have been observed experimentally by electrical conductance and magnetization measurements. Using low-temperature (LT) scanning tunneling microscopy or spectroscopy (STM/S), the Abrikosov lattice was observed previously. In the present study, we investigated magnetic field-dependent superconductivity of nanosized Pb islands through local measurements of superconductivity and its imaging using LTSTM/S.

A typical Pb island is shown in Fig. 1(a). Its thickness was uniform and estimated at 9 monolayers (MLs, 1 ML=0.286 nm). The tunneling conductance at the zero-bias voltage (zero-bias conductance: ZBC) is an appropriate parameter for characterizing the breakdown of the superconductivity. Therefore, we measured the ZBC to characterize the superconductivity.

To elucidate the observed spatial variation of the ZBC, we recorded images of the ZBC under various magnetic fields (Fig. 1). At zero field, the ZBC is small and homogenous in the area. At 0.5 T, the ZBC increases. At 0.6 T, the center has a saturated ZBC, while the periphery has a lower ZBC. Then, at 1.0 T, the entire area has a saturated ZBC, indicating complete breakdown of superconductivity in the entire area. A high ZBC, i.e., breakdown of superconductivity, around the island center observed at 0.6 T implies a vortex formation.

Thus, we demonstrate that visualization of vortex formation and the breakdown of superconductivity by STM/S allow us to determine various critical fields for vortex penetration (expulsion) and for the complete breakdown of superconductivity, i.e., the transition field between the superconducting and normal states.

In conclusion, spatial profiles of superconductivity were obtained by conductance measurements at zero-bias voltage. Critical magnetic fields for vortex penetration and expulsion and for superconductivity breaking were measured for each island. The critical fields depending on the lateral size of the islands and existence of the minimum lateral size for vortex formation were observed [1]. We believe the present study opens up new paths for understanding nano/mesoscopic superconductors including vortices.

Reference

[1] T. Nishio, T. An, A. Nomura, K. Miyachi, T. Eguchi, H.Sakata, S. Lin, N. Hayashi, N. Nakai, M. Machida and Y. Hasegawa, Phys. Rev. Lett. Vol.101, p.167001 (2008).

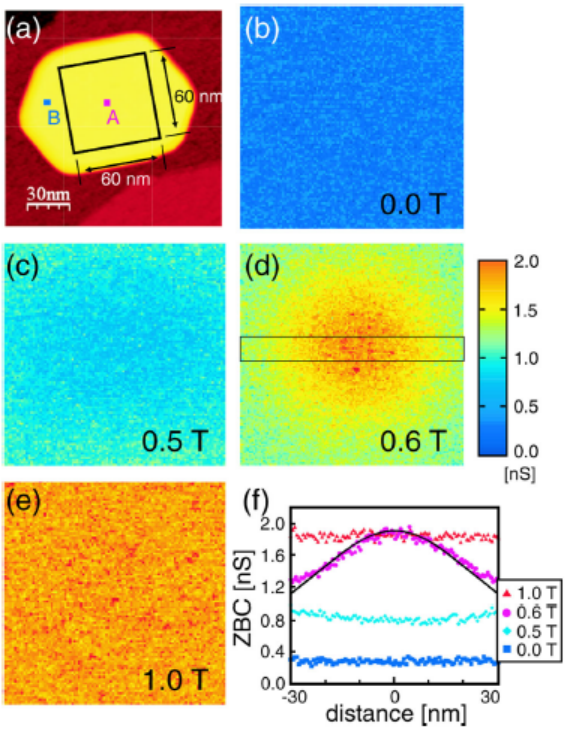

Fig. 1: (a) STM image of a Pb island showing an area where the following ZBC images were taken. (b)-(e) ZBC images taken under various magnetic fields. (f) Cross-sectional ZBC profiles.

1.4.1 Cooperation with superconductor experiment

Nuclear Magnetic Relaxation and Superfluid Density in Fe-Pnictide Superconductors: An Anisotropic ±s-Wave Scenario

Y. Nagai[1)], N. Hayashi, N. Nakai, H. Nakamura, M. Okumura and M. Machida

1) Dept. of Physics, University of Tokyo

Much attention has been focused on novel Fe-based superconductors since the recent discovery of superconductivity at the high temperature 26K in $LaFeAsO_{1-x}F_x$. Up to now, many Fe-based superconductors such as $SmFeAsO_{1-x}F_x$ have been found and intensively investigated. Experimental observations of thermodynamic quantities and others begin now to be reported on those superconductors. Such observations and theoretical analyses of them are important and indispensable for elucidating superconducting properties, especially for Cooper-pairing symmetry on which we focus our attention.

One of the confused points in the experiments for Fe-based superconductors is that the results of the nuclear magnetic relaxation rate seem inconsistent with the superfluid density observations. The nuclear magnetic relaxation rate has the lack of a coherence peak below the critical temperature and exhibits the low temperature power-law behavior. This is seemingly the evidence of unconventional superconductivity with line-node gaps. However, some experiments report that the superfluid density (i.e. penetration depth) does not depend on the temperature at low temperatures, which means that the pairing symmetry is fully gapped s-wave symmetry.

To resolve this contradiction, we investigate the nuclear spin-lattice relaxation rate and the superfluid density on the basis of the realistic effective five-band model. We successfully find that an anisotropic ±s-wave pair function (Fig. 1) can explain consistently the experimental results as follows. Our model leads to the result coinciding well with experimental data of the nuclear magnetic relaxation rate (Fig. 2). Simultaneously, the model reproduces the fully gapped s-wave behavior of the superfluid density (Fig. 3). Hence, we anticipate that the anisotropic ±s-wave pairing can be a possible candidate for the Cooper pairing in the Fe-pnictide superconductors [1].

Reference

[1] Y. Nagai, N. Hayashi, N. Nakai, H. Nakamura, M. Okumura and M. Machida, New J Phys. Vol.10, p.103026 (2008).

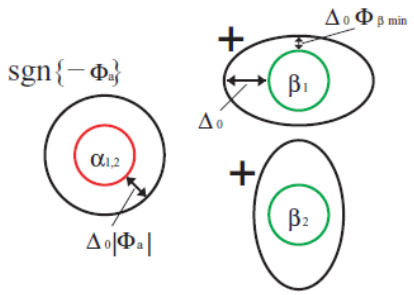

Fig. 1: Schematic figures of the pair functions on each Fermi surface.

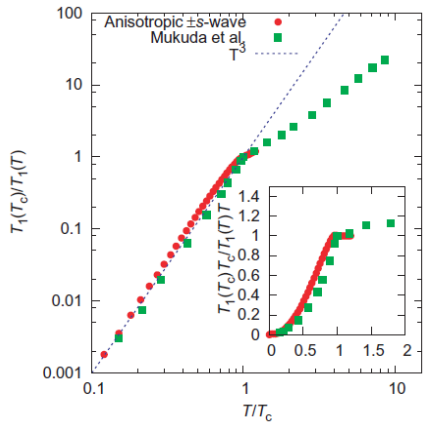

Fig. 2: Temperature dependence of the nuclear magnetic relaxation rate. Experimental data (green squares) and our theoretical result (red circles).

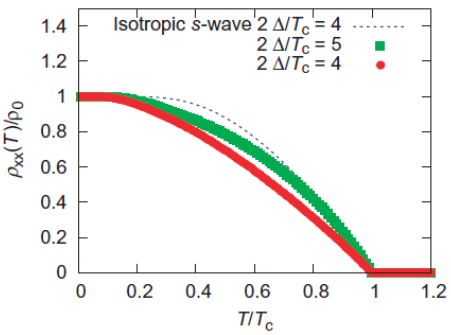

Fig. 3: Temperature dependence of the superfluid density.

1.4.1 Cooperation with superconductor experiment

Kramer-Pesch Approximation for Analyzing Field-Angle-Resolved Measurements Made in Unconventional Superconductors: A Calculation of the Zero-Energy Density of States

Yuki Nagai[1)] and Nobuhiko Hayashi

1) Dept. Phys., University of Tokyo

Much attention has been paid to the investigation of the mechanism of exotic superconductivity emerged in highly correlated materials like high-*Tc* cuprates and heavy fermion compounds, in metallic materials like nonmagnetic borocarbides, and in organic materials like BEDT-TTF salts. Many exotic superconductors (SCs) have zeros of the single-particle excitation gap called nodes on the Fermi surface (FS). It is then important to identify the detailed gap structure: either line or point nodes and their locations on the FS. The identification of them is crucial for understanding the unconventional pairing mechanism of exotic SCs.

In the last decade, the angular dependence on an applied magnetic field has made it easier for us to directly deduce the gap structure including the information on the positions of gap nodes. One such powerful method is the angle-resolved specific heat measurement. By measuring angular-oscillation behavior of the heat capacity with respect to the applied field direction, one can detect the details of the gap structure, especially for the locations of its nodes. Owing to potential abilities to reveal the gap structure in much more various exotic SCs, experimental and theoretical progresses in such field-angle-resolved measurements are highly influential developments in condensed matter physics.

We introduce the so-called Kramer-Pesch approximation (KPA) as a new method to analyze the field-angle-dependent experiments, which improves a previous technique. On the basis of the KPA, we succeed in deriving new equation for the angular-resolved density of states (the density of states is a quantity observed by specific heat measurements). Using the new equation, one can calculate the density of states as a function of the applied field direction.

We show the results obtained for several combinations of FS shape and superconducting gap anisotropy (Figs. 1-3). According to the results for the typical FSs, the FS shape eminently affects the angular-resolved zero-energy density of states, suggesting that one cannot readily identify a superconducting gap in a material without considering its realistic FS shape. That is, we find that the FS anisotropy is an indispensable factor for identifying the superconducting gap symmetry [1].

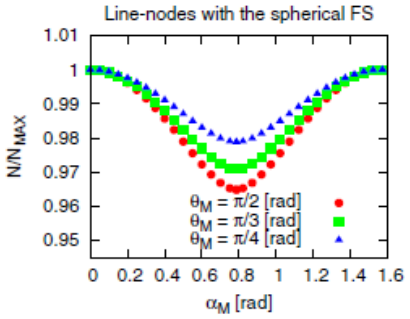

Fig. 1: Field-angle dependence of the zero-energy density of states (Line-node gap on a spherical Fermi surface).

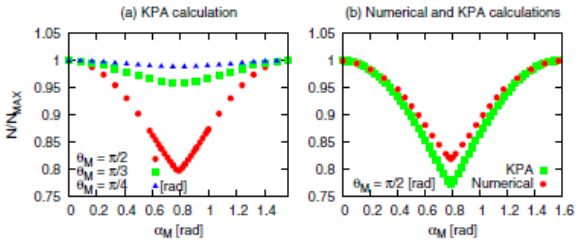

Fig. 2: Field-angle dependence of the zero-energy density of states (Line-node gap on a cylindrical Fermi surface).

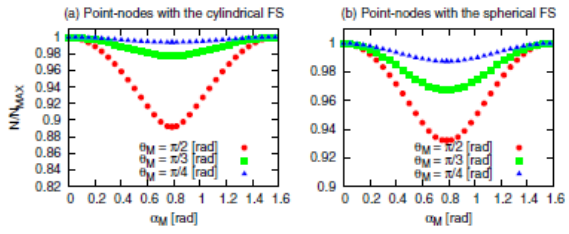

Fig. 3: Field-angle dependence of the zero-energy density of states (Point-node gap on cylindrical and spherical Fermi surfaces).

Reference

[1] Y. Nagai and N. Hayashi, Phys. Rev. Lett. Vol.101, p.097001 (2008).

Calculated Positions of Point Nodes in the Gap Structure of the Borocarbide Superconductor YNi_2B_2C

Yuki Nagai[1)], Yusuke Kato[1)], Nobuhiko Hayashi, Kunihiko Yamauchi[2)] and Hisatomo Harima[3)]

1) University of Tokyo 2) CNR-INFM, Italy 3) Kobe University

The discovery of the nonmagnetic borocarbide superconductor YNi2B2C has considerable attention because of the growing evidence for highly anisotropic superconducting gap and high superconducting transition temperature 15.5 K. To identify the superconducting gap structure, the field-angle-dependent (FAD) heat capacity has been measured in YNi2B2C. The local density of states (LDOS) in the isolated vortex of YNi2B2C was also measured by scanning tunneling microscopy (STM) and scanning tunneling spectroscopy (STS). The vortex core was found to be fourfold star-shaped in real space.

The purpose of our study is to determine the gap structure consistent with the STM/STS and the FAD heat capacity. To determine the superconducting gap function of YNi2B2C, we calculate the LDOS around a single vortex core (Fig. 1) with the use of Eilenberger theory and the band structure calculated by local density approximation, assuming a gap structure with point nodes at different positions (Fig. 2). We also calculate the FAD heat capacity in the vortex state (Fig. 3).

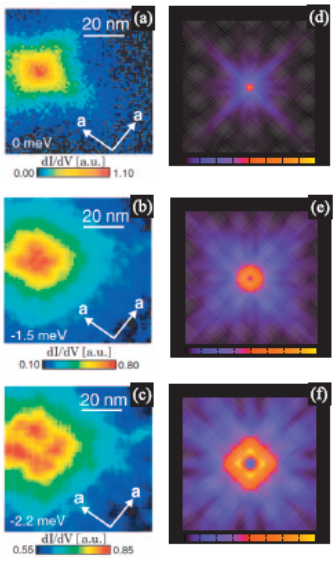

Fig. 1: The local density of states (LDOS) around a single vortex core. Left (right) column: experimental (our theoretical) results.

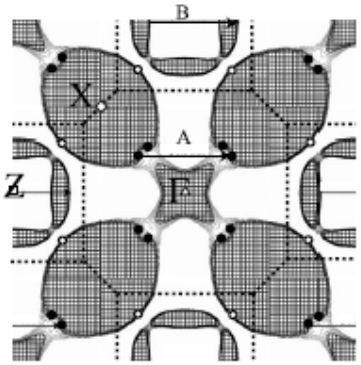

Fig. 2: Positions (filled dots) of the point nodes in the superconducting gap on the Fermi surface.

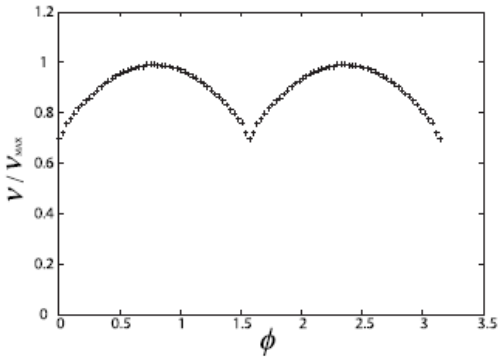

Fig. 3: Anglar dependence of the heat capacity.

Comparing our theoretical results with the experiments, we propose the gap structure of YNi2B2C, which has the point nodes and gap minima along <110> (Fig. 2). Our gap structure is consistent with all results of angular-resolved experiments.

Reference

[1] Y. Nagai, Y. Kato, N. Hayashi, K. Yamauchi and H. Harima, Phys. Rev. B Vol.76, p.214514 (2007).

1.4.2 Computational design of superconductor-based innovative quantum devices

Josephson Effect between Conventional and Non-Centrosymmetric Superconductors

Nobuhiko Hayashi, Christian Iniotakis[1], Masahiko Machida and Manfred Sigrist[1]

1) ETH Zurich, Switzerland

Much attention has recently been focused on the superconductors without inversion symmetry, motivated by the discovery of superconductivity in the non-centrosymmetric heavy-fermion material CePt3Si [1]. The lack of an inversion center in the crystal lattice induces antisymmetric spin–orbit coupling. This spin–orbit coupling has the Rashba form in systems such as CePt3Si where mirror symmetry about a single plane is lacking. Owing to such an antisymmetric spin–orbit coupling, the Fermi surface is split into two sheets through the spin-degeneracy lifting. Moreover, the Cooper pairing state can be “parity-mixed”, namely “spin-singlet–triplet mixed”, which is not possible in centrosymmetric systems. We find that a feature in the electronic spin structure on the Fermi surfaces plays an important role and affects the Josephson pair tunneling in the non-centrosymmetric superconductor.

The Josephson effect between a conventional (s-wave spin-singlet) superconductor and an unconventional superconductor provides a way to probe the spin degree of freedom of the unconventional Cooper pairing. For the non-centrosymmetric superconductor CePt3Si, such an experiment was performed by Sumiyama et al. [2]. Al/CePt3Si junctions were prepared and their Josephson effect was investigated applying weak magnetic fields in order to observe the interference patterns in the supercurrent. A Fraunhofer-shaped pattern was observed for the tunnel junction along the in-plane axis of the tetragonal crystal in CePt3Si, while a very irregular pattern appeared along the c-axis. We propose a scenario to address this experiment. Important in our approach is the influence of Rashba spin–orbit coupling on the Josephson effect. We derive an expression for the dc-Josephson current between a conventional superconductor and a non-centrosymmetric one with Rashba spin–orbit coupling. The expression derived is then used to discuss the specific differences between differently oriented Josephson junctions, in order to give an explanation for the observation in the Al/CePt3Si junctions.

We succeed in deriving the expression for the Josephson current–phase relation for such a junction as follows. (Refer to Ref. [3] for details of these equations.)

$$J = N_{\mathrm{F}}^{L} v_{\mathrm{F}}^{L} \int_{\hat{\boldsymbol{n}}\cdot\hat{\boldsymbol{k}}^{L}>0} \frac{\mathrm{d}\Omega_{k}^{L}}{4\pi} \hat{\boldsymbol{n}}\cdot\hat{\boldsymbol{k}}^{L} T \sum_{\omega_n} K^{L},$$

$$\begin{aligned} K^{L} = {} & \frac{\pi(1+\delta)}{D_{\mathrm{I}}} w_0 \,\mathrm{Im}\{\Psi_s \Delta_{\mathrm{I}}^{*}\} + \frac{\pi(1-\delta)}{D_{\mathrm{II}}} w_0 \,\mathrm{Im}\{\Psi_s \Delta_{\mathrm{II}}^{*}\} \\ & + \frac{\pi(1+\delta)}{D_{\mathrm{I}}} [(-\bar{k}_y^{R}) w_x + \bar{k}_x^{R} w_y] \,\mathrm{Im}\{\Psi_s \Delta_{\mathrm{I}}^{*}\} \\ & + \frac{-\pi(1-\delta)}{D_{\mathrm{II}}} [(-\bar{k}_y^{R}) w_x + \bar{k}_x^{R} w_y] \,\mathrm{Im}\{\Psi_s \Delta_{\mathrm{II}}^{*}\}, \end{aligned}$$

It allows us to give a possible explanation for the recent experimental results [2] for the Al/CePt3Si junction.

The above equations are the main result of our study [3]. The spin-triplet-like Josephson coupling, namely the third and fourth terms in the above second equation can lead to π-junctions, resulting in the absence of the Fraunhofer pattern. The origin of this spin-triplet-like Josephson coupling is *not* a spin-triplet Cooper pairing, but is due to the characteristic spin structure on the Fermi surfaces induced by Rashba spin–orbit coupling in the non-centrosymmetric superconductor.

References

[1] E. Bauer et al., Phys. Rev. Lett. Vol.92, p.027003 (2004).

[2] A. Sumiyama et al., J. Phys. Soc. Jpn. Vol.74, p. 3041 (2005).

[3] N. Hayashi, C. Iniotakis, M. Machida and M. Sigrist, J. Phys. Chem. Solids Vol.69, pp.3225-3227 (2008).

1.4.2 Computational design of superconductor-based innovative quantum devices

Josephson Effect between Conventional and Rashba Superconductors

Nobuhiko Hayashi, Christian Iniotakis[1)], Masahiko Machida and Manfred Sigrist[1)]

1) ETH Zurich, Switzerland

Superconductors without inversion symmetry, the so-called non-centrosymmetric superconductors, have received much interest during recent years. The lack of an inversion center in the crystal lattice induces antisymmetric spin–orbit coupling, leading to important modifications of the superconducting phase. The antisymmetric spin–orbit coupling displays the Rashba form in systems such as CePt3Si [1] where mirror symmetry about a single plane is missing. The specific spin structure on the Fermi surfaces due to the Rashba spin-orbit coupling plays an important role in connection with the Josephson effect. We aim at the properties of the Josephson effect between a conventional superconductor and a non-centrosymmetric superconductor with Rashba spin-orbit coupling.

We study the Josephson effect between a conventional s-wave superconductor and a non-centrosymmetric superconductor with Rashba spin－orbit coupling [3]. Rashba spin−orbit coupling affects the Josephson pair tunneling in a characteristic way. The Josephson coupling can be decomposed into two parts, a 'spin-singlet-like' and a 'spin-triplet-like' component. The latter component can lead to a shift of the Josephson phase by π relative to the former coupling. This has important implications on interference effects and may explain some recent experimental results [2] for the Al/CePt3Si junction.

Considering a Josephson junction between a spin-singlet s-wave superconductor and a non-centrosymmetric one with Rashba spin－orbit coupling, we calculate the supercurrent J flowing across the junction. The calculations can be done by utilizing bulk Green functions. We succeed in deriving the expression for the Josephson current–phase relation for such a junction as follows. (Refer to Ref. [3] for details of these equations.)

$$J = N_{\mathrm{F}}^{\mathrm{L}} v_{\mathrm{F}}^{\mathrm{L}} \int_{\hat{\boldsymbol{n}}\cdot\hat{\boldsymbol{k}}^{\mathrm{L}}>0} \frac{d\Omega_{\hat{k}}^{\mathrm{L}}}{4\pi} \hat{\boldsymbol{n}}\cdot\hat{\boldsymbol{k}}^{\mathrm{L}} T \sum_{\omega_n} K,$$

$$\begin{aligned} K = {} & \frac{\pi(1+\delta)}{D_{\mathrm{I}}} \mathrm{Im}\left\{w_0^* \Psi_{\mathrm{s}} \Delta_{\mathrm{I}}^*\right\} + \frac{\pi(1-\delta)}{D_{\mathrm{II}}} \mathrm{Im}\left\{w_0^* \Psi_{\mathrm{s}} \Delta_{\mathrm{II}}^*\right\} \\ & + \frac{\pi(1+\delta)}{D_{\mathrm{I}}} \mathrm{Im}\left\{\bar{\boldsymbol{\lambda}}\cdot\boldsymbol{w}^* \Psi_{\mathrm{s}} \Delta_{\mathrm{I}}^*\right\} \\ & + \frac{-\pi(1-\delta)}{D_{\mathrm{II}}} \mathrm{Im}\left\{\bar{\boldsymbol{\lambda}}\cdot\boldsymbol{w}^* \Psi_{\mathrm{s}} \Delta_{\mathrm{II}}^*\right\}, \end{aligned}$$

It allows us to give a possible explanation for the recent experimental results [2] for the Al/CePt3Si junction. Furthermore, we anticipate that in the absence of an external magnetic field, spontaneous magnetic fluxes could appear along the interface normal to the c axis of CePt3Si owing to random π and 0-junctions, which can be observed experimentally, in principle, by scanning SQUID microscopes.

The above equations are the main result of our study [3]. By the way, the Andreev bound states may be formed at surfaces of certain orientations in non-centrosymmetric superconductors. The influences of such bound states have been neglected here for the qualitative discussions. A more detailed analysis taking this aspect into account is left for future studies.

References

[1] E. Bauer et al., Phys. Rev. Lett. Vol.92, p.027003 (2004).

[2] A. Sumiyama et al., J. Phys. Soc. Jpn. Vol.74, p. 3041 (2005).

[3] N. Hayashi, C. Iniotakis, M. Machida and M. Sigrist, Physica C Vol.468 pp.844-847 (2008).

1.4.2 Computational design of superconductor-based innovative quantum devices

Quantum synchronization effects in intrinsic Josephson junctions

Masahiko Machida, Takuma Kano, Susumu Yamada, Masahiko Okumura, Toshiyuki Imamura[1)], and Tomio Koyama[2)] 1)Faculty of Sci. & Tech., keio Univ., 2) IMR, Tohoku Univ. ,

Since the discovery of "intrinsic Josephson effects" in layered High-Tc superconductors, the Josephson effects have attracted much interest from standpoints of not only fundamental interest but also device application possibility. The reason is that High-Tc superconductor crystal itself is a natural coupled array of a number of atomic-scale Josephson Junctions as schematically shown in the upper panel of Fig.1. The system has been called "intrinsic Josephson junction", in which some possibilities of synchronous electromagnetic excitations over a huge number of stacked junctions have been intensively investigated because such dynamics may open a promising way toward powerful high-frequency radiation source. Moreover, the reproducibility of identical Josephson junction has been so far considered to be a crucial breakthrough point in the Josephson device production, while intrinsic Josephson junctions are completely free from such a problem if one can make a good crystalline.

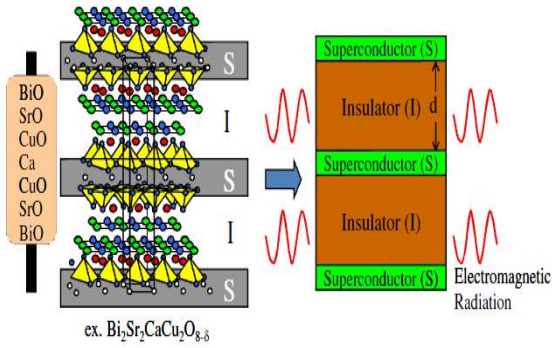

Fig. 1: A schematic figure for a single crystal of layered High-Tc cuprate superconductor, which works as an intrinsic Josephson junction, in which the possibility of the in-phase electromagnetic wave radiation has been examined.

A historical chain of theoretical studies on the intrinsic Josephson effects have clarified an importance of the coupling between stacked neighboring junctions. The dynamics of the superconducting phase in intrinsic Josephson junctions is now well-known to be never understood without the coupling between junctions. Since the recent observation of macroscopic quantum tunneling (MQT) in intrinsic Josephson junctions, a great interest has been aroused on MQT in multi-junction stacked systems. MQT is also expected to be strongly influenced by the coupling. However, the coupling effects on MQT have been little studied except for a few recent works. In this paper, we focus on the quantum dynamics of intrinsic Josephson junctions. A coupling is fully incorporated and effects of the coupling on the quantum dynamics are clarified through large-scale numerical simulations.

The MQT in intrinsic Josephson junctions has been observed by statistical measurements on the switching events into resistive states, i.e., so-called switching into "quasi-particle multi-branches". X.Y.Jin et al., reported that the observed MQT rates depend on the jump destinations. They found that MQT rate is drastically enhanced in the case of the uniform switching, i.e., the collective switching of all junctions. Their finding is that the MQT rate is roughly proportional to the square of the number of junctions. This result implies that MQT collectively occurs and the switching of some junctions induces the jump of other junctions. We expect that this synchronous behavior is caused by the coupling effect. However, there still remains a question why such a collective MQT is enhanced only when the temperature is decreased below the crossover temperature from classical to quantum. In other words, this question is whether the quantum character assists collective or synchronous dynamics or not. In this paper, we therefore examine how the superconducting phase dynamics changes with a crossover from classical to quantum.

We concentrated on the model considering only the capacitive coupling and solved the time evolution of the Schrodinger equation derived from the model Hamiltonian. We found that these results are consistent with the experimental observations.

References

[1] X. Y. Jin et al., Phys. Rev. Lett. **96**, 177003 (2006).
[2] M. Machida et al. Physica C**468,** 689(2008).

1.4.2 Computational design of superconductor-based innovative quantum devices

Collective dynamics of macroscopic quantum tunneling in layered high-Tc superconductor

Masahiko Machida and Tomio Koyama[1)] 1) IMR, Tohoku Univ.

The discovery of macroscopic quantum tunneling (MQT) in YBCO grain boundary junctions and Bi-2212 intrinsic Josephson junctions (IJJs) opened a new frontier on quantum behaviors in superconducting Josephson effects. In Bi-2212 IJJs, the crossover to the quantum regime from the classical (thermal) one occurs about 1K, which is 1-order higher than those in conventional single-junction systems. Furthermore, the dissipation effect that disturbs MQT is fortunately very weak in spite that the symmetry of the order parameter is d-wave which has low-lying nodal quasi-particles. The reason is that the Josephson plasma frequency in IJJs is much higher compared with conventional Josephson junctions and moreover the transfer-integral along the c-direction vanishes for the nodal quasi-particles. These remarkable features in IJJs indicate that IJJs are of great advantage in making superconducting quantum devices.

Very recently, Jin et al. succeeded in observing a novel type of MQT in Bi-2212 IJJs, i.e., the switching to the uniform voltage state where all the junctions are in the voltage state [1]. They reported that the switching rate observed in the multi-photon processes increases with the number of stacked junctions N and the enhancement is much interestingly proportional to the square of N. This result simply suggests that the motion of the phase differences in IJJs is collective in the multi-photon processes. However, it is not so simple to explain why the rate enhancement is related to the square of N. Thus, in this paper, we formulate a theory for the collective MQT based on the model of the capacitively-coupled IJJs and reveal an origin of the square of N in multi-photon assisted MQT. We also revisit the theory for capacitively-coupled IJJs and derive the Hamiltonian based on standard formalism. From the Hamiltonian, we derive the classical equation of motion of the phase difference and discuss the classical collective motion. The details of the classical dynamics were discussed in Ref. [2]. Furthermore, we quantize the Hamiltonian in a collective coordinate and clarify a scheme of quantum energy levels for the capacitively-coupled N IJJs and construct a theory of the multi-photon processes of IJJs [3]. By considering the quantized energy level scheme, we explain the switching rate being proportional to N^2 in the multi-photon processes and moreover predict new features in the switching rate in a low temperature range (～10mK) [3] .

Here, let us show a theoretical result on MQT in IJJs. Since the heart of the result is composed of several mathematical formulas, we here avoid writing down them and instead summarize the result in Fig.1 [3].

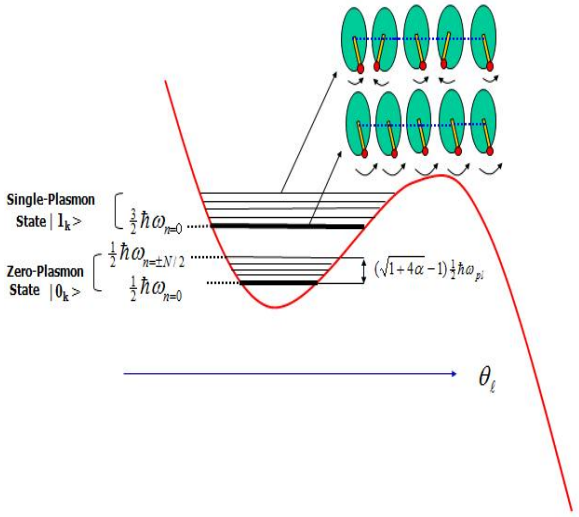

Fig. 1: Energy-level quantization of the longitudinal collective phase oscillation modes in the presence of a bias current. In the N-junction system, the zero- and the single-plasmon states are, respectively, composed of N oscillation modes which are nearly degenerate in the case of the capacitive coupling constant α =1. The zero plasmon state is formed by the zero-point motion of the N plasma modes. We note in this figure that only the zero- and the single-plasmon states are depicted. The situation changes with the magnitude of the bias current .

References

[1] X. Y. Jin et al., Phys. Rev. Lett. **96, 177003 (2006).**

[2] M. Machida, T. Koyama, and M. Tachiki , Phys. Rev. Lett. **83**, 4618 (1999).

[3] M. Machida and T.Koyama, Supercond. Sci. Technol. **19**, S1 (2006).

1.4.3 Large-scale simulation for the fundamental understanding of superconductivity

Vortex microscopic structure in BCS to BEC Fermi superfluids

Masahiko Machida, Tomio Koyama[1)], Yoji Ohashi[2)] 1) IMR, Tohoku Univ. , 2)Faculty of Sci. & Tech., keio Univ.

Very recently, the MIT group has succeeded in observing not only a single-quantized vortex but also a triangular vortex lattice in a two-component atomic Fermi gas. The singly-quantized vortex in a Fermi superfluid is characterized by several inherent spatial lengths. The most well-known length among them is the coherence length, which is a function of the Fermi velocity and the superfluid gap.

In the singly-quantized superconducting vortex we have another well-known characteristic length besides the coherence length, which is related to the slope of the gap function at the center of a vortex. In the low-temperature regime, the length shows linear temperature dependence, which is sharply contrasted with the behavior of the coherence length being nearly independent of temperature. In this paper, we study how the gradient which dominates the behavior of the length scale changes at the BCS-BEC crossover and clarify that the gradient is dependent on microscopic parameters such as the Fermi velocity. In addition, we consider another characteristic gradient in the fermionic gap function which is separately defined outside the first linear slope. Our calculations show that both the gradients are well-defined and reveal their characteristic behaviors, depending on the interaction strength.

Let us present numerical solutions for the single-vortex state. Figures 1(a) and (b) represent the profiles of the fermionic superfluid gap functions Δ along the radial direction, respectively, in the BCS($1/k_F a < 0$) and the BEC ($1/k_F a > 0$) sides. The profiles show a clear difference in these two sides. In the BCS side the first gradient is almost independent of the Feshbach resonance threshold energy ν. This tendency is more clearly seen in the enlarged view as shown in the inset of Fig.1(a). On the other hand, in the BEC side, i.e., ν=20 to ν=1, the first gradient strongly depends on ν as seen in Fig.1(b). Here, we note that the first gradient is proportional to $1/k_F$ in the BCS region and to $\nu-\mu$ (μ is the chemical potential) in the BEC region. The former relation was suggested in the superconducting vortex in the quantum limit. From these relations one understands that the Fermi edge of the fermionic atomic gas is nearly invariant in the BCS regime, whereas it is strongly dependent on ν in the BEC regime. In other words, from the observation of the first gradient, one may detect a signal of the crossover from fermionic to bosonic superfluid states. It is also noted that the linear slope of the first gradient is restricted in the region of $0< r < 1/k_F a$ (See Fig.1(a)). This is because the first gradient is determined only by the Andreev localized-bound states.

Let us next consider the second gradient. As seen in Fig.1(a), The value increases with decreasing ν, i.e., increasing the pairing strength in the BCS side ($1/k_F a < 0$). This behavior is sharply contrasted to the first gradient. On the other hand, the second gradient decreases with decreasing ν, i.e., increasing the pairing strength in the BEC side (see Fig.1(b)) contrary to the BCS side. Thus, one understands that the second gradient is correlated with the fermionic superfluid gap.

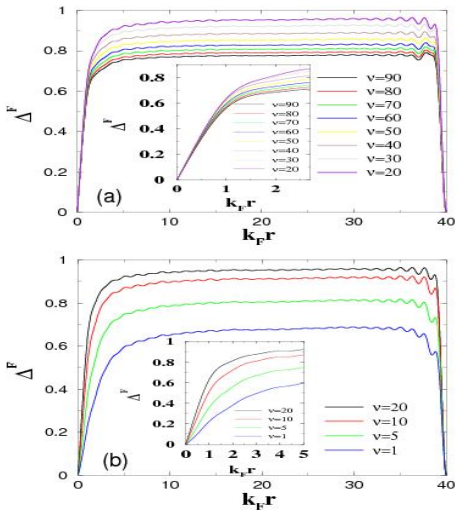

Fig. 1: The radial profile of the fermionic superfluid gap (a) from ν=20 to 90 ($1/k_F a< 0$) and (b) from ν=1 to 20 ($1/k_F a > 0$). The insets in (a) and (b) are the focus views on the central region of the vortex.

In summary, we concludes from the numerical calculations that the first and second gradients behave as specific values characterizing BCS and BEC.

Reference

[1] M. Machida et al. Physica C460-462, 275(2007).

1.4.3 Large-scale simulation for the fundamental understanding of superconductivity

Correlation effects on atom-density profiles of one- and two-dimensional polarized atomic fermi gases loaded on an optical lattice

Masahiko Machida, Susumu Yamada, Masahiko Okumura, Yoji Ohashi[1)], Hideki Matsumoto[2)]

1)Faculty of Sci. & Tech., keio Univ. 2) IMR, Tohoku Univ.

Recently, two-component fermion systems with population imbalance have attracted much attention in various research fields, such as cold atoms, superconductors, and QCD. In the 1960's, effects of the population imbalance have been theoretically investigated in the superconductivity literature. Sarma considered the stability of an interior gap phase (Sarma state). Fulde and Ferrell, and Larkin and Ovchinikov predicted the so-called FFLO state, where the superconducting order parameter is spatially modulated. Very recently, some evidence of the FFLO state has been reported in a heavy fermion superconductor $CeCoIn_5$.

So far, the superfluid Fermi gas with population imbalance has been experimentally studied without an optical lattice. In this paper, we investigate effects of the lattice on the population imbalanced systems. Very recently, there have been several reports on this issue, one of which theoretically claims that FFLO is more stablilized than the non-optical lattice case, and others of which numerically show that FFLO is observable in the one-dimensional attractive Hubbard model by using the density matrix renormalization Group (DMRG) method. Our approach in this paper differs from these works in using the exact diagonalization method mainly and the DMRG method complementarily in order to check whether the exact diagonalization results are small size effects or not. In addition, we focus on the density profile of majority $n_{\uparrow}$ and minority components $n_{\downarrow}$ at T=0 in a one- and two-dimensional lattice trapped systems instead of the stability of the exotic superfluidity FFLO. The reason is that the atom density profile is the most convenient and clear observable for experiments. Moreover, the FFLO requires at least the population imbalance in the atom density profile. Namely, it is crucial point for FFLO whether the population imbalance survives even in the presence of pair instability at T=0 ground state or not.

In this paper, we investigate effects of optical lattice potential in one- and two-dimensional two-component trapped Fermi gases with population imbalances. Using the exact diagonalization and the density matrix renormalization group methods complementarily, we calculate the atom density profile from the ground state many-body wavefunction as a function of attractive interaction strength for various population imbalances. The numerical results reveal that although a phase separation between the superfluid core and the shell cloud of excess atoms occurs as observed in experiments without the optical lattice, the population imbalance generally remains in the core region in contrast to the non-lattice cases. The essence of the numerical results in a strong attractive regime can be explained by an effective model composed of Cooper pairs and excess major fermions.

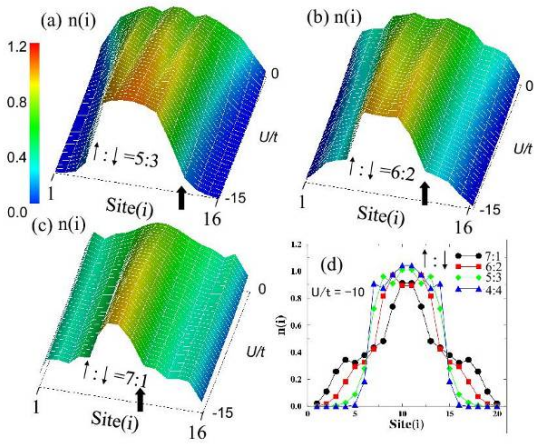

Fig. 1: The exact diagonalization results for U/t dependences (-15< U/t <0) of particle density profiles, n(i) for three imbalance cases, whose ratios of major to minor fermion species are (a) 5:3, (b) 6:2, and (c) 7:1, respectively. In these three cases, the number of total particles, N_F= 8, the site number, N=16 and V/t=1. The panel (d) is a highlight of n(i) at U/t=-10 for the imbalance from 4:4 to 7:1 in N=20. N_F and V/t are the same as (a-c).

References

[1] See, e.g., R.~Casalbuoni and G.~Nardulli, Rev. Mod. Phys. 76, 263 (2004).

[2] M.Machida et al., Phys. Rev. A77, 053614 (2008)

1.4.3 Large-scale simulation for the fundamental understanding of superconductivity

Stripe formation in fermionic atoms on a two-dimensional optical lattice inside a box trap; Density-matrix renormalization-group studies for the repulsive Hubbard model with open boundary conditions

Masahiko Machida, Masahiko Okumura, and Susumu Yamada

Ultra-cold atomic Fermi-gas has attracted not only atomic gas community but also several physicists studying strongly-correlated electron systems. The reason is that the so-called ``optical lattice" formed by counter laser beams creates a periodical lattice potential described by the tight-binding model and the ``Feshbach resonance" enables to access to the Hubbard model with the repulsive on-site interaction. Thus, a research goal in the optical lattice with the Feshbach tuning is to directly observe several controversial issues due to strong correlation as seen in High-Tc cuprate superconductors and other metal oxides in controllable manners.

Generally, ultra-cold Bose and Fermi gases are trapped inside a harmonic trap to avoid the free expansion of atoms. The optical lattice is created inside the trap potential by utilizing the field modulation in the standing waves of lasers. Then, the model Hamiltonian on Fermi atoms is described by the Hubbard model with a harmonic trap potential. In the presence of the harmonic trap potential, specific spatial-patterns appear and have their own novel interests, e.g., how the spin correlation structures change from the Mott domain to metallic edges and whether the holes in the metallic edges form Cooper pairs or not. However, one clearly notices that intrinsic properties of the Hubbard model under a fixed doping are not directly observable. Although the system is quite clean and controllable, there is no direct relationship with solid state physics except for a few artificial cases. In this paper, we therefore suggest that an alternative trap, whose shape is box, enables to experimentally study the Hubbard model with the open boundary condition. By using such a trap shape, we can fully examine the Hubbard model under a fixed doping and an interaction.

Our expecting potential shape is 2-D box created inside the x-y plane with a narrow confinement along z-axis, and 2-D optical lattice is loaded inside the box plane by adding the Gaussian walls or a standing wave light fields with shallow Gaussian envelope curve. Such a stage is just described by 2-D Hubbard model with the open boundary condition. We emphasize that the system becomes the best playground for simulating controversial phenomena of High-Tc superconductors and other layered metal oxides. Furthermore, we would like to point out that ladder type models with the open boundary are recently good targets for advanced DMRG methods and direct comparative studies are possible.

In order to predict atomic density profile under the box trap, we apply the directly-extended density-matrix renormalization group method to 4-leg repulsive Hubbard model with the open boundary condition. Consequently, we find that stripe formation is universal in a low hole doping range and the stripe sensitively changes its structure with variations of U/t and the doping rate as shown in Fig.1. A remarkable change is that a stripe formed by a hole pair turns to one by a bi-hole pair when entering a limited strong U/t range as shown in Fig.1(a) to (b). Furthermore, a systematic calculation reveals that the Hubbard model shows a change from the stripe to the Friedel like oscillation with increasing the doping rate.

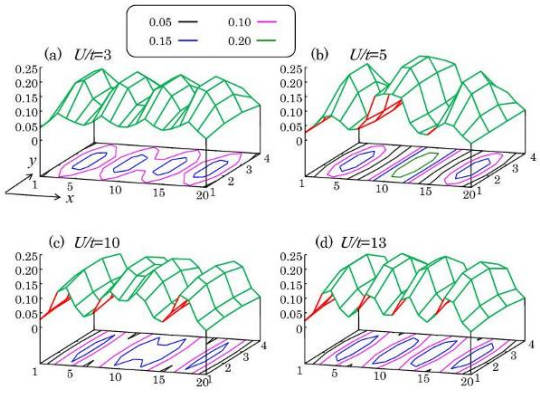

Fig. 1: The dex-DMRG results of the hole density profiles for (a)U/t =3, (b)U/t = 5, (b)U/t =10, and (d)U/t= 13 in the Hubbard model with the open boundary condition. The number of doped holes is 8 and the doping rate is p=0.10.

Reference

[1] M. Machida, M.Okumura, S.Yamada, Phys. Rev. A **77**, 033619 (2008).

1.4.3 Large-scale simulation for the fundamental understanding of superconductivity

Hole Localization in the One-Dimensional Doped Anderson-Hubbard Model

Masahiko Okumura, Susumu Yamada, Nobuhiko Taniguchi[1)], and Masahiko Machida

1) Institute of Physics, University of Tsukuba

Recently, atomic Fermi gas loaded on an optical lattice (FGOL) has attracted a lot of attention, since FGOL is expected to be an excellent testbed to resolve controversial issues in condensed matter physics [1]. One of the advantages of FGOL is a tunability of the interaction between two atoms associated with the Feshbach resonance, which opens up a pathway to systematically study strongly correlated behaviors. Another advantage is the flexibility in making playgrounds such as the periodical lattice, which provides various stages including disorder effects for many-body interacting systems [1].

Among a huge number of proposals on FGOL, one of the unique challenges is a study of interplay between randomness and strong correlation [1]. This is one of the most difficult but important problems in real solids because high-*Tc* superconductor is a typical reality. In high-*Tc* superconductors, their common mother phase is the Mott insulator showing antiferromagnetism. The carrier is doped by chemical substitution, which inevitably brings a random potential. However, the disorder effects in strongly correlated systems have been too complicated issues to study theoretically and experimentally in condensed matters. Thus, its interplay has remained as an unsolved issue. On the other hand, FGOL is a very good experimental reality in systematically examining such a complex issue due to the wide tunability and flexibility.

We study the doped Mott insulator with disorder in a form of the Anderson-Hubbard model [1] in one-dimension, and predict experimental results on FGOL by means of the density-matrix renormalization group (DMRG) method [2,3]. Consequently, we find that the disorder does not destroy the Mott insulator but help the growth of the Mott phase domains contrary to our naïve expectation [4]. Such a nontrivial feature is kept and amplified until the disorder amplitude fully exceeds over the repulsive interaction strength.

We show the ratio of the insulating regions to the total system size [Fig. 1(a)] and an example of the charge distribution in the metallic [Fig. 1(b)], the new insulating [Fig. 1(c)], and the conventional insulating [Fig. 1(d)] phases when two holes are doped. One can find that the flat density regions, which are the Mott insulators assisted by the strong random potential.

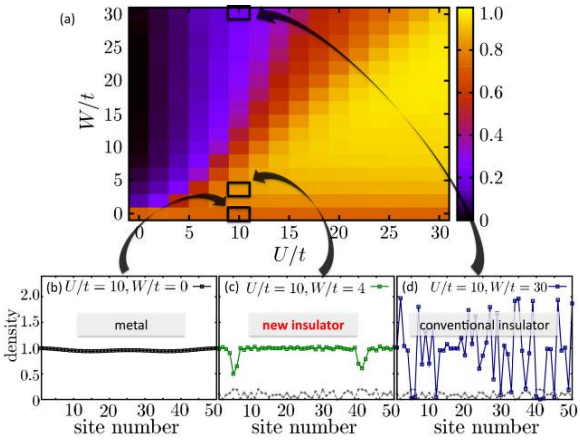

Fig. 1: (a) Ratio of the insulating region to the total system size for several randomness (*W*/*t*) and interaction strength (*U*/*t*). Charge distributions in (b) the metallic phase, (c) the new insulating phase, and (d) the conventional insulating phase.

Our DMRG simulation have revealed that the existence of the new insulator whose origin is the interplay between strong interaction and randomness [4]. It is important future work to extend our analysis above to two-dimensional (2D) system because the High-T_c occurs in the two-dimensional systems. We expect parallelized DMRG is a strong candidate to study the interplay between the strong interaction and strong randomness in 2D systems.

References

[1] M. Lewenstein, A. Sanpera, V. Ahufinger, B. Damski, A. Sen(De), and U. Sen, Advances in Physics **56**, 243 (2007).

[2] S.R. White, Physical Review Letters **69**, 2863 (1992); Physical Review B **48**, 10345 (1993).

[3] U. Schollwock, Review of Modern Physics **77**, 259 (2005); K. Hallberg, Advances in Physics **55**, 477 (2006).

[4] M. Okumura, S. Yamada, N. Taniguchi, and M. Machida, Physical Review Letters **101**, 016407 (2008).

1.4.3 Large-scale simulation for the fundamental understanding of superconductivity

DMRG studies for 1-D random Hubbard chain close to the half-filling

Masahiko Okumura, Susumu Yamada, and Machida Masahiko

Recently, ultracold neutral fermionic atoms have been successfully loaded on an optical lattice. If the system is sufficiently cooled, then it is described by the Hubbard model, which is the most standard model in solid state physics. In atomic gases, a few important parameters, e.g., the interaction strength, the temperature, and so on, are controllable. Moreover, the trap potential shape has been very recently transformed from a harmonic well type to a box shape one [1], and various disorders have been successfully incorporated inside the trap potential [2]. Thus, these technical developments open a possibility to study the random Hubbard model under an open boundary condition. This indicates that the cold atom system is an ideal testbed to investigate one of complicated materials properties, i.e., electronic structure under both strong correlation and randomness, which is currently an important issue in transition metal oxides.

We studied the one-dimensional (1-D) Hubbard model with random potential under the open boundary condition motivated by the two research streamlines in atomic gases and transition metal oxides [3]. We employ the density-matrix renormalization group (DMRG) method [4,5] in order to solve the ground state in such complicated systems as precisely as possible. Especially, we concentrate on a slightly doped region to the half-filling, in which many theoretical treatments fail to predict.

We show the charge distributions for 4-hole case with the fixed interaction strength U/t=20 and various random potential strength (Fig. 1). One finds that the increase in the randomness strength assists formation of the Mott insulating regions. One also confirms the tendency that the Mott plateaus become wider and the hole valleys sharper as the interaction strength increases.

We have studied the 1-D random Hubbard model under the open boundary condition by using DMRG method [3]. Consequently, we found the formation of the Mott plateaus and the hole valleys in the strong coupling and randomness regime. We also observed that the Mott plateaus become wider and the hole valleys deeper as the random potential magnitude increases, while the randomness breaks the Mott plateaus when W (randomness strength) is over U (interaction strength). This observed hole localization is specific to a slightly doped Mott insulator, and the essence is considered to be deeply relevant to the experimental results seen in metal oxides including high-T_c superconductors. We will proceed to extend our approach to two-dimensional case and try to clarify the hole localization behavior in higher dimension in the future. On the other hand, it is interesting to investigate the DOS and LDOS in such systems using the dynamical DMRG [6]. It will inform us of how the Mott gap varies as the repulsive interaction and the randomness change. In addition, we claim that recent advancements in atomic gases enable to directly detect such a localization behavior in the same situation as the present numerical calculation.

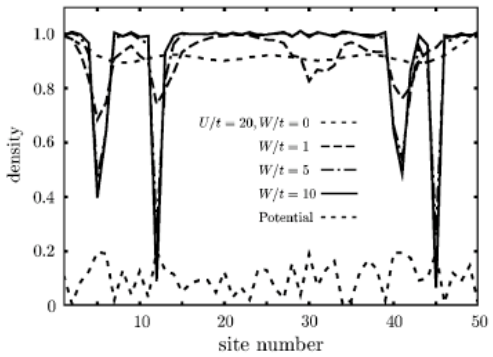

Fig. 1: Charge distribution for 4-hole case with the interaction strength U/t=20 and the randomness strength W/t=0, 1, 5, 10.

References

[1] T.P. Meyrath, F. Schreck, J.L. Hanssen, C.-S. Chuu, and M.G. Raizen, Physical Review A **71**, 041604(R) (2005).

[2] J.E. Lye, L. Fallani, M. Modugno, D.S. Wiersma, C. Fort, and M. Inguscio, Physical Review Letters **95**, 070401 (2005).

[3] M. Okumura, S. Yamada, and M. Machida, Journal of Physics and Chemistry of Solids **69**, 3324 (2008).

[4] S.R. White, Physical Review Letters **69**, 2863 (1992); Physical Review B **48**, 10345 (1993).

[5] U. Schollwock, Review of Modern Physics **77**, 259 (2005); K. Hallberg, Advances in Physics **55**, 477 (2006).

[6] E. Jeckelmann, Phys. Rev. B **66**, 045114 (2002).

1.4.3 Large-scale simulation for the fundamental understanding of superconductivity

Hole loalization in strongly correlated and disorderd systems: DMRG studies for 1-D and 3-leg ladder random Hubbard models

Masahiko Okumura, Susumu Yamada, Nobuhiko Taniguchi[1)], and Masahiko Machida

1) Institute of Physics, University of Tsukuba

Metal–Insulator transition observable in transition metal oxides and the others has been a major focus of research in solid state physics. Electronic states drastically change close to the transition, and emergent phases show very rich varieties depending on crystalline structures and other factors. For example, High-T_c superconductors are weakly coupled layered materials, and their superconductivity emerges close to antiferromagnetic insulator by doping hole career.

Generally, careers, i.e., electrons or holes simply localize in the insulating phase. There are two well-known reasons for the localization. The first one is randomness, which is inevitable in solid states, and the Anderson transition is its consequence. The second one is Coulomb repulsion, which causes the Mott transition and creates rich strongly correlated phases close to the transition.

Recently, an interplay between the randomness and the Coulomb repulsion has attracted much attentions of condensed matter physicists. The reason is that their competition or cooperation may give rise to non-trivial phases, which are much beyond our theoretical expectation. In fact, there is an argument that randomness has an important role on mysterious features observed in under-doped High-T_c superconductors.

As a model system capturing the interplay, the random Hubbard model has been intensively examined. However, the main theoretical target has been limited to the half-filling and the quarter filling, and the doped cases have been never explored. This is because the doped system is too difficult to solve for not only theoretical treatments but also numerical simulations. Namely, any theoretical studies may fail to predict the ground state in the model due to difficulties.

Very recently, we have suggested that the difficulty is broken by employing the density-matrix renormalization group (DMRG) method [1,2]. We study the one-dimensional (1-D) random Hubbard model by using DMRG method and also examine 3-leg ladder random Hubbard model by using directly extended DMRG method [3]. We note that our focus of interest is a slightly doped region very close to the half-filling, which is deeply related to complicated phenomena seen in heavily underdoped High-T_c superconductors.

We show the charge distribution for 2-hole case in the 3-leg random Hubbard model. On clearly find the doped holes are sharply localized and the Mott insulating area appears. This behavior is same as one-dimensional case [4]. Then the hole-localization is expected to be a general phenomenon in low-dimensional random Hubbard model.

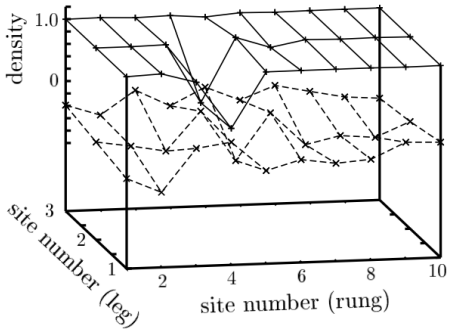

Fig. 1: Charge distribution and random potential for strong interacting fermionic atom system with strong random potential.

We studied 1-D and 3-leg ladder random Hubbard model under the open boundary condition by using DMRG method [3]. We extended our study to 3-leg model. In 3-leg case, we found the formation of the Mott plateau and hole localized valley.

References

[1] S.R. White, Physical Review Letters **69**, 2863 (1992); Physical Review B **48**, 10345 (1993).

[2] U. Schollwock, Review of Modern Physics **77**, 259 (2005); K. Hallberg, Advances in Physics **55**, 477 (2006).

[3] M. Okumura, S. Yamada, N. Taniguchi, and M. Machida, Physica C: superconductivity and its applications **468**, 1241 (2008).

[4] M. Okumura, S. Yamada, N. Taniguchi, and M. Machida, Physical Review Letters **101**, 016407 (2008).

1.4.3 Large-scale simulation for the fundamental understanding of superconductivity

Condition for emergence of complex eigenvalues in the Bogoliubov-de Gennes equations

Yusuke Nakamura[1)], Makoto Mine[2)], Masahiko Okumura and Yoshiya Yamanaka[3)]

1) Department of Materials Science and Engineering, Waseda University
2) Department of Physics, Waseda University
3) Department of Electronic and Photonic Systems, Waseda University

Experiments of the Bose-Einstein condensates (BECs) of neutral atomic gases, first realized in 1995, have been offering challenging subjects in theoretical foundations of quantum many-body problem. Among others, some unstable phenomena of the BECs are very interesting, since to formulate unstable quantum many-body systems is an open problem. Observed examples of such phenomena are the split of a doubly quantized vortex into two singly quantized vortices, the decay of a condensate flowing in an optical lattice, and the decay of the initial configuration in a quenched ferromagnetic spinor BEC. These phenomena are observed at very low temperatures where the dissipative mechanism brought by the thermal cloud is negligibly small. Such instability is called “dynamical instability,” and is distinguished from the “Landau instability,” in which the thermal cloud plays a dissipative role.

For the theoretical investigations of the instability, the Bogoliubov–de Gennes (BdG) equations are employed. The BdG equations follow from linearization of the time-dependent Gross-Pitaevskii (TDGP) equation and determine the excitation spectrum of the condensate. The BdG equations have complex eigenvalues for some cases, and the presence of the complex eigenvalues is interpreted as the sign of dynamical instability. This instability is associated with the decay of the initial configuration of the condensate and can occur even at zero temperature. On the other hand, the Landau instability, which is characterized by the negative eigenvalues and in which the thermal cloud drives the system toward a lower energy state in a dissipative way, is impossible at very low temperature. It is reported that the BdG equations have complex eigenvalues in the cases where the condensate has a highly quantized vortex, where the condensate flows in an optical lattice , and where the condensate has gap solitons, and in the case of the multi-component BECs. It is suggested that some degeneracy between a positive mode and a negative one in the BdG equations is necessary for the emergence of complex eigenvalues.

As for the dynamical instability, another treatment is known, which we refer to as the RK method given by Rossignoli and Kowalski [1]. In this method the quantum Hamiltonian of the quadratic form of creation and annihilation operators is considered, and the complex modes appear as a result of diagonalizing it with unusual operators which are neither bosonic nor fermionic ones. In the previous work [3], our group has analytically derived the condition for the existence of complex modes for the case where the condensate has a highly quantized vortex, by using the RK method. There a small coupling expansion is adopted, and the two-mode approximation on the Hamiltonian is assumed and is essential. The three-mode analysis is also performed, and it is confirmed that the condition for the existence of complex modes is not modified. However, it is not clarified why the two-mode approximation is crucial for the appearance of complex modes.

We studied analytically the BdG equations whose two-component eigenfunctions are not only of positive norm but also of negative norm or of zero norm [2]. It is shown that the degeneracy between a positive-norm mode and a negative-norm one is necessary for the emergence of the complex eigenvalues. To do this, we expand the BdG equations in powers of a shift about a value of the coupling constant at which all the eigenvalues are real. It is emphasized that the present analysis is quite simple and general, not restricted to particular systems. Furthermore, we have confirmed why the two-mode approximation applied in our previous work [3] is valid.

References

[1] R. Rossignoli and A.M. Kowalski, Phys. Rev. A **72**, 032101 (2005).

[2] Y. Nakamura, M. Mine, M. Okumura, and Y. Yamanaka, Physical Review A **77**, 043601 (2008).

[3] E. Fukuyama, M. Mine, M. Okumura, T. Sunaga, and Y. Yamanaka, Physical Review A **76**, 043608 (2007).

1.4.3 Large-scale simulation for the fundamental understanding of superconductivity

Condition for existence of complex modes in a trapped Bose-Einstein condensate with a highly quantized vortex

Eriko Fukuyama[1], Makoto Mine[1], Masahiko Okumura, Tomoka Sunaga[1] and Yoshiya Yamanaka[2]

1) Departmnet of Physics, Waseda University

2) Department of Electronic and Photonic, Waseda University

The Bose-Einstein condensates _BECs_ of neutral atomic gases were realized in 1995, and several kinds of vortices inside the BECs have been observed: the singly quantized vortex, the vortex lattice, and the doubly quantized vortex which was created by the topological phase engineering. In particular, an interesting phenomenon was observed: a doubly quantized vortex decayed into two single quantized vortices spontaneously. The theoretical investigations on the instability of the highly quantized vortex of the neutral atomic BEC were made by several authors. They performed numerical calculation of the Bogoliubov-de Gennes _BdG_ equations, which describe the *c*-number fluctuation around the condensate and are obtained by the linearlization of the time evolution equation of the condensate, that is, the time dependent Gross-Pitaevskii (GP) equation. They found that the equations have complex eigenvalues when a condensate has a vortex with the winding number two, three, or four. The complex eigenvalues cause the blowup or damping of the *c*-number fluctuation. This instability of the condensate, caused by the complex eigenvalues of the BdG equations, is called “dynamical instability.” However, it is still unknown whether a highly quantized vortex with an arbitrary high winding number always brings complex eigenvalues and which eigenvalues become complex. It should also be stressed that the relation between the “dynamical instability” in theoretical concept and the observed decay of the doubly quantized vortex is not elucidated fully and still under investigation. As for the “complex modes,” there is another known treatment, developed by Rossignoli and Kowalski [1]. We refer to it as the RK method. In this method the quantum Hamiltonian of the quadratic form of creation and annihilation operators is considered, and the complex modes appear as a result of diagonalizing it with unusual operators which are neither bosonic nor fermionic ones. Obviously the meaning of the complex modes in the RK method is different from one mentioned above: they are quantum fluctuations in the former, while they are *c*-number ones in the latter. The relation between the complex modes and the complex eigenvalues of the BdG equations has not been established. Furthermore, we point out that the interpretation of the complex eigenvalues of the BdG equations in the case that they are treated as quantum fluctuations, as well as of the complex modes of the RK method, is not simple. We recently proposed an approach of quantum field theory, using the eigenfunctions of the BdG equations including those belonging to the complex eigenvalues and considering the free quantum Hamiltonian consistently, although the content of this paper is not related to the approach directly. In this paper, we derive the conditions for the existence of the complex modes in a trapped BEC with a highly quantized vortex analytically using the RK method within the two-mode approximation and small coupling expansion. Using the condition, we can show that any highly quantized vortex brings the complex modes and identify partially which mode is the complex one. The condition is also useful for checking the results of the numerical calculation.

We derived the analytic expression of the condition for the existence of the complex modes when the condensate has a highly quantized vortex [2], using the method developed by Rossignoli and Kowalski [1] for the small coupling constant, under the two-mode approximation. Finally, we comment that the physical interpretation of the complex modes is not simple and is not settled yet. We recently proposed a quantum field theoretical treatment associated with the complex modes and sought a new interpretation [3,4].

References

[1] R. Rossignoli and A.M. Kowalski, Phys. Rev. A **72**, 032101 (2005).

[2] E. Fukuyama, M. Mine, M. Okumura, T. Sunaga, and Y. Yamanaka, Physical Review A **76**, 043608 (2007).

[3] M. Mine, M. Okumura, T. Sunaga, and Y. Yamanaka, Ann. Phys. (N.Y.) **322**, 2327 (2007)

[4] K. Kobayashi, M. Mine, M. Okumura, and Y. Yamanaka, Ann. Phys. (N.Y.) **323**, 1247 (2008).

1.4.3 Large-scale simulation for the fundamental understanding of superconductivity

Andreev Bound States and Tunneling Characteristics of a Noncentrosymmetric Superconductor

C. Iniotakis[1], N. Hayashi, Y. Sawa[2], T. Yokoyama[2], U. May[1], Y. Tanaka[2] and M. Sigrist[1]

1) ETH Zurich, Switzerland 2) Nagoya University

Since the early 1960s, tunneling spectroscopy has played an important role in gathering information about the gap function of conventional superconductors.1 In the context of unconventional superconductivity, tunneling appeared as a tool to probe the internal phase structure of the Cooper pair wave functions. Surface states with subgap energy, known as Andreev bound states, provide channels for resonant tunneling leading to so-called zero-bias anomalies. The quasiparticle tunneling has emerged as an important phase sensitive probe for unconventional superconductors.

The recent discovery of superconductivity in the heavy fermion compound CePt3Si has motivated intense experimental and theoretical studies, since its crystal symmetry is lacking a center of inversion. The absence of inversion symmetry yields a classification scheme of the pairing symmetry, different from the standard distinction between even- and odd-parity states. Actually, the pairing states in these noncentrosymmetric superconductors can be viewed as states of mixed parity which do not have a definite spin-singlet or spin-triplet configuration.

We address the problem of possible Andreev bound states at the boundaries of a noncentrosymmetric superconductor such as CePt3Si and demonstrate that quasiparticle tunneling could give important information on the gap structure of such a material.

We calculate the normalized differential tunneling conductance for a normal metal/noncentrosymmetric superconductor junction at low temperatures (Figs. 1 and 2).

We find that the superconducting phase with mixed parity can give rise to characteristic zero-bias anomalies in certain junction direction (Fig. 2). Andreev bound states at the interface are the origin of these zero-bias anomalies. The tunneling characteristics for different directions allow us to test the structure of the parity-mixed pairing state [1].

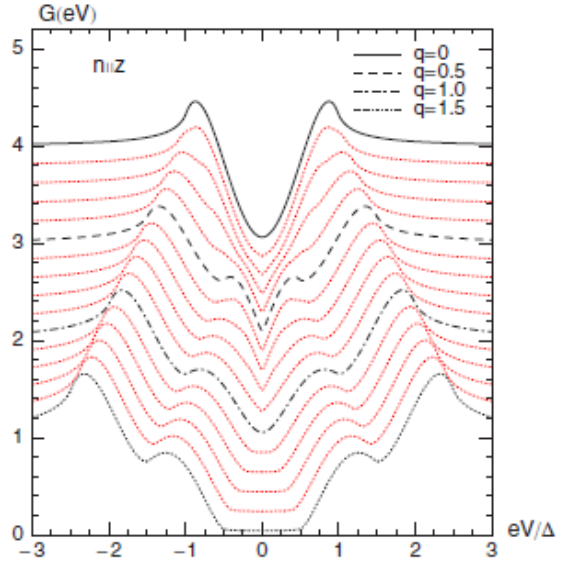

Fig. 1: Calculated tunneling conductance as a function of the bias voltage (the tunneling current flows *parallel* to the *c* axis of CePt3Si).

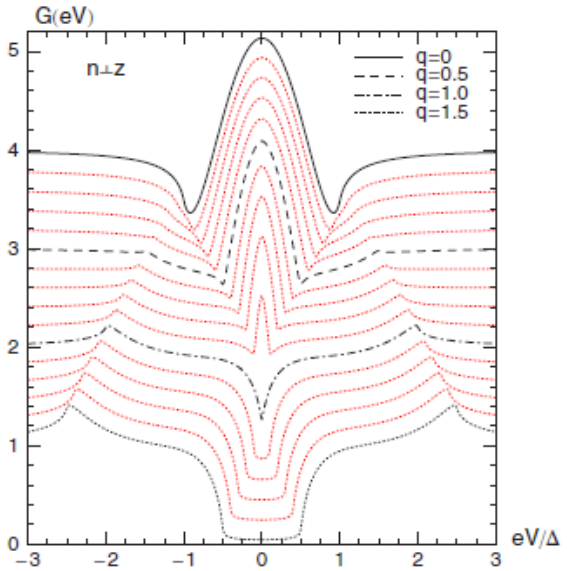

Fig. 2: calculated tunneling conductance as a function of the bias voltage (the tunneling current flows *perpendicular* to the *c* axis of CePt3Si).

Reference

[1] C. Iniotakis, N. Hayashi, Y. Sawa, T. Yokoyama, U. May, Y. Tanaka and M. Sigrist, Phys. Rev. B Vol.76, p.012501 (2007).

1.4.3 Large-scale simulation for the fundamental understanding of superconductivity

Ginzburg-Landau simulation for a vortex around a columnar defect in a superconducting film

Noriyuki Nakai[1)], Nobuhiko Hayashi, Masahiko Machida

1) Center for Computational Science & e-Systems, JAEA

Moving vortices driven by an applied supercurrent lead to the energy loss in superconductors. It is, therefore, necessary for the vortex motion to be suppressed, for an efficient application of superconductors under magnetic fields. Columnar defects are candidate for providing strong vortex-pinning sources. It is important to investigate properties of a columnar defect as a vortex pining.

We study the vortex pinning and depinning phenomena in a superconducting film that contains a single columnar defect. [1] Our simulation study is based on the Ginzburg-Landau theory. As the columnar defect we consider two models, which are metal and insulator. In order to examine how strong the vortex pinning is, we prepare a vortex trapped along a columnar defect. Then, we apply an external magnetic field perpendicular to this columnar defect.

Here, we show that the vortex depinning certainly occurs. The obtained profile of the order parameter under a certain applied field is displayed in Figs. 1 for the metal defect case. In Fig. 1(a) and (b), the amplitude of the order parameter is suppressed at the vortex core. Indeed, in Fig. 1(c) there is a phase singularity at the vortex core where the suppression of the amplitude is situated.

We investigate the thickness and field dependence of the vortex-depinning. As the result by plotting the depinning field, we obtain the pinning-depinning phase diagram for the thickness vs. the applied field in Fig. 2. When the film is thin, the depinning field increases. Moreover, in the insulator case the pinning region in the phase diagram is larger than the metal case. We can see that the pinning force is dependent on the length and the types of the columnar defect. The columnar defect of the insulator seems to be available for the strong pinning source.

Many body effects as the collective pinning cannot appear, because this study considers the single vortex and single columnar defect. For the improvement of the superconducting tape the study on the collective pinning is necessary.

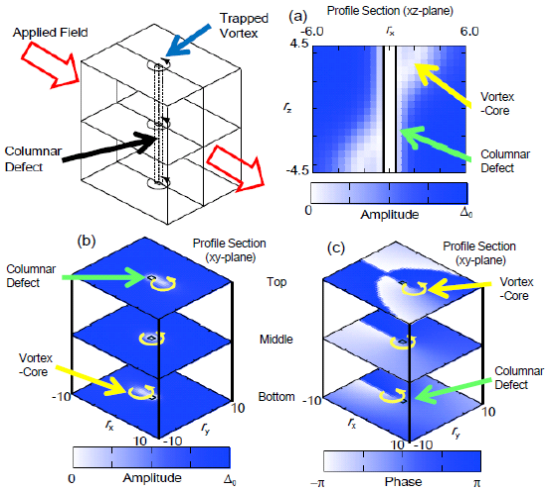

Fig. 1: Of the amplitude of the order parameter profiles for XZ-plane (a) and XY-Plane (b). (c) XY-plane profile of the phase of the order parameter.

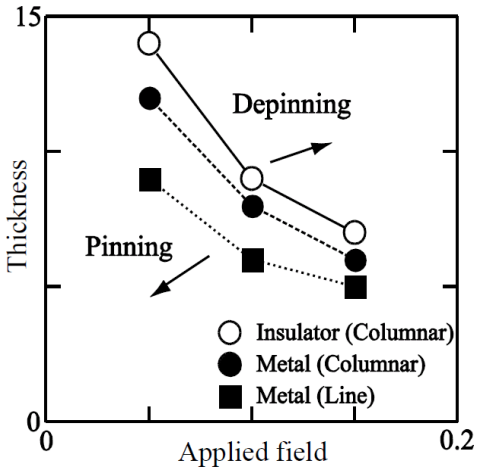

Fig. 2: Pinning-depinning phase diagram for the thickness vs. the applied field.

References (Arial 9pt Bold)

[1] N. Nakai, N. Hayashi and M. Machida, Journal of Physics and Chemistry of Solids Vol. 69, 3301-3303 (2008).

1.4.3 Large-scale simulation for the fundamental understanding of superconductivity

Simulation studies for the vortex depinning dynamics around a columnar defect in superconductors

Noriyuki Nakai[1)], Nobuhiko Hayashi, Masahiko Machida

1) Center for Computational Science & e-Systems, JAEA

The vortex-dynamics of type II superconductors has attracted much attention from many reseachers. One of reasons is that the electric resistivity and this vortex-dynamics is closely correlated. The vortex-motion produces the electric field. For realizing the zero resistivity we have to stop the vortex-motion. On the other hand, the vortex is a circular current of charged particles, therefore we can control its motion by handling the electric and magnetic fields. This property is advantage for the development of the superconducting device.

Because the vortex dynamics is essential for the characteristic of the superconducting material, it is necessary to understand the vortex pinning-dynamics. To study on the vortex-dyanmics and vortex pinning we performed the numerical simulation of the vortex dynamics by using the time-dependent Ginzburg-Landau equation with the complex relaxation rate and Maxwell equation. The simulation considered two pining models. One is metallic case, the other is insulator case. The vortex-flow voltage induced by the vortex-motion and the Hall coefficient were obtained by our simulated calculation.

In Fig. 1 vortex trajectories are shown in the case of the metal-pinning. The vortex-pinning and depinning can be seen at the pinning site. Figure 2 shows the vortex trajectories in the case of the insulator pinning. In contrast, this case does not show the vortex depining at the pinning site.

The difference of the interface between the superconductor and pinning site can be confirmed. In the case of the insulator-pinning site where is trapped vortex, the super current around the pinning site is enhanced as in Fig. 3. This enhanced current generates large repulsive force between the trapped and moving vortices. Because of this large repulsive force the vortex motion is heavily altered by the insulator pinning. As results, vortex motion around the insulator pinning site is slower than the metal pinning case.

By the simulated calculation we investigate that the vortex motion is dependent on the pinning model, which is metal or insulator. Also, the induced voltage by the moving vortices is studied [1].

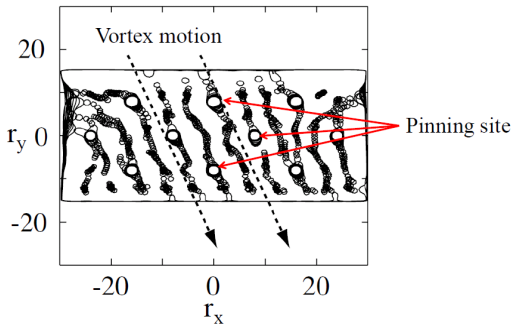

Fig. 1: Vortex trajectory in the metal-pinning case.

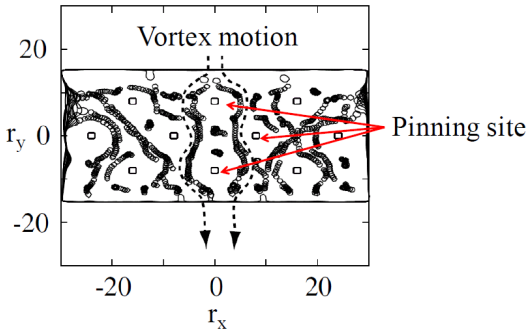

Fig. 2: Vortex trajectory in the insulator-pinning case.

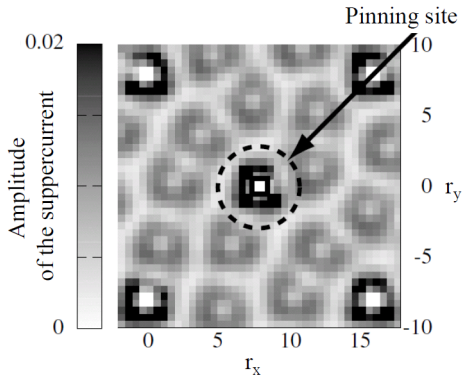

Fig. 3: Supercurrent amplitude in the in the insulator-pinning case

References (Arial 9pt Bold)

[1] N. Nakai, N. Hayashi and M. Machida, Physica C Vol. 468, 1270-1273 (2008).

Ultra large-scale exact-diagonalization for confined fermion-Hubbard model on the Eearth

1.4.3 Large-scale simulation for the fundamental understanding of superconductivity

Simulator: Exploration of superfluidity in confined strongly-correlated systems

Susumu Yamada, Toshiyuki Imamura[1)], Takuma Kano, Yoji Ohashi[2)], Hideki Matsumoto[3)], Masahiko Machida

1) Department of Computer Science, The University of Electro-Communications
2) Faculty of Science and Technology, Keio University
3) Institute of Physics, University of Tsukuba

The successful achievements of the Bose-Einstein condensation in the trapped atomic Bose gas were honored by the Nobel Prize in 2001. After that, atomic physicists have challenged another more difficult condensation in the atomic Fermi gas. The condensation and the resultant superfluidity in fermion system is one of the most universal issues in fundamental physics, since particles which form matters, i.e., electron, proton, neutron, quark, and so on, are fermions and an exploration for their many-body ground states is a central target in modern physics. Motivated by interests based on such a wide background, we numerically explore a possibility of superfluidity in the trapped atomic Fermi gases. Our undertaking model is the fermion-Hubbard model with a trapping potential. The Hubbard model describes a many-body fermion system on a discrete lattice, and the model captures an essence of strongly-correlated electronic structures in solid state systems. Furthermore, whether the model can describe the high temperature superconductivity or not is a main issue in condensed matter physics. If infinite computational resources are permitted, the exact diagonalization is clearly the best approach for the Hubbard model.

In this study, we develop a new type of high performance application which solves the eigenvalue problem of the Hubbard Hamiltonian matrix on the Earth Simulator and present our progress in numerical algorithm and parallelization technique to obtain the best performance and solve the world-record class of large matrices.

In the algorithmic issue, we suggest a new profitable algorithm (PCG method). Comparing between the new method and the conventional one (Lanczos method), we find that the new method is much more excellent except for the memory usage. On the other hand, in the parallelization technique issue, we examine an effect of the hybrid parallelization which combines the inter-node parallelization using MPI for distributed memory with the intra-node parallelization using the automatic parallelization for shared memory in addition to the vectorization. By developing these high-performance computing techniques, we have obtained the excellent performance in the new algorithm and the world record of the large matrix operation (see Tab. 1 and Fig. 1). The calculation results have revealed that when the Coulomb repulsion exceeds a critical value and the confined potential is strong enough to make a Mott insulator region around the potential center, a Cooper pairing function develops between the both sides of the Mott region. This pairing is found to be strongly correlated to the spin structure inside the Mott region, which shows a dimerized character of spin-singlet [1-2].

Tab. 1: The dimension of Hamiltonian matrix.

Model	Number of sites	Number of fermions	Dimension of Hamiltonian	Number of PE's
1	24	12	18,116,083,216	1024
2	21	16	41,408,180,100	2048
3	22	16	102,252,852,900	4096

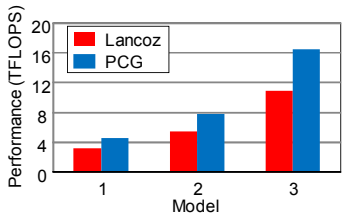

Fig. 1: Performances of the Lanczos method and the PCG method

References

[1] S. Yamada, T. Imamura, T. Kano, Y. Ohashi, H. Matsumoto, M. Machida, Journal of the Earth Simulator, Vol. 7, pp.23-35 (2007).

[2] S. Yamada, T. Imamura, T. M. Machida, Proceedings of Supercomputing 2005 (12-18 November 2005, Tampa, U.S.A) CD-ROM (2005).

1.4.3 Large-scale simulation for the fundamental understanding of superconductivity

Strong pairing and microscopic inhomogeneity of lattice fermion systems

Susumu Yamada, Yoji Ohashi[1)], Hideki Matsumoto[2)], Masahiko Machida

1) Faculty of Science and Technology, Keio University

2) Institute of Physics, University of Tsukuba

The scanning tunneling microscopy (STM) measurement has recently revealed that the density of states (DOS) in the low-energy region, i.e., the energy gap associated with superconductivity shows atomic-scale spatial inhomogeneity in cuprate high-Tc superconductors. This result indicates that the pairing amplitude and the charge density inhomogeneously distribute in atomic scale. Such a microscopic electronic inhomogeneity can be never explained by the conventional BCS theory, since a long coherence of superconductivity beyond atomic scale usually screens atomic-scale inhomogeneity. Thus, the observed inhomogeneity is found to be a key character of novel superconductivity emerged in strongly-correlated systems. In this study, we numerically study this controversial issue, i.e., an interplay between superconductivity and inhomogeneity, based on attractive Hubbard model, which can describe a variety from weak to strong pairing and their superconductivity.

Very recently, the optical lattice created in cold-atom systems has been proven to be quite useful for studying experimentally strongly-correlated systems due to its high controllability, namely the interaction and the lattice structure are almost freely variable. Generally, in solid state systems, such a tuning is extremely difficult. This advantage in the optical lattice has been used to observe the superfluid-insulator transition in an atomic Bose gas and the existence of the Fermi surface in an atomic Fermi gas. However, we note in the atomic gas systems that the translational symmetry is always broken because the gas should be confined by harmonic and other type potentials to avoid an escape of atomic gas. This leads to a new interest how strongly-correlated systems behave in the absence of translational symmetry, while this requires a special attention for a comparison between the optical lattice and the solid state.

We simulate attractive Hubbard models with confinement potentials motivated by two interests. The first one is the prediction of the ground state in the optical lattice, and the second one is the reaction of Cooper pairs on the broken translational symmetry. Especially, we note that the latter interest comes from inhomogeneous superconductivity seen in high-Tc superconductors as the universal observation of the checkerboard pattern inside the vortex core. Thus, we examine the ground state of the attractive Hubbard model with confinement potential using the density-matrix renormalization group (DMRG) methods.

The numerical results reveal that fine inhomogeneous zig-zag patterns universally emerge in the 1-D model case (see Fig. 1) and the zig-zag structure becomes checkerboard type in the 2-D one (see Fig.2). We found that, when the tightly-bound pairs dominate due to the strong attractive interaction, the bound pairs form inhomogeneous patterns in the absence of the translational symmetry. This suggests a novel mechanism of inhomogeneity in strongly correlated fermion systems [1].

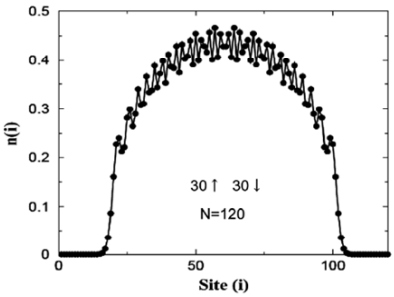

Fig. 1: The particle density profile obtained by the DMRG method. This figure shows the result in a 120-site Hubbard model with 30 up-spins and 30 down-spins [1].

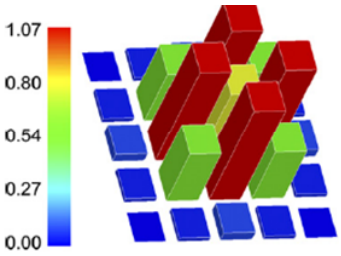

Fig. 2: The particle density profile obtained by the exact diagonalization method. This figure shows the result in a 5×5-site Hubbard model with 10 up-spins and 10 down-spins [1].

Reference

[1] S. Yamada, Y. Ohashi, H. Matsumoto, M. Machida, Physica C , 463–465, pp. 103–106 (2007).

1.4.3 Large-scale simulation for the fundamental understanding of superconductivity

On-site pairing interaction and quantum coherence in strongly correlated systems

Susumu Yamada, Masahiko Machida, Takuma Kano, Toshiyuki Imamura[1)], Tomio Koyama[2)]

1) Department of Computer Science, The University of Electro-Communications

2) IMR, Tohoku University,

Since the observation of the crossover from weakly coupled BCS to BEC of strongly coupled pairs in atomic Fermi gases, its advancements have attracted a number of physicists. In this crossover, there is a significant interest, i.e., how quantum coherent characters change with the variation of the interaction strength. We have not still sufficiently explored the nature of strongly coupled superfluidity. The atomic Fermi gas gives us a timely chance.

The Hubbard model is a typical model describing strong correlations of electrons in solid state materials. The nature of the ground state of the model in the thermodynamical limit is even now a central issue in theoretical studies on strongly correlated fermions, while its dynamics in finite or confined models is a new target in atomic Fermi gases loaded on the optical lattice. In atom gas systems, the optical lattice was successfully created, and the fermion superfluidity on the lattice is now accessible. Such a current advancement raises several fundamental problems, one of which is the relationship between the quantum coherence and the pairing interaction strength as described above. In this research, we numerically investigate the Hubbard model in the presence of the trap potential and study a toy model, i.e., one-dimensional (1-D) Hubbard model embedded in the double-well trap potential (see Fig. 1), to examine quantum dynamical behaviors related to the tunneling between both wells.

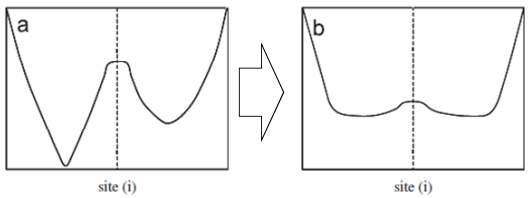

Fig. 1: The time-varying potential shape. At T=0, the shape suddenly changes from left (a) to right (b).

The typical examples of the initial states are given in Fig. 2(a), where pairing interaction $|U/t|$ increases along y-axis ($|U/t|$= 1, 2, 3, 5, and 10 from the front to the back). In Fig. 2, the height and the color of the contour map represent the amplitude of the wave function. It is found that the particles are perfectly confined inside the left-hand side well at the initial time for all $|U/t|$ cases. Moreover, one cannot find out any significant difference of the particle distribution in these initial states. This reason is that the energy scale of the confinement potential is larger than that of the interaction.

Let us show the time evolutions from the initial states after changing the potential shape from asymmetric Fig. 1(a) to symmetric one Fig. 1(b). Fig. 2(b) presents a snapshot for $|U/t|$= 1, 2, 3, 5, and 10 at T=250. It is found that the wave functions smoothly move to the right-hand side when $|U/t|$ is relatively small, while they do not almost do so when $|U/t|$ is large. These results indicate that the dynamics looks like the so-called ‘‘quantum dynamics’’ when the magnitude of $|U/t|$ is small, while the dynamical feature changes to ‘‘classical dynamics’’ when the interaction magnitude becomes large [1].

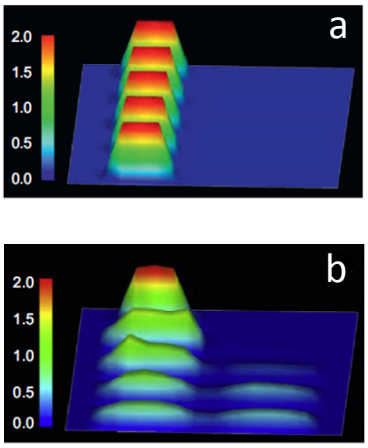

Fig. 2: Particle distributions at T=0 (a) and T=250 (b). From the front, U/t=-1, -2, -3, -5, and -10.

Reference

[1] S. Yamada, M. Machida, T. Kano, T. Imamura, T. Koyama, Journal of Physics and Chemistry of Solids, 69, pp.3395–3397 (2008).

1.4.3 Large-scale simulation for the fundamental understanding of superconductivity

Parallel computing of directly-extended density-matrix renormalization group to two-dimensional strongly correlated quantum systems

Susumu Yamada, Masahiko Okumura, Masahiko Machida

The superfluidity discovered in atomic Fermi gas in 2004 was much beyond our imagination on superfluidity because the attractive interaction between atoms is so strong that the strength results in a room temperature superconductivity if atoms can be replaced by electrons. Recently, this fact has intensively inspired physicists to numerically study strongly-interacting quantum many-body systems in exact ways. One of the numerical approaches on the systems is the Density Matrix Renormalization Group (DMRG) method. The method always keeps the number of the relevant quantum states constant on an increment of the model size by renormalizing the extended states as Fig. 1. The reliable results by the DMRG method are limited only for 1-D or two-leg ladder models in spite of a great demand for 2-D system. The reason is that the direct extension to 2-D requires an enormous memory space while the technical extension based on 1-D algorithm does not keep the accuracy in 1-D systems. Therefore, we parallelize the direct 2-D DMRG code on a large-scale supercomputer and examine the accuracy and the performance for typical lattice models, i.e., Heisenberg and Hubbard models. The parallelization is mainly made on the multiplication of the Hamiltonian matrix and vectors.

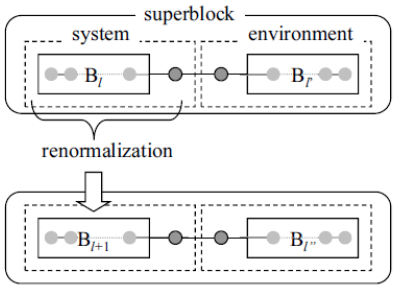

Fig. 1: A schematic figure of the renormalization scheme of DMRG for a 1-D lattice model. The so-called “superblock” is composed of the system and the environment. The rectangles inside the above superblock represent blocks containing l and l' lattice sites, and the dark circles represent single sites. New block B_{l+1} is formed by renormalizing the left block B_l and the left single site (dark circle) while keeping the number of the states in the system block.

Let us present the performance of the direct 2-D DMRG method. A test example is the 7-leg (10×7-site) Heisenberg model. Tab. 1 shows a relationship between the states kept number m and the elapsed time. When m, which is the number of the states kept, is small (see e.g., m = 32), the parallelization effect is found to be poor. However, as m increases, i.e. the size of the Hamiltonian matrix becomes huge, the scalability is improved. In the numerical experiment on m = 128, the elapsed time of the calculation using 128 processors is about three times faster than the case using 32 processors. Another test example is the 4-leg (10 × 4-site) Hubbard model with 38 fermions (19 up-spins, 19 down-spins). Tab. 2 shows a relationship between the states kept number m and the elapsed time. We find that as the number of processors increases from 32 to 128 in m = 128, the elapsed time is reduced to be about one half. These results for both typical models show that the present parallelization scheme is promising, since the obtained ground state approaches to the true ground state with increasing the number of the states kept [1].

Tab. 1: Relationship between the states kept number m and the elapsed time of parallelized DMRG code for 10×7-site Heisenberg model on SGI Altix3700Bx2.

No. of CPU's	Elapsed Time (sec)		
	$m = 32$	$m = 64$	$m = 128$
32	123.46	806.29	6687.38
64	92.85	501.92	3562.31
128	88.84	362.04	2102.81

Tab. 2: Relationship between the states kept number m and the elapsed time of parallelized DMRG code for 10×4-site Hubbard model on SGI Altix3700Bx2.

No. of CPU's	Elapsed Time (sec)		
	$m = 32$	$m = 64$	$m = 128$
32	155.50	745.54	4469.36
64	127.99	645.67	2658.45
128	130.12	515.49	2227.02

Reference

[1] S. Yamada, M. Okumura, M. Machida, Proceedings of the IASTED International Conference on Parallel and Distributed Computing and Networks, (12-14 Febrary 2008, Innsbruck, Austria) 579-076, pp. 175-180 (2008).

1.4.3 Large-scale simulation for the fundamental understanding of superconductivity

High performance computing for eigenvalue solver in density-matrix renormalization group method: Parallelization of the Hamiltonian matrix-vector multiplication

Susumu Yamada, Masahiko Okumura, Masahiko Machida

Quantum lattice systems, e.g. Heisenberg model and Hubbard model, have attracted a tremendous number of physicists since the systems exhibit a lot of interesting phenomenon such as High-Tc superconductivity. In order to understand the systems, some computational methods have been proposed. The most accurate one of them is the exact diagonalization method, which solves the ground state (the smallest eigenvalue and the corresponding eigenvector) of the Hamiltonian matrix derived from the systems. However, the dimension of the Hamiltonian matrix for the exact diagonalization method increases almost exponentially with the number of the lattice sites. Thus, the limit of the simulation on a supercomputer with a terabyte memory system is an about-20-site system[1].

One of methods to overcome the memory-size explosion problem is the Density Matrix Renormalization Group (DMRG) method. The DMRG method keeps the number of the relevant quantum states constant by renormalizing the states of the previous step on enlarging the system (see Fig. 1). Since the DMRG method has been originally developed for 1-D models, many extended method to a 2-D model have been proposed. The DMRG method can be directly extended to an *s*-leg (2-D) model as depicted in Fig. 2. The extension strategy is promising for the excellent accuracy and the good convergence property. However, the method leads to a large amount of memory consumption. Thus, we propose the parallelization technique for the direct extension of DMRG method on a distributed-memory parallel computer, which totally has a huge memory system.

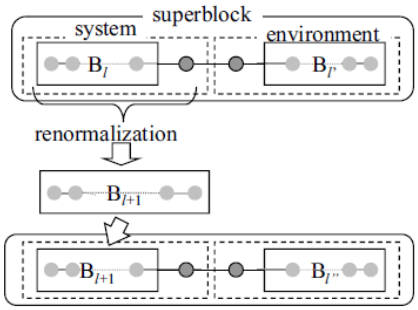

Fig.1 A schematic figure of the renormalization scheme of DMRG method for a 1-D lattice model [2].

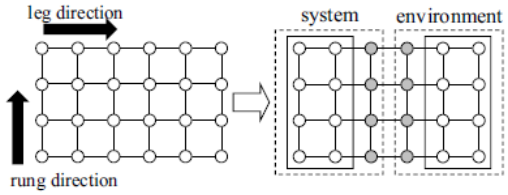

Fig. 2: A superblock configuration in the direct extension of DMRG to a 4-leg model.

We examine the performance of the direct extension 2-D DMRG method on SGI Altix3700Bx2 in Japan Atomic Energy Agency. A test example is 4-leg (10 × 4-site) Hubbard model with 38 fermions (19 up-spins, 19 down-spins). Fig. 3 shows a relationship between the number of states kept *m* and the elapsed time. We find that as the number of processors increases from 32 to 128, the elapsed time is reduced to be about one half, when *m* is about larger than 128. The result shows that the present parallelization scheme is promising, since the obtained ground state approaches to the true ground state with increasing the number of the states kept *m* [2]

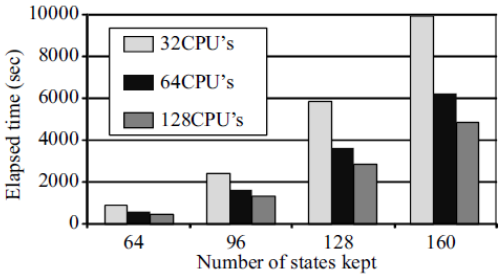

Fig. 3: Relationship between the number m of states kept and the elapsed time of the direct extension DMRG method for 10×4-site Hubbard model on SGI Altix 3700Bx2.

References

[1] S. Yamada, T. Imamura, T. M. Machida, Proceedings of Supercomputing 2005 (12-18 November 2005, Tampa, U.S.A) CD-ROM (2005).

[2] S. Yamada, M. Okumura, M. Machida, Proceedings of 8th International Meeting on High Performance Computing for Computational Science (VECPAR'08) (24-27 June 2008) CD-ROM(2008).

1.4.3 Large-scale simulation for the fundamental understanding of superconductivity

Vortex core structure in strongly correlated superfluidity

Susumu Yamada, Masahiko Okumura, Masahiko Machida, Yoji Ohashi[1)], Hideki Matsumoto[2)],

1) Faculty of Science and Technology, Keio University

2) I IMR, Tohoku University,

The vortex core electronic structure in high-Tc superconductors has attracted much attention because the structure is regarded to reflect their anomalous electronic properties. In high-Tc superconductors, the superconducting state occupies a very wide area in the phase diagram, and the anomalous properties are masked by the superconductivity. On the other hand, the superconducting gap is locally suppressed inside the vortex core under the presence of the magnetic field, and the competing orders against the superconductivity are expected to emerge inside the vortex core. Such an interesting idea has been intensively studied by experimentalists who mainly operate the scanning tunneling microscope, and peculiar spatially modulated structures have been actually observed inside the vortex core. In this study, we suggest an artificial but fruitful way to theoretically study the peculiar states inside the vortex core. We create a local situation similar to the vortex core and exactly check which kind of orders emerge.

The high-Tc superconductivity emerges by doping hole carriers. Thus, the depressed matter inside high-Tc superconducting vortex core corresponds to the hole carrier, and the core region locally approaches the non-doped phase. Such a situation can be similarly realized by trapping electrons inside a local region or by locally expelling holes from the region. This is considered to be qualitatively equivalent to a system created by trapping Fermi atoms loaded on an optical lattice inside a harmonic well or other types of wells. Therefore, we study 1-D optical lattice trapped inside the harmonic well potential by using the density matrix renormalization group (DMRG) method. The present calculation is the first exact calculation although the model system is artificial one. We employ 1-D repulsive Hubbard model with a harmonic trap potential which is given by

$$H_{\mathrm{Hubbard}} = -t\sum_{i,j,\sigma}^{N}(a_{j\sigma}^{\dagger}a_{i\sigma} + H.C.) + U\sum_{i}^{N} n_{i\uparrow}n_{i\downarrow} + V\left(\frac{2}{N-1}\right)^{2} \times \sum_{i,\sigma} n_{i\sigma}\left(i - \frac{N+1}{2}\right)^{2},$$

where $a_{i\sigma}^{\dagger}$ and $a_{i\sigma}$ are the creation and annihilation operators of an electron (a Fermi atom in atomic Fermi gas) with spin (pseudo spin in atomic Fermi gas) $\sigma = \uparrow$ or $\downarrow$ respectively. And, N is the number of the sites of the system. The Hamiltonian includes the on-site repulsive interaction U (>0), as well as a harmonic confinement (trap) potential characterized by V. Fig. 1 shows the numerical results of the Hubbard model with changing the repulsive interaction, the spin polarization ratio, and the number of Fermi particles. The present results are useful for atomic Fermi gases loaded on the optical lattice, while the observed antiferromagnetic local order and its long modulation is very similar to the structure inside the vortex core. We believe that although more careful investigations are required, the present model and calculation capture the essence of the modulate structures inside high-Tc superconducting vortex core.

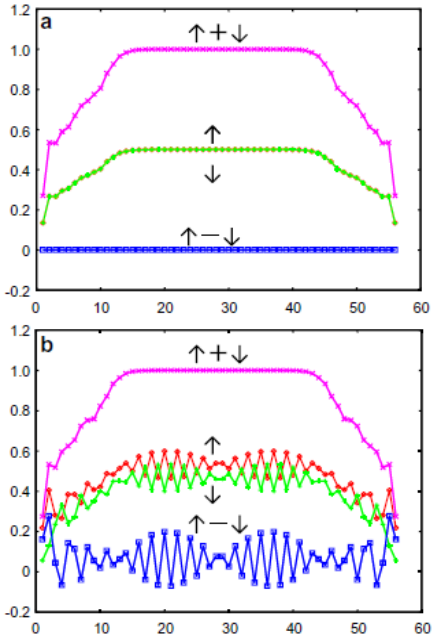

Fig. 1: The DMRG results of the distribution profiles of $n_{\uparrow}+n_{\downarrow}$, $n_{\uparrow}$, $n_{\downarrow}$, $n_{\uparrow}-n_{\downarrow}$ for (a) (24↑, 24↓) and (b) (26↑, 22↓). In all cases, U/t = 7, V/t = 1, and N = 56.

Reference

[1] S. Yamada, M. Okumura,M. Machida, Y. Ohashi, H. Matsumoto, Physica C, 468, pp. 1237–1240 (2008).

1.4.4 Multiscale simulation of nuclear materials and fuels

Modeling of Hydrogen Thermal Desorption Profile of Pure Iron and Eutectoid Steel

Ken-ichi EBIHARA, Tomoaki SUZUDO, Hideo KABURAKI, Kenichi TAKAI[1], and Shigeto TAKEBAYASHI[2]
1) Faculty of Sci.& Tech., Sophia Univ. 2) Nippon Steel Corporation

We have developed a numerical model to simulate the hydrogen desorption profiles for pure iron and eutectoid steel, which is obtained in thermal desorption analysis (TDA). Our model incorporates the equation of McNabb and Foster without the hydrogen diffusion term combined with the Oriani's local equilibrium theory. It is found that the present numerical model successfully simulates the hydrogen desorption profile both for pure iron and for eutectoid steel. We further verify the model by discussing the trapping site concentration.

The thermal desorption analysis (TDA) is one of the experimental methods for identifying different hydrogen trapping states. The TDA measures the amount of hydrogen desorbed from an alloy specimen heated at a constant rate and derives a relation between the desorption rate and the specimen temperature. This relation is called a hydrogen desorption profile, in which are observed several characteristic desorption peaks at certain temperatures. Those peaks correspond to hydrogen trapping states. From hydrogen desorption profiles, we obtain information on hydrogen states and trapping sites, namely microstructural defects,such as vacancies, dislocations, grain boundaries, and interfaces between different phases.

Our proposed model calculates the desorption profile as follows: (Step 1) The initial conditions are set for hydrogen concentration at the interstitial sites C, temperature T, and the occupation ratio at each trap site θ_i ; $C=C_{init}^{total}$, $T=T_{init}$, $\theta_1=\theta_2=0$. (Step 2) By the equilibrium calculation, the amount of hydrogen at the interstitial site, C^{eq}, and at trapping sites, $N_1\theta_1^{eq}$, $N_2\theta_2^{eq}$, is obtained where N_i means the trap site density. (Step3) Hydrogen in the interstitial site is removed as the desorbed hydrogen; $C_{out}=C^{eq}$, i.e. setting the amount of hydrogen at the interstitial site at 0. (Step 4) The hydrogen evolution rate which is plotted on desorption profiles is obtained by dividing the removed hydrogen by a time step (dt) and the ratio of the initial specimen mass and the hydrogen atom mass, M_{init}^{total}/m_H, and temperature is increased by ΔT=[heating rate x dt]. Then (Step 2) is applied to the hydrogen state of (Step 3) with new temperature. (Step 2), (Step 3) and (Step 4) are repeated until the desorbed hydrogen becomes less than a certain threshold.

The numerical calculations have been conducted for the desorption profiles of pure iron and eutectoid steel, and the simulated profiles are in good agreement with the experimental profiles as shown in Fig.1. In the experiment, the specimens which are deformed with the different rate are heated in 200K/hr from the room temperature. In these simulations, the binding energy of the trap site, E_v=61.0kJ/mol for vacancy, E_d=58.6kJ/mol for dislocation, and E_i=84.0kJ/mol for the interface between ferrite and pearlite phases are used and the trap site density N_v=0.5~1.02x10^{26}/m^3, N_d= 3.0~5.3x10^{26}/m^3 for pure iron, and N_v=0.2~0.5x10^{25}/m^3, N_d=0.7~1.7x10^{25}/m^3, N_i=0.0~2.1x10^{25}/m^3 are used. We consider that more detailed knowledge for hydrogen diffusion and microstructures in the alloys is required to verify the numerical model, the simulation results, and the trap site density for each defect.

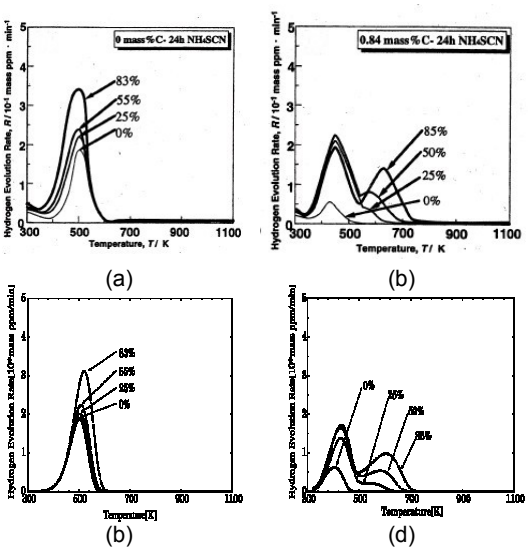

Fig.1 Comparison between experimental and simulation results:(a) and (b) are the experimental results for pure iron and eutectoid steel. (c)and (d) are the simulation results of pure iron and eutectoid steel.

References

[1] Ebihara, et al. Int. ISIJ, Vol.47, 1131(2007).
[2] Ebihara, et al. Tetsu-to-Hagané, Vol.94, 522(2008).

1.4.4 Multiscale simulation of nuclear materials and fuels

Decohesion of iron grain boundaries by sulfur or phosphorous segregation: First-principles calculations

Masatake Yamaguchi, Yutaka Nishiyama, and Hideo Kaburaki

We performed first-principles calculations to simulate the grain boundary decohesion in ferromagnetic bcc iron (Fe) Σ3(111) symmetrical tilt grain boundaries by progressively adding solute atoms [sulfur (S) or phosphorous (P)] to the boundaries. We show that there are two mechanisms of decohesion: (i) fracture surface stabilization with reference to the grain boundary by the segregated solute atoms without interaction between them, and (ii) grain boundary destabilization by a repulsive interaction among the segregated and neighboring solute atoms. It is found that the dominant mechanism for the S-induced decohesion is the former (i), while that for P is the latter (ii). This difference makes P a much weaker embrittling element comparing with S because the mechanism (ii) simultaneously brings about the reduction of the grain boundary segregation energy.

Although sulfur (S) and phosphorous (P) are famous embrittling elements that segregate to iron (Fe) grain boundaries (GBs) and thereby cause intergranular racture, it is not well known why and how these elements weaken Fe GBs. The difference in the embrittling ability between S and P is also not well understood. Experiments using Fe-S-C and Fe-P-C alloys indicate that the shift of ductile-to-brittle transition temperature (DBTT) with respect to the S increase in the GB is 40 K, which is two times larger than that by P (20 K). The S-induced GB embrittlement of Fe occurs even when the bulk S concentration is only several tens atomic parts per million (at. ppm, 0.0001 at. %), while the P-induced one occurs when the bulk P concentration is more than (900 at. ppm.)

The change in the cohesive energy (reversible work of fracture) of the GB, 2γ, plays a key role in such intergranular fracture. A ductile-to-brittle transition occurs when the energy release rate of fracture (2γ) becomes smaller than that of the dislocation nucleation and motion at the crack tip. In addition, analyses of the experiments show that the DBTT is inversely related to the total fracture energy, which is the sum of 2γ plus the work of plastic deformation γp ($\Gamma = 2\gamma + \gamma_p$). Even when γ*p* is much larger than 2γ, γ_p should become zero if 2γ is zero; this means that γ*p* must depend on 2γ in some way. Therefore, the DBTT correlates inversely with 2γ. Furthermore, 2γ is directly related to the fracture surface energy ($2\gamma_s$) and the GB energy (γ_{gb}), which are affected by segregation through the surface segregation energy ($\Delta E^{seg}_{s,total}$) and the GB one ($\Delta E^{seg}_{gb,total}$),

$$2\gamma = (2\gamma_s - \Delta E^{seg}_{s,total} / A) - (\gamma_{gb} - \Delta E^{seg}_{gb,total}/A).$$

Here, $\Delta E^{seg}_{s,total}$ and $\Delta E^{seg}_{gb,total}$ are defined as the (positive) energy gain for total solute atoms which transfer from inner bulk region to the surface and the GB, respectively. *A* is the area of the GB plane on which we consider segregation in a unit cell.

Our calculations indicate that S is a strong embrittling element while P is a weak one, which is consistent with the experiments mentioned in the beginning of this paper. The significant decrease of $\Delta E^{seg}_{gb,av}$ with increasing segregation for the P case indicates that the P embrittlement requires a much higher bulk P oncentration than the S case. Supposing that $\Delta E^{seg}_{gb,av}$ is 1.0 eV for S and 0.5 eV for P, the required bulk concentration for strong segregation can be estimated as about 1 at. ppm for S and 100–1000 at. ppm for P, respectively. This is consistent with the experiments. The rate of decrease of 2γ for the S case in the range of 0–4 (4–8) atoms segregation is about 4.0(1.4) times larger than that for P. This is also consistent with the experimental fact that the DBTT shift by S is two times larger than that by P (S: 40 K and P: 20 K for 1 at% in a GB).

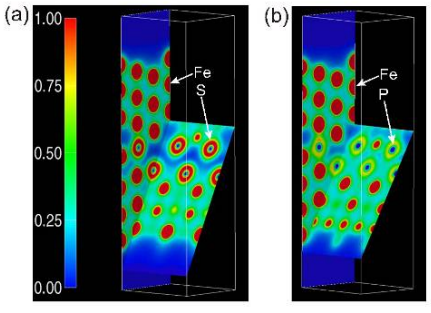

Fig. 6 Calculated electron density maps (electron/Å^3) for the case of 8 atoms segregated at sites 0 and 2 (two atomic layers, 14.4 atom/nm^2). (a) S, (b) P.

Reference

[1] M. Yamaguchi, Y. Nishiyama, H. Kaburaki, Phys. Rev. B 76, 035418(2007).

Molecular dynamics study on the formation of stacking fault tetrahedra and unfaulting of Frank loops in fcc metals

Tomoko Kadoyoshi, Hideo Kaburaki, Futoshi Shimizu, Hajime Kimizuka[1)], Shiro Jitsukawa, Ju Li[2)]
1) Japan Research Institute,Ltd. 2) The Ohio State University

Irradiation of face centered cubic (fcc) metals by charged or neutron particles induces atomic collision cascades, where varieties of defect clusters nucleate from the migration and coalescence of self-interstitial atoms and vacancies. Typical clusters that form from this displacement cascade process are hexagonal dislocation loops called Frank loops containing the stacking fault with the Burgers vector 1/3<111>. These defects are well observed by transmission electron microscopy [1] and are considered to cause significant effects of irradiation hardening and fracture due to dislocation channeling. It is predicted that unfaulting of Frank loops may lead to the formation of dislocation channeling through the absorption of these unfaulted loops by gliding dislocations. However, detailed mechanistic processes of these Frank loops are not well known due to the resolution limit of electron microscopy and the applicability of the elasticity theory down to the range of 1-5nm.

We study these processes by the molecular dynamics method [2]. Critical conditions have been determined for intrinsic transformation of a vacancy Frank loop into a stacking fault tetrahedron in a face centered cubic metal by the molecular dynamics method . We found that a stacking fault tetrahedron can be formed from the scalene hexagonal vacancy Frank loops of wide range of sizes due to the dissociation of dislocations (Fig.1). We have also found atomistically the dynamical process in which vacancy and interstitial faulted Frank loops transform into perfect loops by the application of the external shear stress (Fig.2). We have determined numerically the critical shear stress for the initiation of unfaulting as functions of the size of a Frank loop and temperature. We also have suggested a mechanism that greatly reduces the critical shear stress.

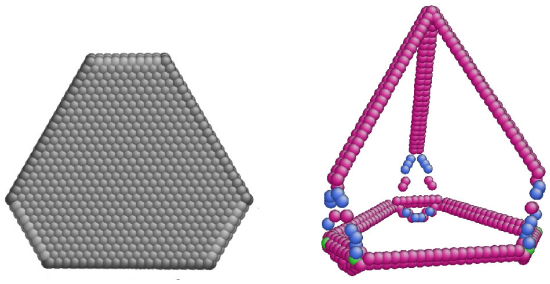

Fig.1: Formation of an incomplete stacking fault tetrahedron from the scalene hexagonal vacancy loop with two different sides.

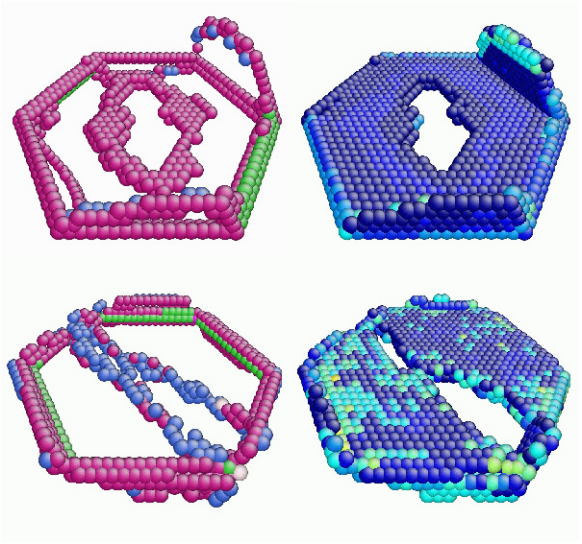

Fig. 2: Unfaulting of a vacancy and an interstitial Frank loop of aluminum containing 721 lattice sites under the fast shear strain rate condition.

References

[1] S.Amelinckx, Dislocations in Solids 2, Oxford: North-Holland Publ.Co.(1979).
[2] T.Kadoyoshi, et al., Act Mat.55, 3073(2007).

1.4.4 Multiscale simulation of nuclear materials and fuels

Simulation for intergranular stress corrosion cracking based on a three-dimensional polycrystalline model

Masayuki Kamaya[1] and Mitsuhiro Itakura

1) Institute of Nuclear Safety System, Inc

In stress corrosion cracking of stainless steel, two different schemes of analysis of crack growth should be employed for the crack initiation phase and crack growth phase. However, this distinction is not clear-cut in the crack initiation phase, since the vicinity of the pre-existing crack is a preferential area of crack initiation due to concentration of stress. Therefore, initiation of crack tends to occur at the tip of a pre-existing crack and it can be regarded as crack growth. In this study, the contribution of this type of apparent crack growth, referred to as initiation dominant growth (IDG), to crack growth was evaluate by a Monte Carlo simulation. A three-dimensional polycrystalline body was generated by Voronoi tessellation. The cracks were assumed to grow along grain boundaries. The effect of stress-concentration around pre-existing cracks was taken into account by applying the finite element method. Initiation and propagation of the cracks were modeled based on concepts of damage mechanics. The simulation could reproduce the changes in number of cracks and the sum of crack length obtained experimentally as well as preferential crack initiation at the stress-concentration zones and suppression of crack initiation in stress-shielding zones. It was shown that the contribution of IDG to crack growth was large for small cracks, and that damage by crack initiation accounted for more than 50% of total damage even when the length of a crack was 0.6 mm at the surface.

In this study, the effects of IDG on crack growth were evaluated using a Monte Carlo simulation that accounts for the influence of local stress on crack initiation. The target of the simulation was SCC of stainless steel, which was tested in the previous study. In the tests, multiple cracks were initiated and grew along grain boundaries. The changes in crack distribution, number of cracks, and crack length were recorded using an in-situ observation system. In the simulation, a polycrystalline body was generated by Voronoi tessellation, and finite element analysis (FEA) was performed for the polycrystalline body to evaluate the local stress distribution induced by pre-existing cracks. The initiation and propagation of cracks were modeled based on concepts of damage mechanics.

Fig.1 shows crack configuration after 1500 grain boundary fractures. One can see a number of long cracks generated by the IDG mechanism. The basic shapes of plots of the number of cracks and sum of crack lengths, plotted against time, also show the effects of IDG, and agree well with experimental results. Thus, the simulation indicates that the IDG mechanism plays an important role in SCC crack initiation in the incubation time.

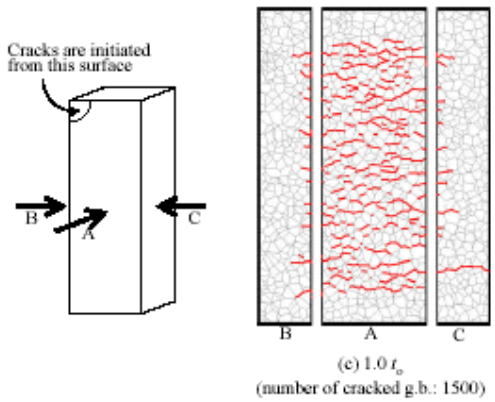

Fig. 1: The geometry of simulation cell (left) and crack configuration after 1500 grain boundary cracks (right). The red lines show fractured grain boundaries.

References

[1] M.Kamaya and M.Itakura, Engineering Fracture Mechanics 76 (2009) 386–401.

1.4.4 Multiscale simulation of nuclear materials and fuels

A three-dimensional meso-scale computer modeling for bubble growth in metals

Tomoaki Suzudo, Hideo Kaburaki, Mitsuhiro Itakurta, Eiichi Wakai[1)]
1)Nuclear Science & Engineering Directrate, Japan Atomic Energy Agency

Helium atoms are produced in metals through transmutation reactions in the irradiation process of high-energy neutrons. Since they tend to precipitate into vacant space because of their high insolubility, bubbles nucleate and grow in metals leading to the microstructural changes and the degradation of mechanical properties; this is of a particular concern in relevance to the first wall integrity for the future fusion reactors and to helium embrittlement in nuclear reactor structural materials, especially in fast breeder reactors.

We investigated a new approach to model the bubble growth in metals. In high temperatures, inert gas atoms and vacancies become highly mobile and it is expected that the pressure of the bubbles would reach its equilibrium with the surface tension. We thus assumed that the bubble state in high temperatures be modeled without atomistic details. In addition, such equilibrium is dynamically attained by a process driven by energy minimization (relaxation) and thermal fluctuation. The thermal fluctuation also causes the bubbles to migrate and eventually their coalescence and coarsening. The bubble growth kinetics thus can be modeled by a meso-scale Monte-Carlo methodology. For this purpose, we adopted a Monte-Carlo simulation model with a three-dimensional lattice system, that is, the material is divided into a number of small cubes, and these cubes are arranged on a regular lattice. This type of meso-scale modeling method is commonly adopted in the field of recrystallization and grain growth, where a grain is represented as aggregated fragments (or elements) that have the same crystallographic orientation. Also in the present model, a bubble is similarly expressed by aggregated fragments all of which contain no solid atoms. The calculation dynamics is driven by the interactions between neighboring cubes such as in cellular automata. The adopted Monte-Carlo algorithm is the Metropolis method. A shape of a bubble is not pre-defined, but self-organized by the balance between energy minimization and fluctuation in the Monte-Carlo dynamics. In addition, the size and the pressure of bubbles can be derived in the same manner. Events in the simulation, such as the migration and the coalescence of bubbles, are not explicitly implemented using the pre-defined rules of reactions as adopted in conventional methodologies, but automatically appear as a result of the fluctuation in the Monte-Carlo dynamics.

We confirmed the validity of the model by reproducing analytical results for bubbles in equilibrium and experimental evidences related to helium bubble growth during post-irradiation annealing. In addition, the bubble size distribution derived by this model is explained by the log-normal distribution, which is also observed in experiment under the same condition. We believe that this approach was successful in simulating the actual bubble growth process, and that the bubble growth at elevated temperatures is a process driven by the energy minimization and the thermal fluctuation. We also extended the model to the study of the interaction between bubbles and grain boundaries and succeeded to produce numerically some self-organized lenticular bubbles on a grain boundary (Fig. 1), which is theoretically predicted and is experimentally found.

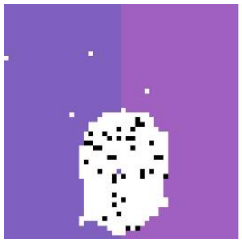

Fig 1. A lenticular bubble on a grain boundary indicated by a vertical line for 10000 Monte-Carlo steps.

The present approach is superior to conventional ones in producing easily the visual information including animations over the bubble growth. Such information can be directly compared with micrographs and in-situ observations.

References

[1] T. Suzudo et al., Modeling Simul. Mater. Sci. Eng. 16, 055003 (2008).

1.5 Computational Quantum Bioinformatics

This is a blank page.

1.5.1 Large-scale computer simulations for molecular biology

Properties of the nucleic-acid bases in free and Watson-Crick hydrogen-bonded states: computational insights into the sequence-dependent features of double-helical DNA

A. R. Srinivasan[1)], Ronald R. Sauers[1)], Marcia O. Fenley[2)], Alexander H. Boschitsch[3)], Atsushi Matsumoto[4)], Andrew V. Colasanti[1)], Wilma K. Olson[1)]

1) Department of Chemistry & Chemical Biology, Rutgers, the State University of New Jersey, USA 2) Department of Physics, Institute of Molecular Biophysics, Florida State University, USA 3) Continuum Dynamics, Inc., USA 4) CCSE, JAEA

The nucleic-acid bases carry structural and energetic signatures that contribute to the unique features of genetic sequences. Here, we review the connection between the chemical structure of the constituent nucleotides and the polymeric properties of DNA. The sequence-dependent accumulation of charge on the major- and minor-groove edges of the Watson–Crick base pairs, obtained from ab initio calculations, presents unique motifs for direct sequence recognition. The optimization of base interactions generates a propellering of base-pair planes of the same handedness as that found in high-resolution double-helical structures. The optimized base pairs also deform along conformational pathways, i.e., normal modes, of the same type induced by the binding of proteins. Empirical energy computations that incorporate the properties of the base pairs account satisfactorily for general features of the next level of double-helical structure, but miss key sequence-dependent differences in dimeric structure and deformability. The latter discrepancies appear to reflect factors other than intrinsic base-pair structure.

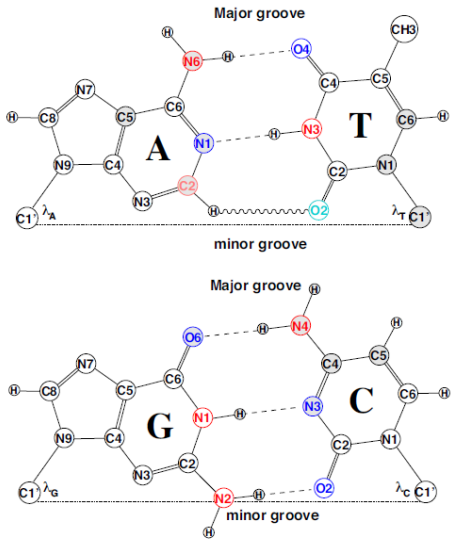

Fig. 1 Comparative hydrogen-bonding interactions, chemical structures (including double bonds), and displacement of bases comprising normal A·T and G·C Watson–Crick pairs. Hydrogen bonds are designated by dashed lines and the "weak" CH···O bond of the A·T base-pair by a thin wavy line.

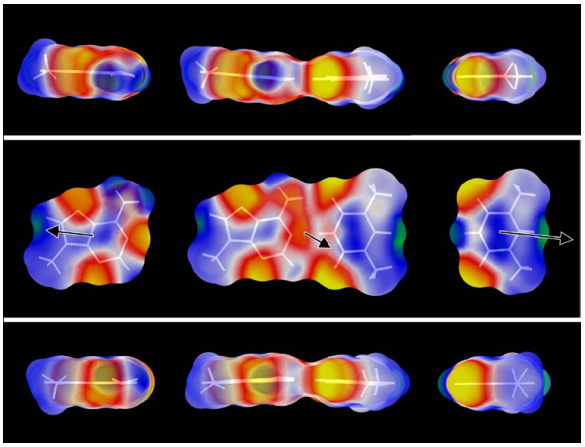

Fig. 2 Electrostatic potential surfaces of the methylated (purine N9 and pyrimidine N1) form of an optimized A·T base pair and its adenine (left) and thymine (right) components in a simulated aqueous environment. Views looking down the major- and minor-groove edges (top and bottom rows of images, respectively) and perpendicular to the base and base-pair planes (middle row). White wireframe models of the respective molecules are superimposed on the electrostatic potential surfaces. Dipole-moment vectors, noted by black arrows, are drawn in accordance with the computed structure and charges. The surfaces of bases and base pairs are color-coded such that the areas of greatest negative potential are yellow, those of greatest positive potential are green, and the intermediate regions of negative, neutral, and positive potential vary, respectively, from red to white and blue.

Key Interactions in Integrin Ectodomain Responsible for Global Conformational Change Detected by Elastic Network Normal-Mode Analysis

Atsushi Matsumoto[1)], Tetsuji Kamata[2)],Junichi Takagi[3)],Kenji Iwasaki[3)],and Kei Yura[1)]
1) JAEA, Kansai, 2) Department of Anatomy, Keio University School of Medicine, 3)Institute for Protein Research, Laboratory of Protein Synthesis and Expression,Osaka University

Integrin, a membrane protein with a huge extracellular domain, participates in cell-cell and cell-extracellular-matrix interactions for metazoan. A group of integrins is known to perform a large-scale structural change when the protein is activated, but the activation mechanism and generality of the conformational change remain to be elucidated. We performed normal-mode analysis of the elastic network model on integrin αVβ3 ectodomain in the bent form and identified key residues that influenced molecular motions. Iterative normal-mode calculations demonstrated that the specific nonbonded interactions involving the key residues work as a snap to keep integrin in the bent form.

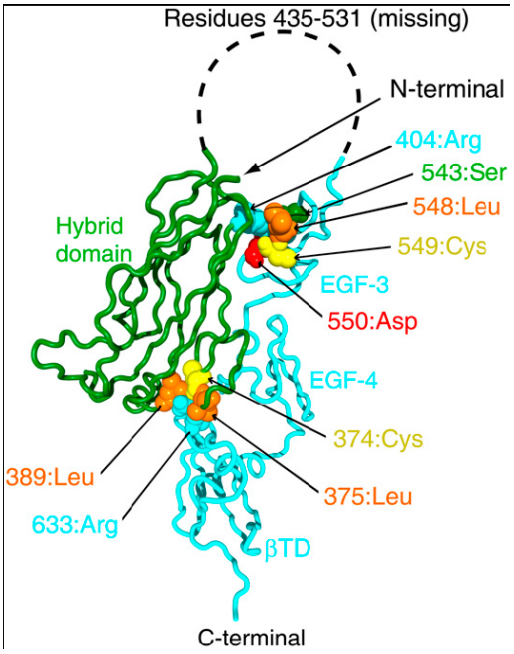

Fig. 1 Three-dimensional structure of integrin β3-chain. Arg633 and Arg404, with their nearby residues, are shown by a space-filling model.

The importance of the key residues for the conformational change was further verified by mutation experiments, in which integrin αIIbβ3 was used. The conservation pattern of amino acid residues among the integrin family showed that the characteristic pattern of residues seen around these key residues is found in the limited groups of integrin β-chains. This conservation pattern suggests that the molecular mechanism of the conformational change relying on the interactions found in integrin αVβ3 is unique to the limited types of integrins.

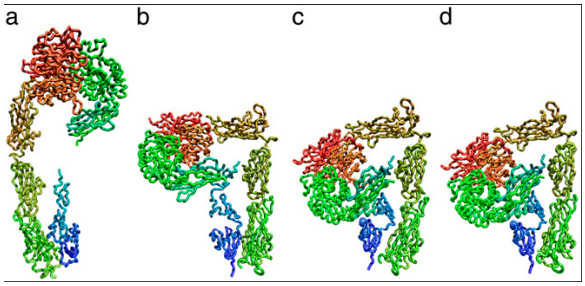

Fig. 2 (a–d) Backbone structures of integrin at the end of 4 different iterative normal-mode calculations 1–4, respectively (Table 1).

Table 1. Summary of four iterative normal mode calculations

Calculation No.	Interaction A	Interaction B	Final conformation
1	–	–	Extended
2	–	+	L-shaped
3	+	–	Bent
4	+	+	Bent

Interaction A refers to the interactions of Arg633 with Cys374, Gly388, and Leu389, and interaction B to those of Arg404 with Ser543, Leu548, Cys549 and Asp550 plus the interactions between Glu364 and Ser551. The plus and minus symbols mean that the springs representing these interactions exist or not exist, respectively.

Synthesis of Pinguisane-Type Sesquiterpenoids Acutifolone A, Pinguisenol, and

1.5.1 Large-scale computer simulations for molecular biology

Bisacutifolones by a Diels-Alder Dimerization Reaction

Junichi Shiina[1)], Masataka Oikawa[2)], Kensuke Nakamura[2)], Rika Obata[1)] and Shigeru Nishiyama[1)]
1) Department of Chemistry, Faculty of Science and Technology, Keio University, 2) CCSE, JAEA

Plants produce numerous kind of secondary metabolites to protect themselves. Number of such compounds isolated from plants are found to be useful, and being exploited. Some of these compounds are not abundant and need to be chemically synthesized to fulfill the needs. Computational prediction often plays an important role, for the development of efficient synthetic methods.

Livewort produces a number of sesquiterpenoids with important biological activities. Asakawa and co-workers have isolated pinguisane-type sesquiterpenoids with antimicrobial and antitumor activities (Fig.1).[1]

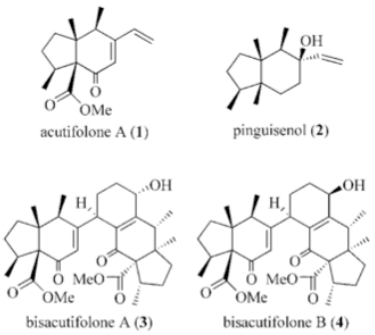

Fig. 1: Pinguisane-type sesquiterpenoids isolated from livewort

In the present work, these compounds are synthesized by means of intramolecular Diels-Alder reaction as a key step. The reaction potentially leads to number of compounds including unwanted products (Fig.2), and knowledge of chemical stability of intermediates or transition states that leads to each product is extremely useful to control the most appropriate reaction condition.

By using the computer system at JAEA, we carried out *ab initio* quantum chemical calculations to compare the relative stability of transition states (Fig.3), and predicted the ratio of the products. During the process, computational prediction helped determine the stereo -chemistry of the reaction products, which was not appropriately identified by experimental measurements, and contributed for the optimization of the reaction condition to obtain the desired natural product.

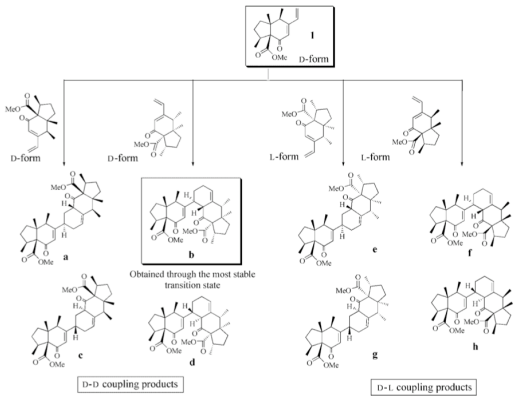

Fig. 2: Potential reaction pathways that includes the one leads to the target natural product

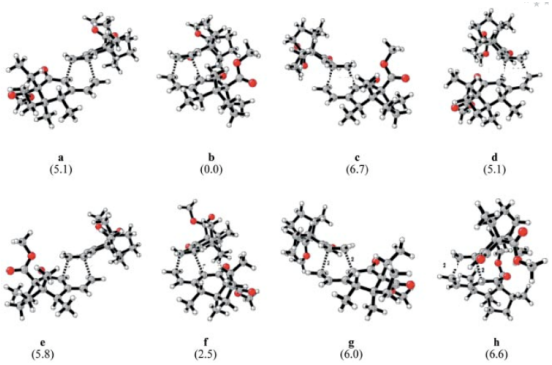

Fig. 3: Transition state structures for the Diels-Alder dimerization, numbers in parenthesis are relative energy in kcal/mol

Transition states were optimized at the RHF/3-21G level. Among possible rotational conformations of the side chains, each structure was confirmed to be the minimum energy, using AM1 calculations. Single point density functional calculations (B3LYP/6-31G(d)) were performed to estimate the precise relative energy of the transition states. All calculations were performed by using Gaussian program package. [2]

References

[1] Y. Asakawa, J.Hattori Bot. Lab. Vol.84, 91 (1998)
[2] M. J. Frisch et al. Gaussian03 Revision B.05, Gaussian Inc., Pittsburgh, PA, (2003)

1.5.1 Large-scale computer simulations for molecular biology

Discrimination of Class I Cyclobutane Pyrimidine Dimer Photolyase from Blue Light Photoreceptors by Single Methionine Residue

Yuji Miyazawa[1)], Hirotaka Nishioka[2)], Kei Yura[3)], Takahisa Yamato[1)]

1)Graduate School of Science, Nagoya University 2) Graduate School of Environmental and Human Science, Meijo University, 3) CCSE, JAEA

DNA photolyase recognizes ultraviolet-damaged DNA and breaks improperly formed covalent bonds within the cyclobutane pyrimidine dimer by a light-activated electron transfer reaction between the flavin adenine dinucleotide, the electron donor, and cyclobutane pyrimidine dimer, the electron acceptor. Theoretical analysis of the electron-tunneling pathways of the DNA photolyase derived from Anacystis nidulans can reveal the active role of the protein environment in the electron transfer reaction. Here, we report the unexpectedly important role of the single methionine residue, Met-353, where busy trafficking of electron-tunneling currents is observed. The amino acid conservation pattern of Met-353 in the homologous sequences perfectly correlates with experimentally verified annotation as photolyases. The bioinformatics sequence analysis also suggests that the residue plays a pivotal role in biological function. Consistent findings from different disciplines of computational biology strongly suggest the pivotal role of Met-353 in the biological function of DNA photolyase.

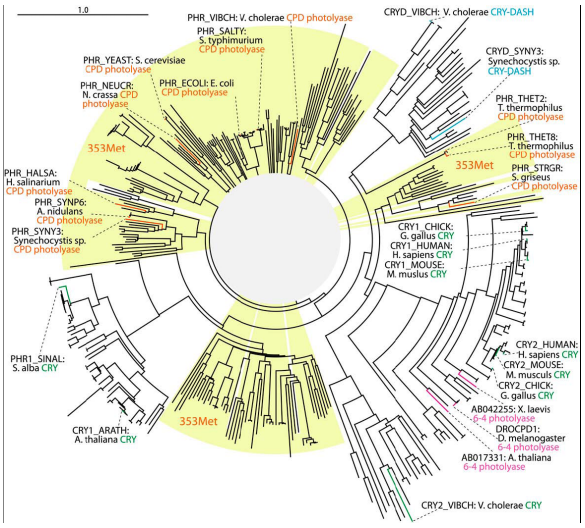

Fig 1. A dendrogram based on amino acid sequences in the photolyase blue light photoreceptor family. A root of the dendrogram was located in the gray circle at the center, but the exact location is unclear because of uncertainty in the branching order of the dendrogram. A branch with a yellow background represents amino acid sequences with Met at the site corresponding to 353 of A. nidulans CPD photolyase. For protein sequences with experimentally verified biological function, the protein (gene) ID and species and protein names are shown. A protein with its name in orange has CPD repair function, a protein in green has biological functions related to CRY, a protein in cyan has functions related to CRY-DASH, and a protein in pink has 6-4 photoproduct repair function. The bar at the top left represents a branch length that corresponds to 1.0 amino acid substitutions per site based on Kimura's distance.

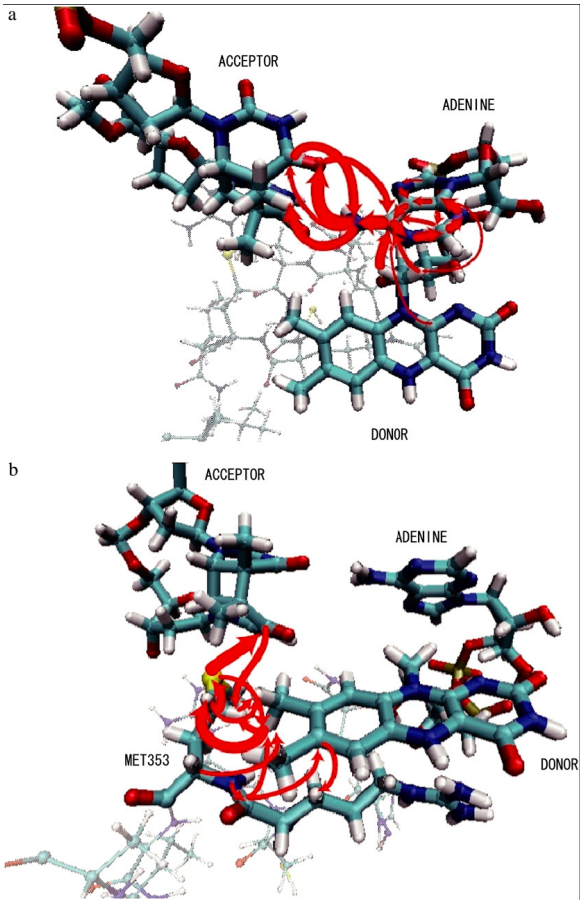

Fig. 2 Electron-tunneling pathways. (a) Adenine route. (b) Met-353 route. Two typical electron-tunneling pathways are shown in these two panels. The width of each arrow is in proportion to the magnitude of the interatomic electron-tunneling current.

1.5.1 Large-scale computer simulations for molecular biology

coliSNP database server mapping nsSNPs on protein structures

Hidetoshi Kono[1)], Tomo Yuasa[2)], Shinya Nishiue[3)] and Kei Yura[4)]
1) Quantum Beam Science Directorate, JAEA, 2) Bioinformatics Department, Mitsubishi Space Software CO. LTD,
3)Department of Bioengineering, Nagaoka University of Technology, 4) CCSE, JAEA

We have developed coliSNP, a database server (http://yayoi.kansai.jaea.go.jp/colisnp) that maps non-synonymous single nucleotide polymorphisms (nsSNPs) on the three-dimensional (3D) structure of proteins. Once a week, the SNP data from the dbSNP database and the protein structure data from the Protein Data Bank (PDB) are downloaded, and the correspondence of the two data sets is automatically tabulated in the coliSNP database. Given an amino acid sequence, protein name or PDB ID, the server will immediately provide known nsSNP information, including the amino acid mutation caused by the nsSNP, the solvent accessibility, the secondary structure and the flanking residues of the mutated residue in a single page. The position of the nsSNP within the amino acid sequence and on the 3D structure of the protein can also be observed. The database provides key information with which to judge whether an observed nsSNP critically affects protein function and/or stability. As far as we know, this is the only web-based nsSNP database that automatically compiles SNP and protein information in a concise manner.

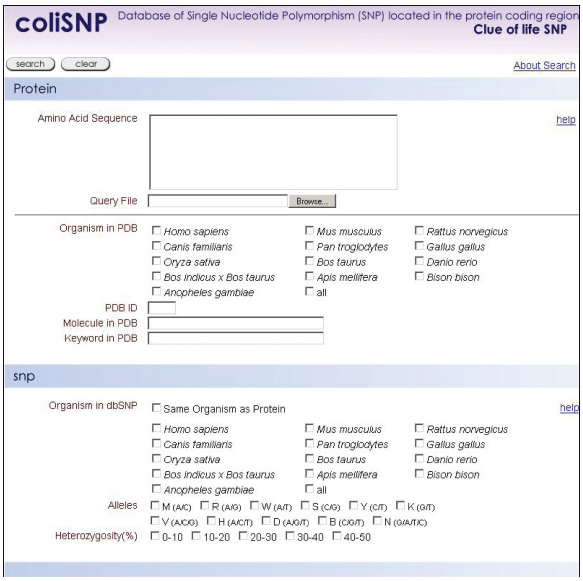

Fig. 1. The coliSNP search interface. The user can use the protein section, SNP section or both to set the search conditions.

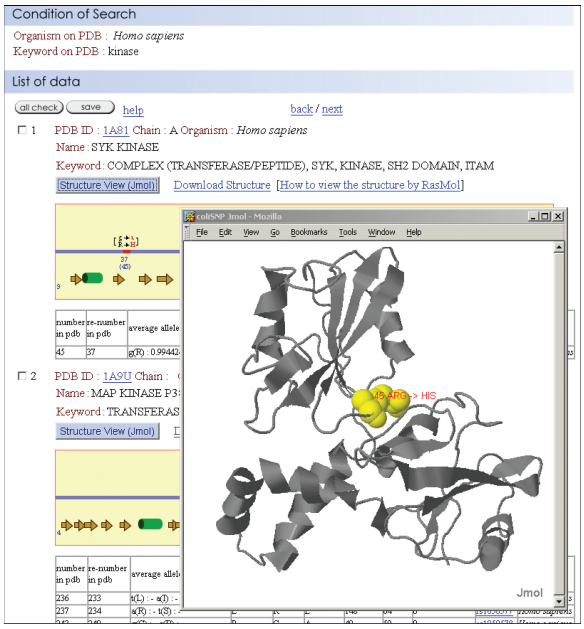

Fig. 2. A typical search result. nsSNP information is provided with structural information on the mutated amino acid residue—e.g. the secondary structure and solvent accessibility.

2. Publication & Presentation List

List of Paper

1.1 Computer Science / Grid Computing

1) Kimiaki Saito, Naoya Teshima, Yoshio Suzuki, Norihiro Nakajima, Hidetoshi Saito, Etsuo Kunieda, Tatsuya Fujisaki, "Gridization of IMAGINE for the remote assistance of radiation therapy", FUJITSU Family Association FY2008 (2009) (Japanese).
2) Yoshio Suzuki, Akemi Nishida, Fumimasa Araya, Noriyuki Kushida, Taku Akutsu, Naoya Teshima, Kohei Nakajima, Makoto Kondo, Sachiko Hayashi, Tetsuo Aoyagi and Norihiro Nakajima, “Development of Three-dimensional Virtual Plant Vibration Simulator on Grid Computing Environment ITBL-IS/AEGIS”, Journal of Power and Energy Systems, Vol.3, No.1, Special Issue on 16th International Conference on Nuclear Engineering pp.60-71 (2009).
3) Yoshio Suzuki, Norihiro Nakajima, Fumimasa Araya, Osamu Hazama, Akemi Nishida, Noriyuki Kushida, Taku Akutsu, Naoya Teshima, Kohei Nakajima, Makoto kondo, Sachiko Hayashi, Tetsuo Aoyagi, “Development of Three-dimensional Virtual Plant Vibration Simulator on Grid Computing Environment ITBL-IS/AEGIS," Proceedings of 16th International Conference on Nuclear Engineering (Orlando, Florida, U.S.A., 2008.5.11-15) CD-ROM (2008).
4) Yuichi Tsujita, Tatsumi Arima, Kazuya Idemitsu, Yoshio Suzuki, Hideo Kimura, “Building an Application-specific Grid Computing Environment Using ITBL for Nuclear Material Engineering” Proceedings of 16th International Conference on Nuclear Engineering (Orlando, Florida, U.S.A., 2008.5.11-15) CD-ROM (2008).
5) Kohei Nakajima, Yoshio Suzuki, Naoya Teshima, Shin-ichiro Sugimoto, Shinobu Yoshimura, Norihiro Nakajima, "Method to Unconsiously Use Grid middleware; Proposal of Seamless API and Its Application to Mechanics System", FY2008 Collected Papers of NEC C&C Systems Users Association (2008) (Japanese).
6) Yoshio Suzuki, Kohei Nakajima, Noriyuki Kushida, Chiaki Kino, Takahiro Minami, Nobuko Matsumoto, Tetsuo Aoyagi, Norihiro Nakajima, Katsuyuki Iba, Nobuhiko Hayashi, Takahisa Ozeki, Toshiyuki Totsuka, Hideya Nakanishi and Yoshio Nagayama, “Research and Development of Fusion Grid Infrastructure Based on Atomic Energy Grid InfraStructure (AEGIS),” Sixth IAEA Technical Meeting on Control, Data Acquisition, and Remote Participation for Fusion Research (Inuyama, Japan, 2007.6.4-8), Fusion Engineering and Design Vol.83 pp.511-515 (2008).
7) Katsuyuki Iba, Takahisa Ozeki, Toshiyuki Totsuka, Yoshio Suzuki, Takayuki Oshima, Shinya Sakaba, Minoru Sato, Mitsuhiro Suzuki, Kiyotaka Hamamatsu and Kimihiro Kiyono “Development and verification of remote research environment based on “Fusion research grid”” Sixth IAEA Technical Meeting on Control, Data Acquisition, and Remote Participation for Fusion Research (Inuyama, Japan, 2007.6.4-8), Fusion Engineering and Design Vol.83 pp.495-497 (2008).
8) Toshiyuki Totsuka, Yoshio Suzuki, Shinya Sakata, Takayuki Oshima, Katsuyuki Iba “Development of the Advanced JT-60 Man-Machine Interfacing System for Remote Experiments” Sixth IAEA Technical Meeting on Control, Data Acquisition, and Remote Participation for Fusion Research (Inuyama, Japan, 2007.6.4-8), Fusion Engineering and Design Vol.83 pp.287-290 (2008).
9) Yoshio Suzuki, “Research and Development of Application Programming Interface for Grid environment”, FUJITSU Family Association FY2007 selected paper (2008) (Japanese).
10) Yoshio Suzuki, Noriyuki Kushida, Naoya Teshima, Kohei Nakajima, Akemi Nishida, and Norihiro Nakajima, “Atomic Energy Grid Infrastructure (AEGIS) and Interoperation with Other Grids”, High Performance Computing on Vector Systems 2008 M. Resch, S. Roller, K. Benkert, M. Gelle, W. Bez, H. Kobayashi, T. Hirayama (Eds.) Springer-Verlag Berlin Heidelberg, pp 65-77 (2008).
11) Noriyuki Kushida, Yoshio Suzuki, Naoya Teshima, Norihiro Nakajima, Yves Caniou and Michel Dayde, “Seamless

connection of ITBL computers from Grid-TLSE toward international matrix prediction system" the Proceedings of 8th International Meeting High Performance Computing for Computational Science (Toulouse, France, 2008.6.24-27) CD-ROM (2008).

12) Noriyuki Kushida, Yoshio Suzuki, Naoya Teshima, Norihiro Nakajima, Yves Caniou, Michel Dayde, and Pierre Ramet, "Toward an International Sparse Linear Algebra Expert System by Interconnecting the ITBL Computational Grid with the Grid-TLSE Platform", FUJITSU Family Association FY2007 (2008) (Japanese).
13) Noriyuki Kushida, Yoshio Suzuki, Naoya Teshima, and Norihiro Nakajima "Developemnt of ITBL-UNICORE Grid interoperable system", FY2007 Collected Papers of NEC C&C Systems Users Association (2007) (Japanese).
14) Chiaki Kino, Yoshio Suzuki, Noriyuki Kushida, Akemi Nishida, Sachiko Hayashi and Norihiro Nakajima, "Development of Cognitive Methodology based Data Analysis System", High Performance Computing on Vector Systems 2008, M. Resch, S. Roller, K. Benkert, M. Gelle, W. Bez, H. Kobayashi, T. Hirayama (Eds.) Springer-Verlag Berlin Heidelberg, pp.89-97 (2008).
15) Chiaki Kinio, Yoshio Suzuki, Akemi Nishida, Noriyuki, Kushida, Sachiko Hayashi, and Norihiro Nakajima, "Concept Design of Cognitive methodology based Data Analysis System", Transactions of JSCES, Vol.2008, Paper No.20080018 pp.1-8 (2008) (Japanese).
16) Yoshio Suzuki, Akemi Nishida, Tomonori Yamada, Fumimasa Araya, Sachiko Hayashi, Norihiro Nakajima, and Toshio Hirayama, "Cerebral Methodology Based Computing for Estimating Validity of Simulation Results", International Conference for High Performance Computing, Networking, Storage and Analysis (SC08) Analytics Challenge Finalist (2008).
17) Chiaki Kino, Noriyuki Kushida, Yoshio Suzuki and Norihiro Nakajima, "Cognitive methodology based Data Analysis System for Large Scale Data", International Conference for High Performance Computing, Networking, Storage and Analysis (SC07) Analytics Challenge Finalist (2007).

1.2 Computational Vibration Science

18) Tomonori Yamada, Fumimasa Araya, Akemi Nishida, Noriyuki Kushida, and Norihiro Nakajima, "Proposal of Vibration Table in an Extended World by Grid Computing Technology for Assembled Structures," Theoretical and Applied Mechanics Japan, Vol.57, pp.81-87 (2009).
19) A. Nishida, F. Araya, T. Yamada, N. Kushida, H. Takemiya and N. Nakajima, " Development and Application Research of Vibration Simulator for Full-scale Nuclear Power Station ," Additional Materials of Nuclear Safety Research Forum 2009, pp.25-29 (2009).
20) A. Nishida, F. Araya, H. Matsubara, O. Hazama and N. Nakajima, " Development and Application Research of Vibration Simulator for Full-scale Nuclear Power Station ," Additional Materials of Nuclear Safety Research Forum 2008, pp.93-97 (2008).
21) Akemi Nishida, "Effect of Timoshenko coefficient in wave propagation analysis of a three-dimensional frame structure", Theoretical and Applied Mechanics Japan, Vol.56, pp.57-65 (2007)
22) H. Matsubara and G. Yagawa, Application and accuracy of basis functions implementated in a patch-by-patch approximation of mixed-type finite element, Journal of Applied mechnics, JSCE, Vol.10 (2007).

1.3 Computational Fluid Dynamics & Fusion Science

23) Masato Ida, Takashi Naoe, and Masatoshi Futakawa, "On the effect of microbubble injection on cavitation bubble dynamics in liquid mercury," Nuclear Instruments and Methods in Physics Research A, Vol.600, No.2, pp.367-375 (2009).
24) Masato Ida, "Bubble-bubble interaction: A potential source of cavitation noise," Physical Review E, Vol.79, No.1, pp.016307-1～016307-7 (2009).
25) Tadashi Watanabe, "Frequency shift and aspect ratio of a rotating-oscillating liquid droplet," Physics Letters A, 373, pp.867-870 (2009).
26) Yasuhiro Idomura, Masato Ida, and Shinji Tokuda, "Conservative gyrokinetic Vlasov simulation," Communications

in Nonlinear Science and Numerical Simulation 13, pp.227-233 (2008).

27) Kazunori Shinohara, Hiroshi Okuda, Satoshi Ito, Norihiro Nakajima, Masato Ida, "Shape optimization using adjoint variable method for reducing drag in Stokes flow," International Journal for Numerical Methods in Fluids. Vol 58 Issue 2, pp.119-159 (2008).

28) Masatoshi Futakawa, Hiroyuki Kogawa, Shoichi Hasegawa, Takashi Naoe, Masato Ida, Katsuhiro Haga, Takashi Wakui, Nobuatsu Tanaka, Yoichiro Matsumoto, and Yujiro Ikeda, "Mitigation technologies for damage induced by pressure waves in high-power mercury spallation neutron sources (II) - Bubbling effect to reduce pressure wave -," Journal of Nuclear Science and Technology 45(10), pp.1041-1048 (2008).

29) Tadashi Watanabe, "Numerical simulation of oscillations and rotations of a free liquid droplet using the level set method," Computers and Fluids, 37, pp.91-98 (2008).

30) Tadashi Watanabe, "Zero frequency shift of an oscillating-rotating liquid droplet," Physics Letters A, 372, pp.482-485 (2008).

31) Tadashi Watanabe, "Numerical simulation of an oscillating-rotating liquid droplet," Computers and Simulation in Modern Science, Vol. I, pp.81-85 (2008).

32) Tadashi Watanabe, "Flow field and oscillation frequency of a rotating liquid droplet," WSEAS TRANSACTIONS on FLUID MECHANICS, 2 Vol. 3, pp164-174 (2008).

33) Takashi Naoe, Masato Ida, and Masatoshi Futakawa, "Cavitation damage reduction by microbubble injection," Nuclear Instruments and Methods in Physics Research Section A 586(3), pp.382-386 (2008).

34) Yasuhiro Idomura, Masato Ida, Takuma Kano, Nobuyuki Aiba, and Shinji Tokuda, "Conservative global gyrokinetic toroidal full-f five dimensional Vlasov simulation," Computer Physics Communications 179(6), pp.391-403 (2008).

35) M. Ida, T. Naoe, M. Futakawa, "Suppression of cavitation inception by gas bubble injection: A numerical study focusing on bubble-bubble interaction," Physical Review E, 76, 4, 046309-1, 046309-10

36) M. Ida, T. Naoe, M. Futakawa, "Direct observation and theoretical study of cavitation bubbles in liquid mercury," Physical Review E 75, 046304 (2007)

37) Yasuhiro Idomura, Masato Ida, Shinji Tokuda and Laurent Villard, "New conservative gyrokinetic full-f Vlasov code and its comparison to gyrokinetic δf particle-in-cell code," Journal of Computational Physics 226(1), pp.244-262, (2007).

1.4 Computational Materials Science

38) Takashi Ichinomiya, Yasumasa Nishiura, Blas Uberuaga, Kurt Sickafus, Mitsuhiro Itakura, Y. Chen, Yasunori Kaneta, and Motoyasu Kinoshita, "Temperature accelerated dynamics study of migration process of oxygen defects in UO2," Journal of Nuclear Materials, Vol.384, pp.315-321 (2009).

39) Masayuki Kamaya, Mitsuhiro Itakura, "Simulation for intergranular stress corrosion cracking based on a three-dimensional polycrystalline model," Engineering Fracture Mechanics, Vol.76, pp.386-401 (2009).

40) Ashwin Ramasubramaniam, Mitsuhiro Itakura, Michael Ortiz, Emily Carter, "Effect of atomic scale plasticity on hydrogen diffusion in iron: Quantum mechanically informed and on-the-fly kineticMonte Carlo simulations," Journal of Materials Research, Vol.23, No.10, pp.2757-2773 (2008).

41) Toshiyuki Takayanagi, Takehiro Yoshikawa, Akira Kakizaki, Motoyuki Shiga, and Masanori Tachikawa, "Molecular dynamics simulations of small glycine-(H2O)n (n = 2-7) clusters on semiempirical PM6 potential energy surfaces," Journal of Molecular Structure (THEOCHEM), Vol.869, pp.29-36, (2008)

42) Haruki Motegi, Akira Kakizaki, Toshiyuki Takayanagi, Yuriko Taketsugu, Tetsuya Taketsugu, and Motoyuki Shiga, "Path-integral molecular dynamics simulations of BeO embedded in helium clusters: Formation of the stable HeBeO complex," Chemical Physics, Vol.354, pp.38-43, (2008)

43) Kimichi Suzuki, Motoyuki Shiga, and Masanori Tachikawa, "Temperature and isotope effects on water cluster ions with path integral molecular dynamics based on 4th order Trotter expansion, " Journal of Chemical Physics, Vol.129, No.144310, pp.1-8, (2008)

44) M. Okumura, S. Yamada, and M. Machida, "DMRG studies for 1-D random Hubbard chain close to the half-filling," J. Phys. Chem. Solids 69, pp.3324-3326 (2008).

45) N. Nakai, N. Hayashi, and M. Machida, "Ginzburg-Landau simulation for a vortex around a columnar defect in a superconducting film," J. Phys. Chem. Solids 69, pp.3301-3303 (2008).
46) N. Hayashi, C. Iniotakis, M. Machida, and M. Sigrist, "Josephson effect between conventional and non-centrosymmetric superconductors," J. Phys. Chem. Solids 69, pp.3225-3227 (2008).
47) S. Yamada, M. Machida, T. Kano, T. Imamura, and T. koyama, "On-site pairing interaction and quantum coherence in strongly correlated systems," Special Issue of the Journal of Physics and Chemistry of Solids, 69, pp.3395-3397 (2008).
48) S. Yamada, M. Okumura, M. Machida, Y. Ohashi, and H. Matsumoto, "Vortex core structure in strongly correlated superfluidity," Physica C, Vol.468, pp.1237-1240 (2008).
49) Masahiko Okumura, Susumu Yamada, Nobuhiko Taniguchi, Masahiko Machida, "Hole localization in strongly correlated and disordered systems: DMRG studies for 1-D and 3-leg ladder random Hubbard models," Physica C 468, pp.1241-1244 (2008).
50) Noriyuki Nakai, Nobuhiko Hayashi, Masahiko Machida, "Simulation studies for the vortex-depinning dynamics around a columnar defect in superconductors," Physica C 468, pp.1270-1273 (2008).
51) Takahiro Nishio, Toshu An, Atsushi Nomura, Kousuke Miyachi, Toyoaki Eguchi, Hideaki Sakata, Shizeng Lin, Nobuhiko Hayashi, Noriyuki Nakai, Masahiko Machida, Yukio Hasegawa, "Superconducting Pb Island Nanostructures Studied by Scanning Tunneling Microscopy and Spectroscopy," Phys. Rev. Lett. 101, 167001 (2008).
52) Yuki Nagai, Nobuhiko Hayashi, Noriyuki Nakai, Hiroki Nakamura, Masahiko Okumura, Masahiko Machida, "Nuclear magnetic relaxation and superfluid density in Fe-pnictide superconductors: An anisotropic ± s-wave scenario," New J. Phys. 10, pp.103026-1-103026-17 (2008).
53) Masahiko Machida, Tomio Koyama, and Hideki Matsumoto, "Synchronization Effects in Intrinsic Josephson junctions by Non-equilibrium Heating," Journal of Physics: Conference Series 129, p.012027 (2008).
54) Yuki Nagai, Nobuhiko Hayashi, "Kramer-Pesch approximation for analyzing field-angle-resolved easurements made in unconventional superconductors: A calculation of the zero-energy density of states," Phys. Rev. Lett.101, pp.097001-4 (2008)
55) Masahiko Okumura, Yamada Susumu, Nobuhiko Taniguchi, Masahiko Machida, "Hole Localization in One-Dimensional Doped Anderson-Hubbard Model," Phys. Rev. Lett. 101, pp.0164071-4（2008）
56) Masahiko Machida, Susumu Yamada, Masahiko Okumura, Yoji Ohashi, Hideki Matsumoto, "Correlation Effects on Atom Density Profiles of 1-D and 2-D Polarized Atomic-Fermi-Gas Loaded on Optical Lattice," Physical Review A 77, pp.053614-053614 (2008).
57) Masahiko Machida, Masahiko Okumura, Susumu Yamada, "Stripe formation in fermionic atoms on a two-dimensional optical lattice inside a box trap: Density-matrix renormalization-group studies for the repulsive Hubbard model with open boundary conditions," Physical Review A77, pp.033619-033623 (2008).
58) Masahiko Machida, Takuma Kano, Susumu Yamada, Masahiko Okumura, Toshiyuki Imamura, Tomio Koyama, "Quantum Synchronization Effects in Intrinsic Josephson Junctions," Physica C 468, pp.689-694 (2008 年).
59) N. Hayashi, C. Iniotakis, M. Machida, and M. Sigrist, "Josephson effect between conventional and Rashba superconductors," Physica C 468, p.844 (2008).
60) M. Machida, T. Kano, S. Yamada, M. Okumura, T. Imamura, and T. Koyama,"Quantum Synchronization Effects in Intrinsic Josephson Junctions," Physica C 468, p.689 (2008).
61) T. Suzudo, H. Kaburaki, M. Itakura, E. Wakai, "A three-dimensional meso-scale computer modeling for bubble growth in metals," Modelling Simul. Mater. Sci. Eng. 16, p.055003 (2008)
62) Y. Nakamura, M. Mine, M. Okumura, and Y. Yamanaka, "Condition for emergence of complex eigenvalues in the Bogoliubov-de Gennes equations," Physical Review A77, pp.043601-043607 (2008).
63) Masahiko Machida, Masahiko Okumura, Susumu Yamada,"Stripe formation in fermionic atoms on a two-dimensional optical lattice inside a box trap: Density-matrix renormalization-group studies for the repulsive Hubbard model with open boundary conditions," Physical Review A 77, pp.033619-033623 (2008).
64) Yusuke Nakamura, Sinjo Mime, Masahiko Okumura, Yuya Nakayama, "Condition for emergence of complex eigenvalues in the Bogoliubov-de Gennes equations," Physical Review A77, pp.043601-043606(2008).

65) Tomio Koyama, Masahiko Machida, Masaru Kato and Takekazu Ishida, "Quantum dynamics of the phase difference in an assembly of closed 0-π Josephson junctions made by d- and s-wave superconductors," Physica C: Superconductivity, Volumes 460-462, Part 2, 1 September 2007, pp. 1305-1306
66) Takekazu Ishida, Masatoshi Nishikawa, Shigehito Miki, Hisashi Shimakage, Zhen Wang, Kazuo Satoh, Tsutomu Yotsuya, Masahiko Machida and Masaru Kato, "Superconducting radiation detector by using a microfabricated MgB2 meander line," Physica C: Superconductivity, Volumes 460-462, Part 1, 1 September 2007, pp. 618-619
67) Y. Nagai, Y. Kato, N. Hayashi, K. Yamauchi, and H. Harima, "Calculated positions of point nodes in the gap structure of the borocarbide superconductor YNi2B2C," Phys. Rev. B 76, p.214514 (2007).
68) H. Suematsu, M. Kato, M. Machida, T. Koyama and T. Ishida, "Quasi-particle spectrum of giant vortex states in a square nanoscopic superconducting plate," Physica C, pp.463-465 (2007) pp.262-265.
69) T. Koyama, M. Machida, M. Kato and T. Ishida, "Macroscopic quantum effect in intrinsic Josephson junctions containing magnetic flux," Physica C, 463-465 (2007) pp.985-988.
70) M. Kato, T. Koyama, M. Machida and T. Ishida, "Anisotropic superconductors in nano-structures," Physica C: Volumes 463-465, (2007) p.254.
71) H. Suematsu, M. Kato, M. Machida, T. Koyama and T. Ishida, "Quasi-particle spectrum of giant vortex states in a square nanoscopic superconducting plate," Physica C: Volumes 463-465, (2007) p.262.
72) M. Machida and T. Koyama, "Theory for collective macroscopic tunneling in high-Tc intrinsic Josephson junctions," Physica C: Superconductivity, Volumes 463-465, 1 October 2007, pp. 84-88
73) S. Yamada, M. Machida, Y. Ohashi and H. Matsumoto, "Strong pairing and microscopic inhomogeneity of lattice fermion systems," Physica C: Superconductivity, Volumes 463-465, 1 October 2007, pp. 103-106
74) Tomio Koyama and Masahiko Machida, Quantum correction to the discrete breather in capacitively-coupled intrinsic Josephson junctions, Physica C: Superconductivity, Volumes 460-462, Part 2, 1 September 2007, pp. 1321-1322.
75) Masaru Kato, Tomio Koyama, Masahiko Machida and Takekazu Ishida, Superconducting symmetries of nano-structured anisotropic superconductors, Physica C: Superconductivity, Volumes 460-462, Part 2, 1 September 2007, pp. 1436-1437.
76) Ken-ichi Ebihara, Tomoaki Suzudo, Hideo Kaburaki, Kenichi Takai, Shigeto Takebayashi Modeling of Hydrogen Thermal Desorption of Pure Iron and Eutectoid Steel, ISIJ International, 47(8), 2007, pp.1131-1140
77) Masatake Yamaguchi, Yutaka Nishiyama and Hideo Kaburaki Decohesion of iron grain boundaries by sulfur or phosphorous segregation: First-principles calculations. Physical Review B 76, p.035418 (2007)
78) S. Yamada, T. Imamura, T. Kano, Y. Ohashi, H. Matsumoto, and M. Machida Ultra Large-scale Exact-diagonalization for Confined Fermion-Hubbard Model on the Earth Simulator: Exploration of Supuerfluidity in Confined Strongly-Correlated Systems, Journal of the Earth Simulator, Vol. 7, June 2007 pp.23-35
79) Masahiko Machida, Tomio Koyama and Yoji Ohashi, Vortex structure in weak to strong coupling superconductors: Crossover from BCS to BEC Physica C: Superconductivity, Volumes 445-448, 1, pp. 194-197
80) Masahiko Machida, Susumu Yamada, Yoji Ohashi and Hideki Matsumoto "Novel pairing in the Hubbard model with confinement potential," Physica C: Superconductivity, Volumes 445-448, 1 October 2006, pp. 90-93

1.5 Computational Quantum Bioinformatics

81) A. R. Srinivasan, Ronald R. Sauers, Marcia O. Fenley, Alexander H. Boschitsch, Atsushi Matsumto, Andrew V. Colasanti, and Wilma K. Olson, "Properties of the nucleic-acid bases in free and Watson-Crick hydrogen-bonded states: computational insights into the sequence-dependent features of double-helical DNA," Biophys Review, Vol.1, No.1, pp.13-20 (2009).
82) A.Matsumoto, T.Kamata, J.Takagi, K.Iwasaki, K.Yura, "Key interactions in ectodomain of integrin responsible for global conformational change detected by elastic network normal mode analysis," Biophys. J, 95, pp.2895-2908 (2008).
83) C. Yamasaki et al., "The H-Invitational Database (H-InvDB), a comprehensive annotation resource for human genes and transcripts - Genome Information Integration Project And H-Invitational 2," Nucleic Acids Research, 36

(2008) D793-D799 (K. Yura is the 75^th author of 136).

84) Go, M., Yura, K., Shionyu, M. (2007) Contribution of computational biology and structural genomics to understand genome and transcriptome. "Proceedings of the International Symposium on Frontiers of Computational Science 2005 (ISFCS2005)", (eds. Y. Kaneda, H. Kawamura and M. Sasai), Springer, pp.75-80.

85) H. Kono, T. Yuasa, S. Nishiue, and K. Yura, "coliSNP database server mapping nsSNPs on protein structures," Nucleic Acids Research, 36 (2008) pp.D409-D413.

86) Gong, X., Nakamura, K., Yu, H., Yura, K., Go, N. (2007) BAAQ: An Infrastructure for Application Integration and Knowledge Discovery in Bioinformatics. IEEE Transactions on Information Technology in Biomedicine, 11 (4), pp.428-434.

87) Miyazawa, Y., Nishioka, H., Yura, K., Yamato, T. (2008) "Discrimination of class I cyclobutane pyrimidine dimer photolyase from blue light photoreceptors by single methionine residue," Biophysical Journal, 94, pp.2194-2203.

88) Shiina, J., Oikawa, M., Nakamura, K., Obata, R., and Nishiyama, S. (2007) Synthesis of pingusane-type sesquiterpenoids, acutifolone A and pinguisenol along with bisacutifolones through the Diels-Alder dimerization reaction., European Journal of Organic Chemistry, 31, pp. 5190-5197.

List of Oral Presentation

1.1 Computer Science / Grid Computing

1) Guehee Kim, Yoshio Suzuki, Akemi Nishida, and Hiroshi Takemiya, "Development of APIs for Desktop Supercomputing", 9th Teraflop Workshop (Tohoku University, Sendai, Miyagi, Japan, 2008.11.12-13) (2008) (Invited).

2) Yves Caniou, Noriyuki Kushida, Naoya Teshima, "Implementing interoperability between the AEGIS and DIET GridRPCmiddleware to build an International Sparse Linear Algebra Expert System", The Second International Conference on Advanced Engineering Computing and Applications in Sciences (Valencia, Spain, 2008.9.29-10.4) (2008).

3) Chiaki Kino, Tomoaki Kunugi, and Zensaku Kawara, "Numerical simulation on heat transfer of falling film flow along a vertical wall," Proceedings of 2007 ASME-JSME Thermal Engineering Summer Heat Transfer Conference(HT2007) (Vancouver, British Columbia, CANADA, 2007.7.9) (2007).

4) Noriyuki Kushida, "One approach of new parallel architecture for real space descretization methods", REDIMPS (Tokyo, Japan, 2007.5.29) (2007).

5) Noriyuki Kushida, "One approach of new parallel architecture for Real Space Descritization methods", (16th CCSE Workshop on High Performance Computing on Vector Based Architectures - Recent Achievements and Future Directions - Japan Atomic Energy Agency) (Tokyo, Japan, 2007.4.23) (2007).

1.2 Computational Vibration Science

6) Tomonori Yamada, "Construction of Vibration Table in an Extended World for Safety Assessment of Nuclear Power Plants", 9th Teraflop Workshop (Tohoku University, Sendai, Miyagi, Japan, 2008.11.12-13) (2008) (Invited).

7) Norihiro Nakajima, Fumimasa Araya, Akemi Nishida, Yoshio Suzuki, Masato Ida, Tomonori Yamada, Noriyuki Kushida, Kim G, Chiaki Kino, Hiroshi Takemiya, "A large scale simulation for impact and blast loading issues," International Symposium on Structures under Earthquake, Impact, and Blast Loading 2008(IB08), pp.119-123 (Osaka, Japan, 2008.10.10-11) (2008) (Invited).

8) Akemi Nishida, "Impact analysis of three-dimensional frame structures -An Application for piping structures of a nuclear power plant-," International Symposium on Structures under Earthquake, Impact, and Blast Loading 2008(IB08), pp.129-134 (Osaka, Japan, 2008.10.10-11) (2008) (invited).

9) Osamu Hazama, Noriyuki Kushida, Hitoshi Matsubara, Akemi Nishida, Yoshio Suzuki, Fumimasa Araya, Tetsuo Aoyagi and Norihiro Nakajima, “Integrated Framework for Simulating Behaviors of Nuclear Power Plants under Earthquakes”, Proceedings of 9th MpCCI User Forum, pp.118-125 (Schloss Birlinghoven, Sankt Augustin,

Germany, 2008.2.19-20) (2008).
10) Noriyuki Kushida, Yoshio Suzuki, Osamu Hazama, Hitoshi Matsubara, Akemi Nishida, Fumimasa Araya, Tetsuo Aoyagi and Norihiro Nakajima, "R&D of Nuclear Power Plant Simulator on Atomic Energy Grid Infrastructure," Proceedings of 8th MpCCI User Forum, pp.102-107 (Sankt Augustin, Germany, 2007.2.13-14) (2007).
11) Osamu Hazama, "Transient thermal stress analysis of a spherically curved tubesheet", REDIMPS (Tokyo, Japan, 2007.5.29) (2007).
12) M. Tani, N. Nakajima, A. Nishida, Y. Suzuki, H. Matsubara, O. Hazama, N. Kushida, and K. Kawasaki, "A METHODOLOGY OF STRUCTURAL ANALYSIS FOR NUCLEAR POWER PLANT SIZE OF ASSEMBLY," Joint International Topical Meeting on Mathematics & Computations and Supercomputing in Nuclear Applications (M & C + SNA 2007) (Monterey, USA, 2007.4.16) (2007)

1.3 Computational Fluid Dynamics & Fusion Science

13) T.Watanabe, "Numerical Simulation of Oscillating-Rotating Liquid Droplet," Proc. 3rd IASME/WSEAS Int. Conf. Continuum Mechanics (CM'08) (Cambridge, UK, 2008.2.23-25) (2008).
14) T.Watanabe, "Oscillation frequency and deformation of levitated droplets," Proc. XXII Int. Congress Theoretical and Applied Mechanics (ICTAM 2008) (Adelaide、Austraria, 2008.8.24-29) (2008).
15) M. Futakawa, H. Kogawa, S. Hasegawa, M. Ida, K. Haga, T. Wakui, T. Naoe, N. Tanaka, Y. Matsumoto, and Y. Ikeda, "R&D on pressure-wave mitigation technology in mercury target," 18th Meeting of the International Collaboration on Advanced Neutron Sources (ICANS-XVIII) (2007).
16) Masato Ida, Takashi Naoe, and Masatoshi Futakawa, "Numerical study of gas and cavitation bubble dynamics in liquid mercury under negative pressure," (5th Joint ASME/JSME Fluids Engineering Conference) (San Diego, California, USA, 2007.7.31) (2007)
17) T.Watanabe, "Parallel Computations of Droplet Oscillations," Proc. Int. Conf. on Parallel Computational Fluid Dynamics,37 (Antalya, Turkey, 2007.5.21-24) (2007).
18) Yasuhiro Idomura, "Performances of first principle fusion plasma turbulence simulations on SX and Altix" (16th CCSE Workshop on High Performance Computing on Vector Based Architectures - Recent Achievements and Future Directions - Japan Atomic Energy Agency) (Tokyo, Japan, 2007.4.23) (2007).

1.4 Computational Materials Science

19) Hiroki Nakamura, Masahiko Machida, Alfred Baron, Tatsuo Fukuda, and Shinichi Shamoto, "Effects of Magnetic Ordering on Phonon Spectra in Iron-based Superconductors: First Principle Calculation and Theoretical Analysis," 2009 APS March meeting (Pittsburgh, USA, 2009/03/16-20).
20) Masahiko Okumura, Susumu Yamada, Nobuhiko Taniguchi, Masahiko Machida, "Magnetizm Localization and Hole Localization in Fermionic Atoms Loaded on Optical Lattice," 2009 APS March meeting, (Pittsburgh, USA, 2009/03/16-20).
21) Masahiko Okumura, Hiroaki Onishi, Susumu Yamada, and Masahiko Machida, "Spin and Charge Dynamics in Atomic Fermions Loaded on Optical Lattice," 2009 APS March meeting, (Pittsburgh, USA, 2009/03/16-20).
22) Masahiko Okumura, Susumu Yamada, and Masahiko Machida, "Parallelized DMRG studies for atomic Fermi gas loaded on optical lattice," Supercomputing in Solid State Physics 2009 (Kashiwa, Japan, 2009/02/18).
23) Masahiko Machida, "±S-wave Scenario in Iron-based Superconductors: Thermodynamics and Josephson Effects," (International Workshop on Iron Related High-Tc Superconductors (IRiSes2009), Tokyo, Japan, Jan. 25, 2009)
24) Ken-ichi Ebihara, Masatake Yamaguchi, Hideo Kaburaki, and Yutaka Nishiyama, "Rate Theory Modeling of Irradiation-induced Phosphorus Segregation in FCC nickel Using First Principles Calculations," 2008 MRS Fall Meeting (Boston, USA, 2008.12.1-5).
25) T. Suzudo, H. Kaburaki, and M. Itakura, "Modeling Study of Grain Sub-division Observed at High Burnup Nuclear Fuel," The 4th International Meeting of Multi-scale Materials Modeling (Florida State University, USA, 2008.10.29).
26) Mitsuhiro Itakura, Hideo Kaburaki, Masatake Yamaguchi and Tomoko Kadoyoshi, "Coupled Simulation of Grain

Boundary Decohesion and Hydrogen Segregation," The 4th International Meeting of Multi-scale Materials Modeling (Florida State University, USA, 2008.10.28).

27) Masahiko Okumura, Noriyuki Nakai, Hiroki Nakamura, Nobuhiko Hayashi, Susumu Yamada, and Masahiko Machida, "Exact Diagonalization Studies on Two-Band Minimal Model for Iron-Based Superconductors," 21th International Symposium on Superconductivity (Tsukuba, Japan, 2008.10.27-29).

28) Noriyuki Nakai, Nobuhiko Hayashi, and Masahiko Machida, "Simulation study for the orientation of the driven vortex lattice in an amorphous superconductor," 21st International Symposium on Superconductivity (Tsukuba, Japan, 2008.10.27-29).

29) Noriyuki Nakai, Nobuhiko Hayashi, and Masahiko Machida, "TDGL simulation for the driven vortex-latice in an amorphous superconductor," International Workshop on Nanostructured Superconductors: From fundamentals to applications (Freudenstadt, Germany, 2008.9.13-17).

30) Nobuhiko Hayashi, "New theoretical method for analyzing the field-angle-dependent measurements made in unconventional superconductors," International Workshop on Nanostructured Superconductors: From fundamentals to applications (Freudenstadt, Germany, 2008.9.13-17).

31) Susumu Yamada, Masahiko Okumura, Masahiko Machida, "High Performance Computing for Eigenvalue Solver in Density-Matrix Renormalization Group Method: Parallelization of the Hamiltonian Matrix-vector Multiplication," Conference Proceedings of 8th international Meeting on High performance Computing for Computational Science, pp.448-454 (2008.09)

32) Susumu Yamada, Masahiko Okumura, Masahiko Machida, "Parallel Computing of Directly-Extended Density-Matrix Renormalization Group to Two-Dimensional Strongly Correlated Quantum Systems," Proceedings of 26th IASTED International Multi-Conference, pp.175-180 (2008.09)

33) Masahiko Okumura, Susumu Yamada, Masahiko Machida: "Ground States of Cold Neutral Fermions in 2-Dimensional Optical Lattices: Effects of Strong Correlation in Square and Triangular Lattices," The 21th International Conference on Atomic Physics (Storrs, Connecticut, USA, 2008.07.28)

34) Masahiko Machida, Takuma Kano, Masahiko Okumura, Noriyuki Nakai, Nobuhiko Hayashi, "Population Imbalanced Two-component Fermi Superfluidity inside Box-shape Trap Self-consistent Calculations of T = 0 BdG Equation," The 21th International Conference on Atomic Physics（Storrs, Connecticut, USA, 2008.07.28)

35) Y. Nishiyama, M. Yamaguchi, K. Onizawa, A. Iwase, H. Matsuzawa, "Irradiation-Induced Intergranular Solutes Segregation and Their Effects on Ductile-to-Brittle Transition Temperature in Reactor Pressure Vessel Steels," ASTM 24th Symposium on Effects of Radiation on Nuclear Materials and the Nuclear Fuel Cycle (Denver, U.S.A., 2008.06.26)

36) Machida Masahiko, "Quantum Synchronization and Electromagnetic Wave Emission in Intrinsic Josephson Junctions," International Conference on Theoretical Physics (Dubna, Russia, 2008.07.08)

37) Machida Masahiko, "Quantum dynamics, synchronization, and electromagnetic wave emission in intrinsic Josephson junctions," The 6th International Symposium on Intrinsic Josephson Effect and Plasma Oscillations in High-Tc Superconductors (Pohang, Korea, 2008.07.17)

38) N. Hayashi, "Josephson effect between conventional and Rashba superconductors," Whorkshop on NON-CENTROSYMMETRIC SUPERCONDUCTORS, (Zurich Switzerland, 2008.5.30-31).

39) Susumu Yamada, Masahiko Okumura, and Masahiko Machida, "Parallel Computing of Directly-Extended Density-Matrix Renormalization Group to Two-Dimensional Strongly Correlated Quantum," The IASTED International Conference on Parallel and Distributed Computing and Networks, Innsbruck (Austria), 2008.2.12-14.

40) T. Suzudo, H. Kaburaki, M. Itakura, et al., "Modeling studies of recovery process induced by fission/ion truck in UO2/CeO2," New Crossover Project International Workshop-4, November 13-14, 2007, Tokyo, Japan.

41) M. Machida, International Conference "Vortex V," "Quantum Synchronization Effects in Intrinsic Josephson Junctions," (Invited Talk, Sep. 13, 2007, Rhodes, Greek)

42) M. Machida "Quantum Synchronization Effects and Related Electromagnetic Excitation in Intrinsic Josephson Junctions," in APCTP Workshop on Superconductivity and Mesoscopic Quantum Phenomena (Invited Talk, Pohang, Aug. 20, Korea).

43) M. Machida "Electromagnetic Excitation of Intrinsic Josephson Junctions in Classical and Quantum Regimes," in

Korean Superconductivity Society Meeting (Invited Talk, Yong-Pyong, Aug. 18, Korea)

44) H. Kaburaki and T. Tajima "Recent progress of supercomputing research in nuclear fields in Japan," Joint International Topical Meeting on Mathematics & Computations and Supercomputing in Nuclear Applications (M & C + SNA 2007) (Monterey, USA, 2007.4.16)

45) M. Yamaguchi and H. Kaburaki "First principles calculations on the grain boundary cohesion in BCC Fe," Joint International Topical Meeting on Mathematics & Computations and Supercomputing in Nuclear Applications (M & C + SNA 2007) (Monterey, USA, 2007.4.16)

46) M. Itakura, T. Kadoyoshi and H. Kaburaki "Molecular Dynamics and quasi-two dimensional dislocation dynamics simulation on the Orowan pinning mechanism of a mixed dislocation in FCC metals," Joint International Topical Meeting on Mathematics & Computations and Supercomputing in Nuclear Applications (M & C + SNA 2007) (Monterey, USA, 2007.4.16)

47) T. Suzudo, H. Kaburaki and E. Wakai "A THREE-DIMENSIONAL MESO-SCALE MODELING FOR HELIUM BUBBLE GROWTH IN METALS," Joint International Topical Meeting on Mathematics & Computations and Supercomputing in Nuclear Applications (M & C + SNA 2007) (Monterey, USA, 2007.4.16)

48) M. Machida "High-Performance computing for exact quantum many-body simulation on the Earth Simulator" (16^th CCSE Workshop on High Performance Computing on Vector Based Architectures - Recent Achievements and Future Directions - Japan Atomic Energy Agency) (Tokyo, 2007.4.23)

1.5 Computational Quantum Bioinformatics

49) A. Matsumoto and H. Ishida, "Structural analysis of ribosome based on the elastic network normal mode analysis and fitting technique," The 6th Asian Biophysical Association (ABA) Symposium（Hong Kong University of Science and Technology, Hong Kong, January 11-15, 2009)

50) Kei Yura, "Amino acid residue doublet propensity in the protein-RNA interface and its application to RNA interface prediction," Workshop on Computational Biophysics（Nov. 20-21, 2007, Noyori Conference Hall, Nagoya University, Japan）

51) A. Matsumoto,“Structural analysis of robosome based on the elastic network normal mode analysis and fittintg technique”, BioMaps Seminar (Mar. 26, 2008, Rutgers, The State University of New Jersey, USA)

52) A. Matsumoto,“Structural analysis of robosome based on the elastic network normal mode analysis and fittintg technique”, Japan-UK symposium on conformational changes in proteins and nucleic acids which constitute biological macro-molecules. (Dec. 20, 2007, Pacifico Yokohama, Yokohama, Japan)

3. Awards

1) 6th Division CG Award, Computational Science and Engineering Division of the Japan Atomic Energy Society, (23 March 2009), Akemi Nishida, Fumimasa Araya, "Application of SEM to Impact Response Analysis of Pipe Structure"

2) Certificate of Merit for Best Presentation, Computational mechanics division of the Japan society of mechanical engineers (March, 2008), Masato Ida, "Suppression of Mercury Cavitation by Gas Bubble Injection"

3) Computer Science Research and dvelopment Office, JAEA R&D Merit Award (2009), "Achievement of Research for Advanced Computer Utilization".

4) FUJITSU Family Association FY2008 (2009), Kimiaki Saito, Naoya Teshima, Yoshio Suzuki, Norihiro Nakajima, Hidetoshi Saito, Etsuo Kunieda, Tatsuya Fujisaki, "Gridization of IMAGINE for the remote assistance of radiation therapy" (Japanese).

5) FY2008 Collected Papers of NEC C&C Systems Users Association (2008), Kohei Nakajima, Yoshio Suzuki, Naoya Teshima, Shin-ichiro Sugimoto, Shinobu Yoshimura, Norihiro Nakajima, "Method to Unconsiously Use Grid middleware; Proposal of Seamless API and Its Application to Mechanics System" (Japanese).

6) FY2007 Collected Papers of NEC C&C Systems Users Association (2007),.Noriyuki Kushida, Yoshio Suzuki,

Naoya Teshima, and Norihiro Nakajima "Developemnt of ITBL-UNICORE Grid interoperable system" (Japanese).

7) International Conference for High Performance Computing, Networking, Storage and Analysis (SC08) Analytics Challenge Finalist (2008), Yoshio Suzuki, Akemi Nishida, Tomonori Yamada, Fumimasa Araya, Sachiko Hayashi, Norihiro Nakajima, and Toshio Hirayama, "Cerebral Methodology Based Computing for Estimating Validity of Simulation Results".
8) International Conference for High Performance Computing, Networking, Storage and Analysis (SC07) Analytics Challenge Finalist (2007), Chiaki Kino, Noriyuki Kushida, Yoshio Suzuki and Norihiro Nakajima, “Cognitive methodology based Data Analysis System for Large Scale Data”.
9) Outstanding Paper Award of The Japan Society for Computational Engineering and Science (2007), Susumu Yamada.

4. External Funds

1) "Development of physical model describing the dynamic interaction characteristics of component connections for the analysis of an entire nuclear facility", Innovative Nuclear Research and Development Program (MEXT) 10,397K Yen (FY2007), 6,567K Yen (FY2008)
2) "Research and Development of International Matrix solver Prediction System on French-Japan International GRID Computing Environment" (REDIMPS) (JST) 4,500 K Yen (FY2006-FY2009)
3) "R&D of Grid Middle Utilization Technology" (MEXT) 75,737 K Yen (FY2006-FY2007)
4) "Generation of High Dimensional Volume Map", Grants-in-Aid for Scientific Research, Grant-in-Aid for Young Scientists (B) (MEXT) 1,016 K Yen (FY2007-FY2008)
5) "Simulation for Predicting Quake-Proof Capability of Nuclear Power Plants", Core Research for Evolutional Science and Technology (JST) 650 K Yen (FY2007), 19,400K Yen (FY2008)
6) "Development of a large scale simulator for cavitation bubble clouds and theoretical study", Grants-in-Aid for Scientific Research, Grant-in-Aid for Young Scientists (B) (MEXT) 900 K Yen (FY2007)
7) "Theoretical and computational study of liquid-metal cavitation",Grants-in-Aid for Scientific Research, Grant-in-Aid for Young Scientists (B) (MEXT) 900 K Yen (FY2007)
8) "The prediction of the irradiation-induced embrittlement of reactor pressure vessel steels in high-irradiation region" (JNES), 5000 K Yen (FY2007-FY2008)
9) "Framework Development for Multi-scale and Multi-physics Simulations toward Novel Applications of Superconductivity" (CREST), 45,000K Yen/Year (FY2006-2011)
10) "Large-scale Simulation Studies for Quantum Turbulence I, II" (MEXT), 1000 K Yen/year (FY2006-FY2009)
11) "New crossover project" (MEXT), 6300 K Yen (FY 2007), 1800 K Yen (FY 2008)
12) "R&D Project on Irradiation Damage Management Technology for Structural Materials of Long-life Nuclear Plant" (MEXT), 700 K Yen (FY 2007) , 300 K Yen (FY 2008)
13) "Fundamental Studies on Technologies for Steel Materials with Enhanced Strength and Functions" (JRCM), 2343 K Yen (FY 2007), 21375 K Yen (FY 2008)
14) Building atomic resolution structures from low-resolution data of supra-molecules (JST, CREST) 1,670 K Yen (FY2007)
15) Structural bioinfomatics for elucidating complex structures of proteins (MEXT) 11,383 K Yen (FY2007)
16) Database search and functional analysis of transition-metal-binding proteins (JSPS) 3,120 K Yen (FY2007-FY2008)

5. Staff List of CCSE (R&D Office) in FY2007-FY2008

Director:	Toshio Hirayama
Duputy Director:	Norihiro Nakajima
Duputy Director:	Masayuki Tani

- Computer Science Reseaerch and Development Office

General Manager:	Norihiro Nakajima (until May 2008)
General Manager:	Hiroshi Takemiya (since June 2008)
Duputy General Manager:	Tetsuo Aoyagi

- R&D Team for Computer Science

Team Leader (Assistant Principal Researcher):	Yoshio Suzuki
Senior Post-Doctoral Fellow:	Hiroko Miyamura (since October 2008)
Collaborating Enginner:	Nobuko Matsumoto (until June 2007)
	Takahiro Minami (until June 2007)
	Kohei Nakajima
	Taku Akutsu
	Sachiko Hayashi (since July 2007)
	Naoya Teshima (since July 2007)
Post-Doctoral Fellow:	Chiaki Kino
	Guehee Kim (since April 2008)

- R&D Team for full-scale simulation technology

Team Leader (Assistant Principal Researcher):	Akemi Nishida
Assistant Principal Researcher:	Fumimasa Araya
Reseach Engineer:	Masato Ida
Reseach Engineer:	Noriyuki Kushida
Research Engineer:	Hideo Kimura (until December 2007)
Senior Post-Doctoral Fellow:	Osamu Hazama (until March 2008)
	Tomonori Yamada (since April 2008)
Post-Doctoral Fellow:	Hitoshi Matsubara (until March 2008)

- R&D Team for Quantum Energy Simulator

Duputy Director:	Hiroshi Matsuoka
Principal Researcher:	Shinji Tokuda (until September 2007)

- Simulation Technology Resaerch and Development Office

General Manager:	Masahiko Machida

- Material Simulator Team

Duputy Director:	Hideo Kaburaki
Assistant Principal Researcher:	Tomoaki Suzudo
Assistant Principal Researcher:	Masatake Yamaguchi
Assistant Principal Researcher:	Mitsuhiro Itakura
Reseach Engineer:	Narimasa Sasa
Assistant Principal Researcher:	Susumu Yamada
Assistant Principal Researcher:	Motoyuki Shiga

Collaborating Enginner:	Tomoko Kadoyoshi

- Quantum Bioinformatics Team

Team leader (Assistant Principal Researcher):	Kei Yura (until March 2008)
Assistant Principal Researcher:	Atsushi Matsumoto
Senior Post-Doctoral Fellow:	Kensuke Nakamura (until October 2008)

- CREST Special Topic Team

Post-Doctoral Fellow:	Nobuhiko Hayashi
Post-Doctoral Fellow:	Noriyuki Nakai
Post-Doctoral Fellow:	Masahiko Okumura

This is a blank page.

国際単位系（SI）

表１．SI 基本単位

基本量	SI 基本単位	
	名称	記号
長さ	メートル	m
質量	キログラム	kg
時間	秒	s
電流	アンペア	A
熱力学温度	ケルビン	K
物質量	モル	mol
光度	カンデラ	cd

表２．基本単位を用いて表されるSI組立単位の例

組立量	SI 基本単位	
	名称	記号
面積	平方メートル	m^2
体積	立法メートル	m^3
速さ，速度	メートル毎秒	m/s
加速度	メートル毎秒毎秒	m/s^2
波数	毎メートル	m^{-1}
密度，質量密度	キログラム毎立方メートル	kg/m^3
面積密度	キログラム毎平方メートル	kg/m^2
比体積	立方メートル毎キログラム	m^3/kg
電流密度	アンペア毎平方メートル	A/m^2
磁界の強さ	アンペア毎メートル	A/m
量濃度[(a)]，濃度	モル毎立方メートル	mol/m^3
質量濃度	キログラム毎立法メートル	kg/m^3
輝度	カンデラ毎平方メートル	cd/m^2
屈折率[(b)]	（数字の） 1	1
比透磁率[(b)]	（数字の） 1	1

(a) 量濃度（amount concentration）は臨床化学の分野では物質濃度（substance concentration）ともよばれる。
(b) これらは無次元量あるいは次元１をもつ量であるが、そのことを表す単位記号である数字の１は通常は表記しない。

表３．固有の名称と記号で表されるSI組立単位

組立量	SI 組立単位			
	名称	記号	他のSI単位による表し方	SI基本単位による表し方
平面角	ラジアン[(b)]	rad	1[(b)]	m/m
立体角	ステラジアン[(b)]	sr[(c)]	1[(b)]	m^2/m^2
周波数	ヘルツ[(d)]	Hz		s^{-1}
力	ニュートン	N		m kg s^{-2}
圧力，応力	パスカル	Pa	N/m^2	m^{-1} kg s^{-2}
エネルギー，仕事，熱量	ジュール	J	N m	m^2 kg s^{-2}
仕事率，工率，放射束	ワット	W	J/s	m^2 kg s^{-3}
電荷，電気量	クーロン	C		s A
電位差（電圧），起電力	ボルト	V	W/A	m^2 kg s^{-3} A^{-1}
静電容量	ファラド	F	C/V	m^{-2} kg^{-1} s^4 A^2
電気抵抗	オーム	Ω	V/A	m^2 kg s^{-3} A^{-2}
コンダクタンス	ジーメンス	S	A/V	m^{-2} kg^{-1} s^3 A^2
磁束	ウエーバ	Wb	Vs	m^2 kg s^{-2} A^{-1}
磁束密度	テスラ	T	Wb/m^2	kg s^{-2} A^{-1}
インダクタンス	ヘンリー	H	Wb/A	m^2 kg s^{-2} A^{-2}
セルシウス温度	セルシウス度[(e)]	℃		K
光束	ルーメン	lm	cd sr[(c)]	cd
照度	ルクス	lx	lm/m^2	m^{-2} cd
放射性核種の放射能[(f)]	ベクレル[(d)]	Bq		s^{-1}
吸収線量，比エネルギー分与，カーマ	グレイ	Gy	J/kg	m^2 s^{-2}
線量当量，周辺線量当量，方向性線量当量，個人線量当量	シーベルト[(g)]	Sv	J/kg	m^2 s^{-2}
酸素活性	カタール	kat		s^{-1} mol

(a)SI接頭語は固有の名称と記号を持つ組立単位と組み合わせても使用できる。しかし接頭語を付した単位はもはやコヒーレントではない。
(b)ラジアンとステラジアンは数字の１に対する単位の特別な名称で、量についての情報をつたえるために使われる。実際には、使用する時には記号rad及びsrが用いられるが、習慣として組立単位としての記号である数字の１は明示されない。
(c)測光学ではステラジアンという名称と記号srを単位の表し方の中に、そのまま維持している。
(d)ヘルツは周期現象についてのみ、ベクレルは放射性核種の統計的過程についてのみ使用される。
(e)セルシウス度はケルビンの特別な名称で、セルシウス温度を表すために使用される。セルシウス度とケルビンの単位の大きさは同一である。したがって、温度差や温度間隔を表す数値はどちらの単位で表しても同じである。
(f)放射性核種の放射能（activity referred to a radionuclide）は、しばしば誤った用語で"radioactivity"と記される。
(g)単位シーベルト（PV,2002,70,205）についてはCIPM勧告2（CI-2002）を参照。

表４．単位の中に固有の名称と記号を含むSI組立単位の例

組立量	SI 組立単位		
	名称	記号	SI 基本単位による表し方
粘度	パスカル秒	Pa s	m^{-1} kg s^{-1}
力のモーメント	ニュートンメートル	N m	m^2 kg s^{-2}
表面張力	ニュートン毎メートル	N/m	kg s^{-2}
角速度	ラジアン毎秒	rad/s	m m^{-1} s^{-1}=s^{-1}
角加速度	ラジアン毎秒毎秒	rad/s^2	m m^{-1} s^{-2}=s^{-2}
熱流密度，放射照度	ワット毎平方メートル	W/m^2	kg s^{-3}
熱容量，エントロピー	ジュール毎ケルビン	J/K	m^2 kg s^{-2} K^{-1}
比熱容量，比エントロピー	ジュール毎キログラム毎ケルビン	J/(kg K)	m^2 s^{-2} K^{-1}
比エネルギー	ジュール毎キログラム	J/kg	m^2 s^{-2}
熱伝導率	ワット毎メートル毎ケルビン	W/(m K)	m kg s^{-3} K^{-1}
体積エネルギー	ジュール毎立方メートル	J/m^3	m^{-1} kg s^{-2}
電界の強さ	ボルト毎メートル	V/m	m kg s^{-3} A^{-1}
電荷密度	クーロン毎立方メートル	C/m^3	m^{-3} sA
表面電荷	クーロン毎平方メートル	C/m^2	m^{-2} sA
電束密度，電気変位	クーロン毎平方メートル	C/m^2	m^{-2} sA
誘電率	ファラド毎メートル	F/m	m^{-3} kg^{-1} s^4 A^2
透磁率	ヘンリー毎メートル	H/m	m kg s^{-2} A^{-2}
モルエネルギー	ジュール毎モル	J/mol	m^2 kg s^{-2} mol^{-1}
モルエントロピー，モル熱容量	ジュール毎モル毎ケルビン	J/(mol K)	m^2 kg s^{-2} K^{-1} mol^{-1}
照射線量（X線及びγ線）	クーロン毎キログラム	C/kg	kg^{-1} sA
吸収線量率	グレイ毎秒	Gy/s	m^2 s^{-3}
放射強度	ワット毎ステラジアン	W/sr	m^4 m^{-2} kg s^{-3}=m^2 kg s^{-3}
放射輝度	ワット毎平方メートル毎ステラジアン	W/(m^2 sr)	m^2 m^{-2} kg s^{-3}=kg s^{-3}
酵素活性濃度	カタール毎立方メートル	kat/m^3	m^{-3} s^{-1} mol

表５．SI 接頭語

乗数	接頭語	記号	乗数	接頭語	記号
10^{24}	ヨタ	Y	10^{-1}	デシ	d
10^{21}	ゼタ	Z	10^{-2}	センチ	c
10^{18}	エクサ	E	10^{-3}	ミリ	m
10^{15}	ペタ	P	10^{-6}	マイクロ	μ
10^{12}	テラ	T	10^{-9}	ナノ	n
10^{9}	ギガ	G	10^{-12}	ピコ	p
10^{6}	メガ	M	10^{-15}	フェムト	f
10^{3}	キロ	k	10^{-18}	アト	a
10^{2}	ヘクト	h	10^{-21}	ゼプト	z
10^{1}	デカ	da	10^{-24}	ヨクト	y

表６．SIに属さないが、SIと併用される単位

名称	記号	SI 単位による値
分	min	1 min=60s
時	h	1h =60 min=3600 s
日	d	1 d=24 h=86 400 s
度	°	1°=(π/180) rad
分	’	1’=(1/60)°=(π/10800) rad
秒	”	1”=(1/60)’=(π/648000) rad
ヘクタール	ha	$1ha=1hm^2=10^4m^2$
リットル	L，l	$1L=11=1dm^3=10^3cm^3=10^{-3}m^3$
トン	t	$1t=10^3$ kg

表７．SIに属さないが、SIと併用される単位で、SI単位で表される数値が実験的に得られるもの

名称	記号	SI 単位で表される数値
電子ボルト	eV	$1eV=1.602\ 176\ 53(14)\times10^{-19}J$
ダルトン	Da	$1Da=1.660\ 538\ 86(28)\times10^{-27}kg$
統一原子質量単位	u	1u=1 Da
天文単位	ua	$1ua=1.495\ 978\ 706\ 91(6)\times10^{11}m$

表８．SIに属さないが、SIと併用されるその他の単位

名称	記号	SI 単位で表される数値
バール	bar	1 bar=0.1MPa=100kPa=10^5Pa
水銀柱ミリメートル	mmHg	1mmHg=133.322Pa
オングストローム	Å	1 Å=0.1nm=100pm=10^{-10}m
海里	M	1 M=1852m
バーン	b	$1\ b=100fm^2=(10^{-12}cm)2=10^{-28}m^2$
ノット	kn	1 kn=(1852/3600)m/s
ネーパ	Np	SI単位との数値的な関係は、対数量の定義に依存。
ベル	B	
デジベル	dB	

表９．固有の名称をもつCGS組立単位

名称	記号	SI 単位で表される数値
エルグ	erg	$1\ erg=10^{-7}$ J
ダイン	dyn	$1\ dyn=10^{-5}$N
ポアズ	P	$1\ P=1\ dyn\ s\ cm^{-2}=0.1Pa\ s$
ストークス	St	$1\ St=1cm^2\ s^{-1}=10^{-4}m^2\ s^{-1}$
スチルブ	sb	$1\ sb=1cd\ cm^{-2}=10^4cd\ m^{-2}$
フォト	ph	$1\ ph=1cd\ sr\ cm^{-2}\ 10^4lx$
ガル	Gal	$1\ Gal=1cm\ s^{-2}=10^{-2}ms^{-2}$
マクスウェル	Mx	$1\ Mx = 1G\ cm^2=10^{-8}Wb$
ガウス	G	$1\ G=1Mx\ cm^{-2}=10^{-4}T$
エルステッド[(c)]	Oe	1 Oe ≙ $(10^3/4\pi)A\ m^{-1}$

(c) ３元系のCGS単位系とSIでは直接比較できないため、等号「 ≙ 」は対応関係を示すものである。

表10．SIに属さないその他の単位の例

名称	記号	SI 単位で表される数値
キュリー	Ci	$1\ Ci=3.7\times10^{10}Bq$
レントゲン	R	$1\ R=2.58\times10^{-4}C/kg$
ラド	rad	$1\ rad=1cGy=10^{-2}Gy$
レム	rem	$1\ rem=1\ cSv=10^{-2}Sv$
ガンマ	γ	1γ=1 nT=10-9T
フェルミ		1フェルミ=1 fm=10-15m
メートル系カラット		1メートル系カラット = 200 mg = 2×10-4kg
トル	Torr	1 Torr = (101 325/760) Pa
標準大気圧	atm	1 atm = 101 325 Pa
カロリー	cal	1cal=4.1858J（「15℃」カロリー），4.1868J（「IT」カロリー）4.184J（「熱化学」カロリー）
ミクロン	μ	1 μ =1μm=10^{-6}m

（第8版，2006年改訂）

この印刷物は再生紙を使用しています